NUCLEAR MAGNETIC RESONANCE STUDIES OF HEMOGLOBIN: FUNCTIONAL STATE CORRELATIONS AND ISOTOPIC ENRICHMENT STRATEGIES

Authors: **Jon S. Morrow**
Yale University
New Haven, Connecticut

Frank R. N. Gurd
Indiana University
Bloomington, Indiana

Referee: Chien Ho
University of Pittsburgh
Pittsburgh, Pennsylvania

I. INTRODUCTION

Hemoglobin is a protein of outstanding biological importance whose function in the transport of oxygen and carbon dioxide is well understood.[1] The functional cycle in the erythrocyte is known in some detail. Allosteric effectors such as organic phosphates, hydrogen ions, and carbon dioxide are recognized, and their adjustments under varying conditions have been described.[1,2] Numerous abnormal forms are known and have been studied in great detail.[1-4]

Hemoglobin is a peculiarly appropriate subject for the application of the modern techniques of protein biochemistry. It is present in high concentration in solution in a cell that is readily harvested. Either in the intact cell or after removal from it, the hemoglobin can be carried through the conversions from the oxy- to the deoxy-state and the structural consequences or interactions with effectors examined under simulated functional conditions. Perhaps most important, hemoglobin has been examined very extensively by X-ray crystallography and much is known thereby about the concerted changes in structure of the four subunits on passing from the unliganded to the liganded state. Not only are the details of the ligand environments specified, but also the adaptations of heme structure and protein conformation within each subunit and at the interfaces between subunits.[5-9]

The following structural and functional properties can be summarized:

1. The normal hemoglobin consists of two pairs of subunits, designated $\alpha_2\beta_2$, which may dissociate under physiological or experimental conditions to the dimer form $\alpha\beta$.
2. Each subunit contains a heme group bound by secondary forces in an elaborate fold of the protein chain with access from the outside to the iron atom for reversible binding of the ligand.
3. The fully deoxygenated structure is distinct for the normal protein from the fully liganded one bearing O_2 or CO at each heme iron.
4. Acceptance of the ligand causes a change in the heme such that its structure is somewhat flattened and the iron is pulled towards the ligand, thereby drawing an attached imidazole group with it. This imidazole group is known as part of the "proximal" histidine residue, residue 87F8 in the α chain and 92F8 in the β chain.[1,10]

5. The various movements of the heme and of attached or abutting protein components cause displacements going out as far as the outer borders of the subunits to the regions of contact with other subunits.

6. Subunit contacts are well defined in at least two conformations, one characteristic of the liganded and the other of the unliganded tetramer. The differences are not limited to the rearrangements described within the given subunit, but the entire tetramer adapts by sliding and rotating the subunits to effect a new stable relationship. The conformations differ, therefore, both within each subunit and in the interactions between the subunits. The unliganded structure is often called the T (or taut) state and the liganded structure the R (or relaxed) state.

7. The combination of crystallographic and solution studies further shows that the R and T states can be represented by forms with varying numbers of ligands bound. This is particularly striking in some abnormal or artificially prepared hemoglobins in which, for example, a fully deoxy form may be found in the R state.

8. A number of the properties of hemoglobin with relation to ligands can be explained in terms of the concerted allosteric model of Monod et al.[11] in which the tetramer is viewed as switching from the T to the R state as binding progresses. This model is easily treated to allow for differences in the α and β subunit interactions.[12,13] The compatibility of ligand acceptance with a predominance of either state is illustrated by the approximate binding sequence, $T_0 \rightarrow T_1 \rightarrow T_2 \rightarrow T_3 \rightarrow R_3 \rightarrow R_4$, where the subscripts represent numbers of oxygen molecules bound per tetramer.[13]

9. The important allosteric effectors influence the R to T transition and impress their effects on the regular ligand interaction pattern. Of primary interest are the specific effects of H^+, CO_2, and organic phosphates, most notably 2,3-diphosphoglycerate. The striking effect of H^+ or CO_2 in diminishing the oxygen affinity of hemoglobin has long been known.[14-16] The dramatic effect of organic phosphate in also lowering the oxygen affinity has only been appreciated in this past decade,[17,18] although it is interesting to note that as early as 1921, Adair et al. speculated[19] that there was "some third substance present . . . which forms an integral part of the oxygen hemoglobin complex."

10. Carbon dioxide effects are modulated primarily by means of carbamino formation with the terminal amino group of the polypeptide chains; eg., $CO_2 + R\text{-}NH_2 \rightleftharpoons RNHCOO^- + H^+$. The combination of crystallographic and solution studies has shown that the carbamino formation favors the T state, and that the phosphates such as 2,3-diphosphoglycerate and inositol hexaphosphate, while competing with carbamino formation at the β chains, are also particularly effective in specifying the T conformation.[20-22] Certain abnormal hemoglobins such as Hb M_{Iwate} are particularly stable in the T state.[4] The R state is usually selected experimentally by saturation with O_2 or CO.

11. A variety of ligand states have been studied, partly to help elucidate the nature of the ligand effect on the heme conformation. These studies are of the greatest importance for the NMR work because the presence of one or more unpaired electrons in the heme will have powerful effects on the nature of the observations that can be made. Secondarily they have made possible the use of valency hybrids to complement certain abnormal hemoglobins.[23,24] For reference, Table 1 lists the electronic configuration of the heme iron in certain states.[25]

12. Kinetics of reactions with O_2 and other ligands have shown that the hemes in α and β chains react at inherently different rates.[26] Relaxation kinetics have shown that the association and dissociation rates for the first O_2 binding are fast, so that the picture of a very taut, inaccessible T state is not entirely appropriate.[27] The last association step is also quite fast. Intermediate stages cannot be resolved, but it can be said that relatively slow processes are involved. Considerable concentrations of intermediate forms other than T_0 and R_4 are evident from this work. Very fast processes, possibly related to local rearrangements in the heme pocket, have been observed by the technique of laser photolysis.[28]

The various hemoglobins discussed below, as well as the primary structure of human and horse hemoglobin, are listed for reference in Table 2.

The main methods that can be applied to hemoglobin solutions, apart from NMR, deal specifically with the ligand or subunit equilibria or with the electronic state of the heme groups, and the effects of various conditions and agents on these properties. In these categories fall many

TABLE 1

Electron Configurations of the Heme Iron in Various State of Hemoglobin

Oxidation state		Fe^{2+}	Fe^{2+}	Fe^{3+}	Fe^{3+}
Spin state		S = 2	S = 0	S = 5/2	S = 1/2
Electron configuration	$d_{x^2-y^2}$	↑ —	——	↑ —	——
	d_{z^2}	↑ —	——	↑ —	——
	d_{xy}, d_{xz}, d_{yz}	↑ —	↑↓	↑ —	↑ —
		↑ —	↑↓	↑ —	↑↓
		↑↓	↑↓	↑ —	↑↓
T_{1e}		·····	-----	$1 \cdot 10^{-10}$ sec	$2 \cdot 10^{-12}$ sec
Examples		Deoxy Hb	HbO_2 HbCO	Ferri Hb	HbCN HbN_3

T_{1e} = longitudinal electron spin relaxation time.

Adapted from Wüthrich, K., *Struct. Bonding*, 8, 53, 1970.

TABLE 2A

Amino Acid Sequence of Various Hemoglobins and Sperm Whale Myoglobin

The sequence of the α and β chains of human adult hemoglobin, the γ-chain of fetal hemoglobin, and the α and β chains of horse hemoglobin are listed so as to emphasize the homologies between the chains. Sperm whale myoglobin is also listed for comparison. Both commonly used nomenclatures are also cited: (1) that based on the sequential residue number; and (2) that based on the sequential residue number in each α-helix, the helices being denoted as A to H.

Sequential residue number									
Hemoglobin			Helical residue number	α Human	α Horse*	γ Human	β Human	β Horse*	Sperm whale myoglobin
α	β and γ	Myoglobin							
	1		NA 1			Gly	Val		
1	2	1	2	Val		His	His	Gln	Val
2	3	2	3	Leu		Phe	Leu		Leu
3	4	3	A 1	Ser		Thr	Thr	Ser	Ser
4	5	4	2	Pro	Ala	Glu	Pro	Gly	Glu
5	6	5	3	Ala		Glu	Glu		Gly
6	7	6	4	Asp		Asp	Glu		Glu
7	8	7	5	Lys		Lys	Lys		Trp
8	9	8	6	Thr		Ala	Ser	Ala	Gln
9	10	9	7	Asn		Thr	Ala		Leu
10	11	10	8	Val		Ile	Val		Val
11	12	11	9	Lys		Thr	Thr	Leu	Leu
12	13	12	10	Ala		Ser	Ala		His
13	14	13	11	Ala		Leu	Leu		Val
14	15	14	12	Trp		Trp	Trp		Trp
15	16	15	13	Gly	Ser	Gly	Gly	Asp	Ala
16	17	16	14	Lys		Lys	Lys		Lys
17	18	17	15	Val		Val	Val		Val
18		18	16	Gly					Glu
19		19	AB 1	Ala	Gly				Ala
20	19	20	B 1	His		Asn	Asn		Asp

*For horse α- and β-chains only those residues are indicated which are different from the corresponding ones in human hemoglobin.

TABLE 2A (Continued)

Amino Acid Sequence of Various Hemoglobins and Sperm Whale Myoglobin

Sequential residue number									
Hemoglobin									
α	β and γ	Myoglobin	Helical residue number	α Human	α Horse*	γ Human	β Human	β Horse*	Sperm whale myoglobin
21	20	21	2	Ala		Val	Val	Glu	Val
22	21	22	3	Gly		Glu	Asp	Glu	Ala
23	22	23	4	Glu		Asp	Glu		Gly
24	23	24	5	Tyr		Ala	Val		His
25	24	25	6	Gly		Gly	Gly		Gly
26	25	26	7	Ala		Gly	Gly		Gln
27	26	27	8	Glu		Glu	Glu		Asp
28	27	28	9	Ala		Thr	Ala		Ile
29	28	29	10	Leu		Leu	Leu		Leu
30	29	30	11	Glu		Gly	Gly		Ile
31	30	31	12	Arg		Arg	Arg		Arg
32	31	32	13	Met		Leu	Leu		Leu
33	32	33	14	Phe		Leu	Leu		Phe
34	33	34	15	Leu		Val	Val		Lys
35	34	35	16	Ser	Gly	Val	Val		Ser
36	35	36	C 1	Phe		Tyr	Tyr		His
37	36	37	2	Pro		Pro	Pro		Pro
38	37	38	3	Thr		Trp	Trp		Glu
39	38	39	4	Thr		Thr	Thr		Thr
40	39	40	5	Lys		Gln	Glu	Gln	Leu
41	40	41	6	Thr		Arg	Arg		Glu
42	41	42	7	Tyr		Phe	Phe		Lys
43	42	43	CD 1	Phe		Phe	Phe		Phe
44	43	44	2	Pro		Asp	Glu	Asp	Asp
45	44	45	3	His		Ser	Ser		Arg
46	45	46	4	Phe		Phe	Phe		Phe
47	46	47	5	Asp		Gly	Gly		Lys
	47	48	6			Asn	Asp		His
48	48	49	7	Leu		Leu	Leu		Leu
49	49	50	8	Ser		Ser	Ser		Lys
	50	51	D 1			Ser	Thr	Gly	Thr
	51	52	2			Ala	Pro		Glu
	52	53	3			Ser	Asp		Ala
	53	54	4			Ala	Ala		Glu
	54	55	5			Ile	Val		Met
50	55	56	6	His		Met	Met		Lys
51	56	57	7	Gly		Gly	Gly		Ala
52	57	58	E 1	Ser		Asp	Asp	Asn	Ser
53	58	59	2	Ala		Pro	Pro		Glu
54	59	60	3	Gln		Lys	Lys		Asp
55	60	61	4	Val		Val	Val		Leu
56	61	62	5	Lys		Lys	Lys		Lys
57	62	63	6	Gly	Ala	Ala	Ala		Lys
58	63	64	7	His		His	His		His
59	64	65	8	Gly		Gly	Gly		Gly
60	65	66	9	Lys		Lys	Lys		Val
61	66	67	10	Lys		Lys	Lys		Thr

TABLE 2A (Continued)

Amino Acid Sequence of Various Hemoglobins and Sperm Whale Myoglobin

Sequential residue number									
Hemoglobin			Helical residue number	α Human	α Horse*	γ Human	β Human	β Horse*	Sperm whale myoglobin
α	β and γ	Myoglobin							
62	67	68	11	Val		Val	Val		Val
63	68	69	12	Ala		Leu	Leu		Leu
64	69	70	13	Asp		Thr	Gly	His	Thr
65	70	71	14	Ala	Gly	Ser	Ala	Ser	Ala
66	71	72	15	Leu		Leu	Phe		Leu
67	72	73	16	Thr		Gly	Ser	Gly	Gly
68	73	74	17	Asn	Leu	Asp	Asp	Glu	Ala
69	74	75	18	Ala		Ala	Ala	Gly	Ile
70	75	76	19	Val		Ile	Leu	Val	Leu
71	76	77	20	Ala	Gly	Lys	Ala	His	Lys
72	77	78	EF 1	His		His	His		Lys
73	78	79	2	Val	Leu	Leu	Leu		Lys
74	79	80	3	Asp		Asp	Asp		Gly
75	80	81	4	Asp		Asp	Asp	Asn	His
76	81	82	5	Met	Leu	Leu	Leu		His
77	82	83	6	Pro		Lys	Lys		Glu
78	83	84	7	Asn	Gly	Gly	Gly		Ala
79	84	85	8	Ala		Thr	Thr		Glu
80	85	86	F 1	Leu		Phe	Phe		Leu
81	86	87	2	Ser		Ala	Ala		Lys
82	87	88	3	Ala	Asp	Gln	Thr	Ala	Pro
83	88	89	4	Leu		Leu	Leu		Leu
84	89	90	5	Ser		Ser	Ser		Ala
85	90	91	6	Asp		Glu	Glu		Gln
86	91	92	7	Leu		Leu	Leu		Ser
87	92	93	8	His		His	His		His
88	93	94	9	Ala		Cys	Cys		Ala
89	94	95	FG 1	His		Asp	Asp		Thr
90	95	96	2	Lys		Lys	Lys		Lys
91	96	97	3	Leu		Leu	Leu		His
92	97	98	4	Arg		His	His		Lys
93	98	99	5	Val		Val	Val		Ile
94	99	100	G 1	Asn		Asn	Asp		Pro
95	100	101	2	Pro		Pro	Pro		Ile
96	101	102	3	Val		Glu	Glu		Lys
97	102	103	4	Asn		Asn	Asn		Tyr
98	103	104	5	Phe		Phe	Phe		Leu
99	104	105	6	Lys		Lys	Arg		Glu
100	105	106	7	Leu		Leu	Leu		Phe
101	106	107	8	Leu		Leu	Leu		Ile
102	107	108	9	Ser		Gly	Gly		Ser
103	108	109	10	His		Asn	Asp	Asn	Glu
104	109	110	11	Cys		Val	Val		Ala
105	110	111	12	Leu		Leu	Leu		Ile
106	111	112	13	Leu		Val	Val	Ala	Ile
107	112	113	14	Val	Ser	Thr	Cys	Leu	His
108	113	114	15	Thr		Val	Val		Val
109	114	115	16	Leu		Leu	Leu	Val	Leu

TABLE 2A (Continued)

Amino Acid Sequence of Various Hemoglobins and Sperm Whale Myoglobin

Sequential residue number									
Hemoglobin			Helical residue number	α Human	α Horse*	γ Human	β Human	β Horse*	Sperm whale myoglobin
α	β and γ	Myoglobin							
110	115	116	17	Ala		Ala	Ala		His
111	116	117	18	Ala	Val	Ile	His	Arg	Ser
112	117	118	19	His		His	His		Arg
113	118	119	GH 1	Leu		Phe	Phe		His
114	119	120	2	Pro		Gly	Gly		Pro
115	120	121	3	Ala	Asn	Lys	Lys		Gly
116	121	122	4	Glu	Asp	Glu	Glu	Asp	Asn
117	122	123	5	Phe		Phe	Phe		Phe
118	123	124	H 1	Thr		Thr	Thr		Gly
119	124	125	2	Pro		Pro	Pro		Ala
120	125	126	3	Ala		Glu	Pro	Glu	Asp
121	126	127	4	Val		Val	Val	Leu	Ala
122	127	128	5	His		Gln	Glu	Gln	Gln
123	128	129	6	Ala		Ala	Ala		Gly
124	129	130	7	Ser		Ser	Ala	Ser	Ala
125	130	131	8	Leu		Trp	Tyr		Met
126	131	132	9	Asp		Gln	Glu	Gln	Asn
127	132	133	10	Lys		Lys	Lys		Lys
128	133	134	11	Phe		Met	Val		Ala
129	134	135	12	Leu		Val	Val		Leu
130	135	136	13	Ala	Ser	Thr	Ala		Glu
131	136	137	14	Ser		Gly	Gly		Leu
132	137	138	15	Val		Val	Val		Phe
133	138	139	16	Ser		Ala	Ala		Arg
134	139	140	17	Thr		Ser	Asp	Asn	Lys
135	140	141	18	Val		Ala	Ala		Asp
136	141	142	19	Leu		Leu	Leu		Ile
137	142	143	20	Thr		Ser	Ala		Ala
138	143	144	21	Ser		Ser	His		Ala
139	144	145	22	Lys		Arg	Lys		Lys
140	145	146	23	Tyr		Tyr	Tyr		Tyr
141	146	147	24	Arg		His	His		Lys
		148	25						Glu
		149	HC 1						Leu
		150	2						Gly
		151	3						Tyr
		152	4						Gln
		153	5						Gly

Adapted from Antonini, E. and Brunori, M., *Hemoglobin and Myoglobin in Their Reactions with Ligands*, North-Holland Publishing, London, 1971.

TABLE 2B

Amino Acid Changes in Some Mutant Hemoglobins

Hemoglobin	Residue number	Position	Substitution From	Substitution To	Chain	Structural consequences
J Capetown	92	FG 4	Arg	Gln	α	This residue makes Van der Waals contact with Arg C6 of neighboring β chain at an $\alpha_1\beta_2$ interface. A hydrogen bond to the β chain with its guanidinium group may also be formed. Replacement may perturb the transition between R and T states.
Chesapeake	92	FG 4	Arg	Leu	α	Similar effect as in Hb J Capetown.
M Iwate	87	F 8	His	Tyr	α	Replacement of the proximal His (see Figure 12) with a Tyr is thought to lead to a stabilization of Fe^{+++} by means of ionic interactions between the phenol group of Tyr and the Fe cation. In addition, the heme is displaced toward helix E. The conformation remains similar to that of the T state, regardless of the state of ligation of the molecule.
Kansas	102	G 4	Asn	Thr	β	The C^{γ} of Thr may interfere with the vinyl or methyl groups of pyrrol II which would displace either heme or helix. In addition, Thr unlike Asn is unable to form a hydrogen bond with Asp G1 of the α chain, leading to enhanced formation of $\alpha\beta$ dimers.
Kempsey	99	E 1	Asp	Asn	β	Loss of COO^- weakens internal hydrogen bond and alters contact with Val G3 of the α chain.

TABLE 2B (Continued)

Amino Acid Changes in Some Mutant Hemoglobins

Hemoglobin	Residue number	Position	Substitution From	Substitution To	Chain	Structural consequences
M Milwaukee	67	E11	Val	Glu	β	As with Hb M Iwate, the COO^- of Glu forms a salt bridge with the cationic iron. The replacement also forces His E7 away from the heme pocket. (See Figure 12.)
S	6	A 3	Glu	Val	β	Replacement with hydrophobic group near surface of molecule diminishes solubility and leads to filamentous aggregation when deoxygenated.
Sydney	67	E 11	Val	Ala	β	Contact of heme with C^{γ},s of Val is lost. Loosens heme group.
Yakima	99	G 1	Asp	His	β	Hydrogen bond between COO^- of G1 β_1 and NH of Glu G3 β_2 is lost. Hydrogen bond potentially formed by His is weaker, and the His side chain makes an additional contact with Leu G7 of the α_1 chain. A contact with C^{γ} of Val G3α is lost.
Zurich	63	E 7	His	Arg	β	The bulky side chain of Arg cannot be accommodated in the heme pocket. As a result, it protrudes at the surface and leaves a large cavity near the ligand binding site of the iron.

Adapted from Perutz, M. F. and Lehmann, H., *Nature*, 219, 902, 1968; Antonini, E. and Brunori, M., *Hemoglobin and Myoglobin in Their Reactions with Ligands*, North-Holland Publishing, London, 1971.

important kinetic observations. Such methods yield only indirect evidence about conformational states of the dissolved protein. Because of its potential for observing individual resonances and for distinguishing between different structures in solution, the NMR method has been urged into application in the past few years.

The present essay examines the role that nuclear magnetic resonance has played in elucidating the details of hemoglobin form and function. The nuclei which have been studied include ^{1}H, ^{13}C, ^{19}F, ^{31}P, ^{17}O, and ^{35}Cl, although the major portion of the work to date involves ^{1}H and ^{13}C. In a very real sense, the era of magnetic resonance studies of proteins has only begun in the past five to eight years, primarily as a result of the development of pulsed Fourier transform and correlation methodology[29,30] and the enhanced resolution and sensitivity afforded by the introduction of spectrometers with superconducting solenoids, operating at polarizing fields in excess of 52,000 G. Only the nuclear magnetic resonance studies will be examined herein, and only those dealing with hemoglobin; studies utilizing electron paramagnetic resonance are beyond the scope of this review.

For the reader unfamiliar with the nuclear magnetic resonance experiment, the basic concepts are briefly reviewed, as well as those aspects of the theory necessary for an appreciation of the hemoglobin studies. No attempt has been made to present a rigorous mathematical treatment, since many such presentations are available.[31,32] Rather, the emphasis is on the presentation of a conceptual outline punctuated with equations whenever a formal representation of ideas is particularly advantageous. Following the introduction of the theory, the experiments themselves are discussed, segregated as to the nucleus under study. Finally, the various studies are considered in aggregate, and future avenues of investigation into the subtleties of hemoglobin function are examined.

II. THEORY

A. Nuclear Magnetization

In addition to charge and mass, many nuclei in their ground state possess a nonvanishing spin angular momentum, $I\hbar$ (integer or half-integer in units of $\hbar$), which gives rise to a dipolar magnetic moment (μ_N) given by

$$\mu_N = \gamma_N \hbar I, \tag{1}$$

where γ_N is the magnetogyric ratio characteristic of a given nucleus N. All nuclei with odd mass number possess this property; nuclei with even mass number may be either spinless or else possess integral values of the spin quantum number I. In the presence of a static external field H_0, the nuclear magnetic moment interacts with the field, assuming $2I + 1$ spin states characterized by equally spaced (Zeeman) energy levels of energy $\gamma_N \hbar I H_0$. Figure 1 depicts graphically the case of an $I = \frac{1}{2}$ system. The separation energy is given by

$$\Delta E = \gamma_N \hbar H_0 = \frac{\mu_N H_0}{I}, \tag{2}$$

corresponding to a frequency (in Hz)

$$\nu_0 = \frac{\gamma_N H_0}{2\pi}. \tag{3}$$

Thus for a system with $I = \frac{1}{2}$ such as ^{1}H, ^{13}C, ^{31}P, or ^{19}F (Table 3), two energy states are possible, corresponding to having the spin aligned either with or against the static applied field H_0. In reality, perfect alignment of the spins with H_0 is not possible, but rather each magnetic moment precesses about H_0 at the Larmor frequency (ν_0) defined by Equation 3. This precession is quite analogous to that of a gyroscope in a gravitational field. Macroscopically, of course, the net magneti-

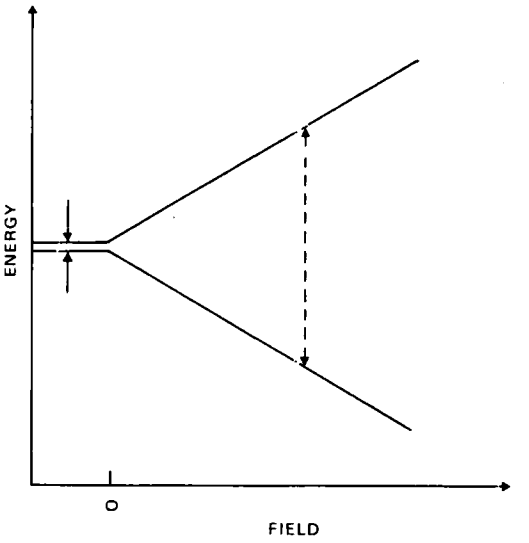

FIGURE 1. Energy level separation for the $I = \frac{1}{2}$ spin system. In the simplest case the field is the static external field H_0. The dashed double arrow symbolizes an energy difference equal to $\gamma \hbar H_0$.

TABLE 3

Physical Constants of Some Typical Magnetic Nuclei

Nucleus	I	γ_N (radians·sec^{-1}·gauss^{-1})	Q ($\times 10^{-24}$ cm^2)	μ(erg·G^{-1})	Relative sensitivity at constant field	Frequency (MHz) for 10 KG field
^{1}H	1/2	26,753	–	2.79268	1.000	42.276
^{2}H	1	4,107	2.74×10^{-2}	0.85738	9.64×10^{-3}	6.5357
^{13}C	1/2	6,728	–	0.70220	1.59×10^{-2}	10.705
^{14}N	1	1,934	7.1×10^{-2}	0.40358	1.01×10^{-3}	3.076
^{15}N	1/2	-2,712	–	-0.28304	1.04×10^{-3}	4.315
^{19}F	1/2	25,179	–	2.6273	8.34×10^{-1}	40.055
^{31}P	1/2	10,840	–	1.1305	6.64×10^{-2}	17.235
^{33}S	3/2	2,054	5.3×10^{-2}	0.64274	2.26×10^{-3}	3.266
^{35}Cl	3/2	2,624	-7.9×10^{-2}	0.82091	4.71×10^{-3}	4.172

zation observed will be coincident with H_0, since in the ensemble average components of the individual magnetic moments not coincident with H_0 will vanish. Moreover, the magnitude of the macroscopic magnetization will be proportional to the excess of spins aligned with H_0, when compared to those opposed to H_0, as given by the Boltzman relationship. Specifically, the populations, P_i, of the spins in the energy levels (F_i) are proportional to exp ($-E_i/kT$). Thus the net magnetization of a sample containing N spins can be shown to be:[32]

$$M = N\gamma\hbar \frac{\sum_{m=-I}^{I} m \exp(\gamma\hbar m H_0/kT)}{\sum_{m=-I}^{I} \exp(\gamma\hbar m H_0/kT)} \quad (4)$$

or, since for nuclear magnetism $\gamma\hbar m H_0/kT$ is very small, a linear expansion of the exponential is permissible, yielding

$$M = \frac{N\gamma^2\hbar^2 I(I+1)}{3kT} H_0 = \chi_0 H_0. \quad (5)$$

The 1/T dependence of the static nuclear magnetic susceptibility (χ_0) is the well-known Curie law. Reference to Figure 2 may help to clarify some of the foregoing points.

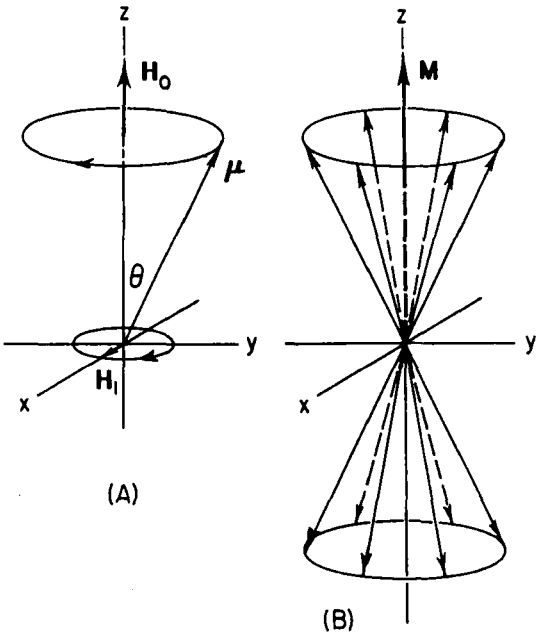

FIGURE 2. A. Precession of a magnetic moment μ about a fixed magnetic field H_0. The radio frequency field H_1 rotates in the xy plane. B. Precession of an ensemble of identical magnetic moments of nuclei with I = ½. The net macroscopic magnetization M is oriented along H_0 and has the equilibrium value M_0.

It should be appreciated that the very small energy separation characteristic of the Zeeman interaction (Equations 2 or 3) constitutes a mixed

blessing for the NMR spectroscopist. It allows the use of radio frequency radiation (~300 MHz or less) to induce transitions between the energy levels necessary for the detection of resonance (see below). Since such radiation is far too weak energetically to induce thermal or electronic transitions, nuclear magnetic resonance is one of the few techniques which allows the observation of a molecule in the complete absence of chemically significant perturbations. Unfortunately, however, the small ΔE of the Zeeman interaction also leads to exceedingly small net macroscopic magnetizations (M, Equations 4 or 5), making detection difficult and demanding large amounts of sample (typically 10^{18} identical nuclear moments). For hemoglobin, this translates to concentrations on the order of 2 to 16 m*M* (in heme), with sample volumes ranging from 0.5 to over 10 ml. Moreover, even at the highest concentrations and sample volumes signal averaging techniques remain necessary, especially for the less sensitive or less abundant isotopes (cf. Table 3).

Detection of the magnetization arising from each set of identical nuclei is accomplished by the application of radio frequency radiation in such a manner that a small magnetic field (H_1) is established rotating in a plane normal to H_0 and at the Larmor frequency of the nucleus of interest (Figure 2A). This rotating H_1 induces rapid transitions between the spin states of that nucleus. The inequality of the populations of the spins in the magnetic energy levels at equilibrium in the applied static magnetic field makes the net absorption of electromagnetic energy greater than the induced emission. Such absorption is detectable by modern electronic and computer techniques. Note that under conditions in which the populations of the spin states are equal, the net magnetization (M) vanishes (cf. Equation 4), and no net absorption can occur. Under such circumstances, the resonance is said to be *saturated.* The process by which the equilibrium population is established is termed *spin-lattice relaxation,* and is characterized by the time constant, T_1. As described below, the measurement of this relaxation time and its mechanistic interpretation offer a powerful means of detecting the thermal motion in the region of the nucleus under observation.

B. Chemical Shift

An inspection of Table 3 reveals the basic resonance frequency at 10 kG of several nuclei of interest for the study of hemoglobin. As shown by Equation 3, this frequency will be linearly dependent on the magnetic field strength H_0. However, if all nuclei of a given type in a molecule resonated at *exactly* the same frequency, nuclear magnetism would be of little use to the chemist. The unique power of the NMR method derives from the fact that a variety of local interactions with surrounding electrons and adjacent nuclear spins will alter the total field acting on any given nucleus. For a simple diamagnetic compound, the origin of these perturbations is primarily twofold: (1) the applied field H_0 induces a Larmor precession of the electronic charges about the nucleus, equivalent to an electric current producing at the nucleus a magnetic field H_d, which opposes H_0, but is proportional to it; (2) the applied H_0 polarizes the electronic cloud about the nucleus, producing an additional magnetic field H_p at the nucleus, which is also proportional to H_0. Thus the resultant field at a given nucleus for a simple diamagnetic compound represents the sum of the above terms:

$$H_{eff} = H_o + H_d + H_p = H_o (1 - \sigma) \quad (6)$$

where σ represents a field-independent shielding constant. Clearly, since the chemical environment of an atom modulates the nature of its electronic configuration, it also affects the precise frequency at which that nucleus will resonate. Hence, σ is termed "chemical shift", and is usually expressed in units of parts per million (ppm).

Other factors may also contribute to or indeed dominate the chemical shift effect. These include the combined effects of diamagnetic and paramagnetic currents on neighboring atoms, electric currents flowing in closed rings of atoms, and nearby paramagnetic centers such as an unpaired electron. These latter contributions are of paramount importance to the ^1H NMR studies of hemoglobin, and are discussed now in greater detail.

C. Ring Current Shifts

The large diamagnetic anisotropies of aromatic molecules have been attributed by Pauling[33] to the circulation of π electrons in the plane of the ring, yielding enhanced diamagnetic susceptibility in a direction perpendicular to the ring (Figure 3). The functional form of the ring current shifts in the case of benzene has been given by Johnson and

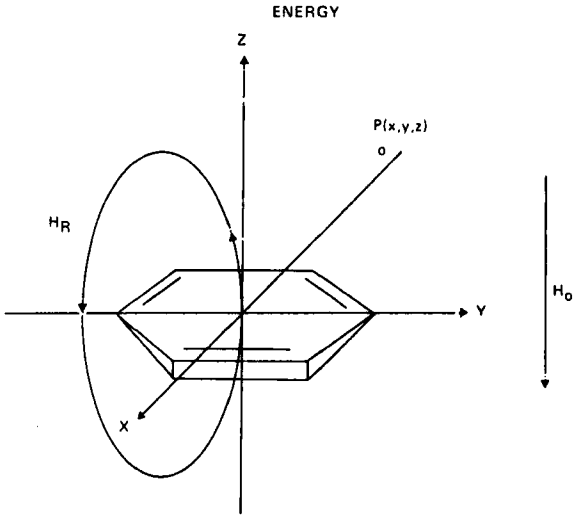

FIGURE 3. The local magnetic ring current field H_R of an aromatic molecule. H_0 is the external polarizing field. The field strength at a point P is determined by the position relative to the aromatic ring and by the size of H_R. H_R depends on the total number of π-electrons in the aromatic molecule. (Redrawn and reprinted from Wüthrich, K., *Struct. Bonding*, 8, 53, 1970. With permission.)

Bovey.[34] For larger conjugated ring systems the ring current shifts may be substantial. The porphyrin ring possesses 18 electrons which may be regarded as circulating in a path embracing 16 or 18 nuclei.[35,36] Appreciable shielding and deshielding contributions to the ring protons result, as indicated by numerous ^{1}H NMR studies of different isolated porphyrins.[37-40] Calculations attempting to predict these shifts accurately on theoretical grounds have been in only qualitative agreement.[37,41] For the case of the porphyrins, Shulman et al.[42] have developed an approximation of the Johnson and Bovey treatment,[34] with empirically derived parameters, which has proved useful in assigning the observed ring current shifted resonances in ^{1}H NMR studies of hemeproteins. In this treatment, the position of a resonance arising from atom i is shifted by ring j with unit normal vector $\check{n}_j$ an amount (in ppm) $\Delta\delta_{ij}$:

$$\Delta\delta_{ij} = D_j \frac{3(r_{ij}\cos\theta + Z_j)^2/(r_{ij} + Z_j)^2 - 1}{r_{ij}^3 + R_j^3}, \qquad (7)$$

where $r_{ij} = |\check{r}_i - \check{r}_j|$, $\cos\theta = (\check{r}_i - \check{r}_j)\cdot\check{n}_j/r_{ij}$, and D_j, Z_j, and R_j are empirical constants, the values of

TABLE 4

Parameters Used to Describe Ring-current Shifts

Ring	D	Z	R
Porphyrin	305.0	6.0	4.0
Tryptophan	19.7	1.84	1.22
Tyrosine and phenylalanine	10.0	1.5	1.0

From Shulman, R. G., Wüthrich, K., Yamane, T., Patel, D. J., and Blumberg, W. E., *J. Mol. Biol.*, 53, 143, 1970. With permission.

which as used by Shulman et al.[42] are given in Table 4. Figure 4[42] shows a plot of the predicted behavior of the ring current shifts of protons about a porphyrin ring, calculated on the bases of Equation 7 and Table 4. The great sensitivity of the chemical shift of nearby protons to their geometry about the ring is apparent.

D. Paramagnetic Phenomena

Under certain conditions, the electronic configuration of the iron of the porphyrin ring in hemoglobin is such that one or more unpaired electrons is produced. These conditions are detailed in Table 1. The presence of an unpaired electron has marked consequences upon the NMR spectrum of compounds containing such paramagnetic centers. The magnetic field produced at the nucleus of a nearby atom due to an unpaired spin can potentially be larger than the applied static field H_0 itself,[32] reducing the nuclear Zeeman coupling (Equation 2) to negligible significance. However, if the lifetime of the electron spin in a given state becomes very short, then only the average value of its magnetization will be apparent to nearby nuclei. This average value will be proportional to the relative populations of the electronic spin states aligned either along or against H_0. The magnitude of this observable magnetization is controlled by a relation analogous to that given by Equation 5. As such, one expects the chemical shift of nuclei under the influence of unpaired electron spins to be proportional to the inverse of temperature, and indeed it is by this criterion that such "hyperfine" shifts are distinguished. Included are primarily two distinct interactions: a scalar coupling of the nuclear and electronic spins mediated by the σ and π molecular

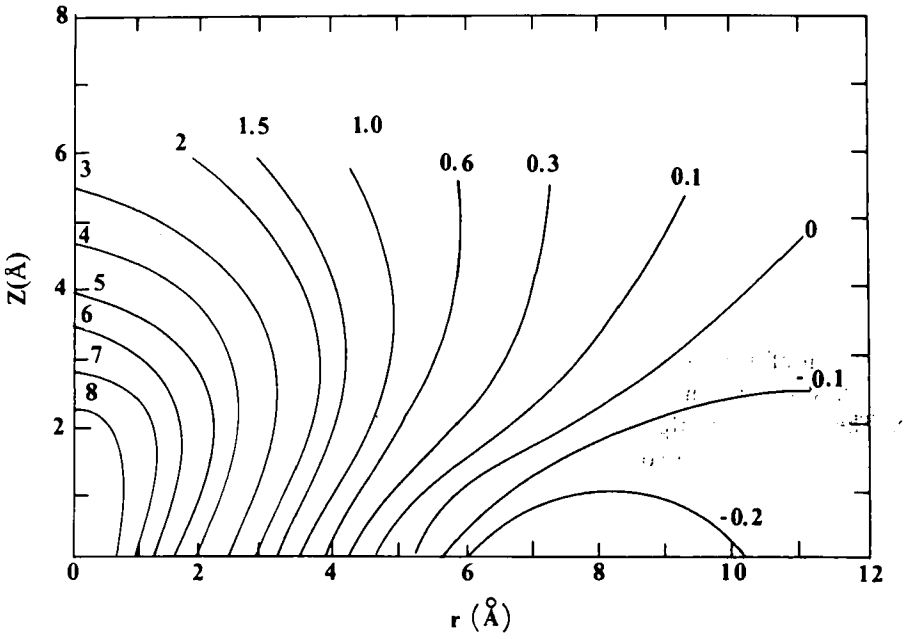

FIGURE 4. Plots of contours of equal ring-current shifts computed by Shulman et al.[42] The coordinates Z and r refer to the distances perpendicular to the plane of the ring and outward in the plane of the ring, respectively. (Redrawn and reprinted from Shulman, R. G., Wüthrich, K., Yamane, T., Patel, D. J., and Blumberg, W. E., *J. Mol. Biol.*, 53, 143, 1970. With permission.)

orbitals; and a dipolar (through space) coupling of the nuclear moments with electrons possessing anisotropic g-tensors.* The former of these is termed the Fermi hyperfine contact shift, while the latter phenomenon is called the pseudocontact shift.

For systems with isotropic g-tensors the expected contact shift in ppm is given by:[43]

$$\Delta\sigma_c = \frac{\Delta\nu_c}{\nu_0} = \frac{A\,\gamma e\,S\,(S+1)}{\gamma_N\,3kT}, \qquad (8)$$

where A is the contact interaction constant characteristic of a given nucleus, S is the total electronic spin, γe is the electron magnetogyric ratio, ν_0 is the Larmor frequency of nucleus N, and T is the absolute temperature. The calculation of the contact shift in systems with anisotropic g-tensors is considerably more involved,[44] although such considerations are necessary to describe properly the hyperfine interactions in iron-porphyrin complexes.[45,46] An examination of the details of such a treatment for azido ferrihemoglobin has been made by Wüthrich.[25] An interesting result of such a treatment is that the hyperfine coupling constant A itself turns out to be temperature dependent.

The pseudocontact shift, $\Delta\delta_{pc}$ (in ppm) is most appropriately expressed for hemoglobin, where rotational tumbling is slow and electron relaxation fast, as:[46]

$$\Delta\delta_{pc} = CK\left\{[g_z^2 - \tfrac{1}{2}(g_x^2 + g_y^2)]\,(1 - 3\cos^2\Omega) + 3/2\,(g_y^2 - g_x^2)\sin^2\Omega\cos 2\Psi\right\}, \qquad (9)$$

where Ω is the polar angle of the radius vector $\check{r}$ from the electron spin to the nucleus, and ψ is the angle between the projection of $\check{r}$ in the xy plane and the x axis. K is a reduction factor for the unpaired spin localized on the metal, while C is given by:

$$C = \frac{\beta^2\,S\,(S+1)}{9\,k\,T\,r^3}, \qquad (10)$$

β is the Bohr magneton. Note that anisotropy of the g-tensor is required in order to have a nonvanishing pseudocontact contribution to the chemical shift, and that the psuedocontact term

*An anisotropic g-tensor for an electron indicates that its magnetic susceptibility is different depending upon its orientation with respect to H_o.

should attenuate outside the immediate vicinity of the unpaired spin due to the r^{-3} dependence.

E. Nuclear Spin-spin Coupling

In analogy with the interaction of the electron and nuclear spins discussed above, nuclear spin-spin interactions also can perturb the observed spectrum. The longer relaxation time of nuclear spins generally precludes an averaging of the resultant magnetic field so that the additional field contributed by the spin of a given nucleus may be either added to or substracted from the local fields at nearby nuclei. The resulting multiplicity of local magnetic environments results in a corresponding multiplicity of resonance lines for each nucleus so perturbed. The mechanism of spin-spin coupling may generally take two forms. Potentially the stronger is through space dipolar coupling, similar to the pseudocontact interaction discussed above. Such coupling is not normally observed for small molecules in solution, since rapid thermal motions effectively nullify the observable dipolar field. However, the motional restriction characteristic of proteins conceivably may limit such averaging, resulting in a substantially more complicated spectrum.

The other form of spin-spin coupling is encountered in practice and represents a scalar interaction mediated by way of the electrons intervening between two nuclei. This interaction occurs by slight polarizations of the spins and orbital motions of the valence electrons, and is not affected by thermal motion nor the external applied field. The result is again a multiplicity of local magnetic environments.

Two interacting nuclei may be *spin decoupled* if one of the nuclei is forced by the application of an external radio frequency field at the appropriate frequency to undergo rapid transitions between energy levels, leading to saturation. The effect on the observed spectrum is a collapse of the multiplet structure, and an *Overhauser enhancement* of the resonances undergoing dipolar relaxation as a result of the nuclear spin-spin coupling. Such a technique is most commonly employed in ^{13}C NMR to remove multiplicity due to heteronuclear ^{13}C-^{1}H spin-spin couplings. The *nuclear Overhauser enhancement* factor (NOE) has been shown to be independent of the number of coupled nuclei involved in the dipolar relaxation mechanism (see below), and is proportional to the magnetogyric ratios and transition probabilities describing the two spin systems. For carbon and hydrogen, this NOE factor becomes[47]

$$X = 1 + \eta$$

where

$$\eta = \frac{\gamma_{1_H}}{\gamma_{13_C}} \left[\frac{W_2 - W_o}{W_2 + 2W_1 + W_o + 2W_1^*} \right] \tag{11}$$

where W_1^* represents transition probabilities related to nondipolar relaxation mechanisms and the remaining W terms refer to dipolar-related transition probabilities. For ^{13}C-^{1}H dipolar relaxation, X may range from a maximal value of 2.988 to 1.153,[47,48] primarily as a function of the rate of molecular reorientation.

F. Nuclear Spin Relaxation

As previously alluded to, the phenomenon of spin relaxation is of primary importance to the study of nuclear magnetism, and a considerable wealth of literature has accumulated describing the various mechanisms involved.[29,31,32,49] Such mechanisms are manifold, and include paramagnetic relaxation, nuclear magnetic dipole-dipole, spin-rotation, chemical shift anisotropy, quadrupolar, and scalar coupling mechanisms. Of primary interest to the study of hemoglobin are paramagnetic relaxation and nuclear magnetic dipole-dipole relaxation. The present discussion will therefore be limited to these mechanisms.

Generally, two time constants are used to characterize the relaxation behavior of a given nucleus, T_1 and T_2, the *spin-lattice* and *spin-spin* relaxation times, respectively. To gain an intuitive appreciation of the significance of these terms, a slightly different conceptualization of the resonance experiment from that presented above will prove useful. Instead of viewing the applied radio frequency field (H_1) as inducing transitions between the Zeeman levels, one can with equal validity[32] view the effect to be a tipping of the magnetization, such that nonvanishing components appear in the x–y plane. Reference to Figures 2 and 5 should clarify this scheme. Transfer of energy from the nuclear spins to the surrounding "lattice" (spin-lattice relaxation) leads to a net decrease in the absolute magnitude of the x–y projection of each nuclear. moment, and hence to a loss of detected signal (detection being

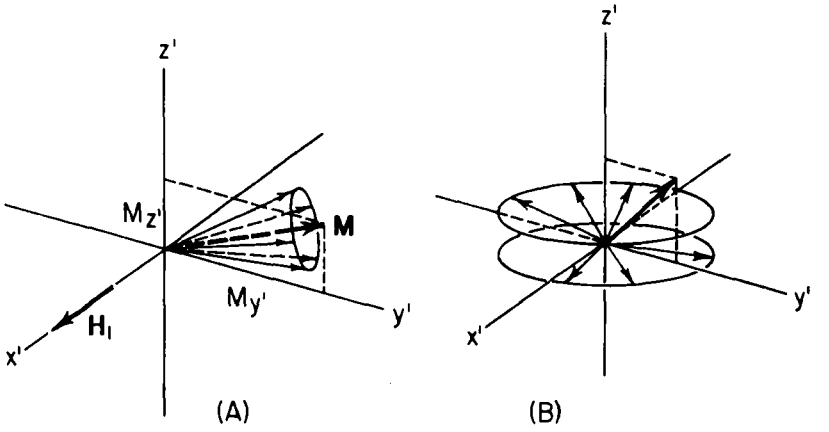

FIGURE 5. A. Tipping of nuclear moments and macroscopic magnetization through an angle and establishment of M y'. B. Dephasing of nuclear moments with reduction of M y'.

by means of a receiver coil sensitive to transient magnetic fields in the x–y plane). Since any energy transfer is basically a resonance phenomenon, only those motions of the surrounding "lattice" which have frequency components near the Larmor frequency of the nucleus of interest will be effective in promoting T_1 relaxation.

Conversely, the lifetime of the observed magnetization in the x–y plane may be limited by a dephasing of the nuclear moments, most commonly by the adiabatic exchange of spin energy directly between two neighboring identical nuclei. Since such spin-spin exchange does not require the thermal motion to have frequencies corresponding to a "resonance," T_2 relaxation will be sensitive to slower components of molecular motion, as well as to static inhomogeneities in H_0.

Both relaxation processes are lifetime-limiting perturbations upon the observed resonance. By the Heisenberg uncertainty principle,

$$\Delta E \Delta t \geq \hbar \tag{12}$$

where ΔE and Δt are the uncertainties in the measurement of energy and time, respectively. Hence, diminished lifetime of a spin state enhances the uncertainty in its precise Larmor frequency (Equation 3), a fact reflected by the increased line width of resonances with short relaxation times. Since $T_2 \leq T_1$,[32] the expected line width at half-height may be expressed as:

$$\Delta\nu = \frac{1}{\pi T_2^*}, \tag{13}$$

where T_2^* represents an apparent T_2 and may include contributions from all factors affecting the line width.

Two factors may be of particular importance in determining the line width: the presence of an unpaired spin and chemical exchange. The latter will be discussed below. In general, for dipolar (or paramagnetic) relaxation due to interactions with spin S, where S may represent either a nuclear or electronic spin, $\frac{1}{T_2}$ may be described for nucleus N of spin I as:[50]

$$\frac{1}{T_{2_N}} = \frac{S(S+1)\gamma_I^2\gamma_S^2\hbar^2}{15\, r^6}\left[4\tau_{c1} + \frac{\tau_{c_2}}{1+(\omega_I-\omega_S)^2\tau_{c_2}^2} + \frac{3\tau_{c1}}{1+\omega_I^2\tau_{c1}^2} + \frac{6\tau_{c2}}{1+\omega_S^2\tau_{c2}^2} + \frac{6\tau_{c2}}{1+(\omega_I+\omega_S)^2\tau_{c2}^2}\right] \tag{14}$$

The corresponding equation for $\frac{1}{T_1}$, the inverse of the spin-lattice relaxation time is:

$$\frac{1}{T_{1_N}} = \frac{2S(S+1)\gamma_I^2\gamma_S^2\hbar^2}{15\, r^6}\left[\frac{\tau_{c2}}{1+(\omega_I-\omega_S)^2\tau_{c2}^2} + \frac{3\tau_{c1}}{1+\omega_I^2\tau_{c1}^2} + \frac{6\tau_{c2}}{1+(\omega_I+\omega_S)^2\tau_{c2}^2}\right], \tag{15}$$

where r is the distance between the spins and ω_i is the Larmor frequency of spin i. The terms $\tau_{c_1}^{-1}$ and $\tau_{c_2}^{-1}$ are the effective correlation times of the coupled magnetic moment vectors given by (neglecting the effects of exchange):

$$\frac{1}{\tau_{c1}} = \frac{1}{T_{1s}} + \sum_i \frac{1}{\tau_i}\,;\quad \frac{1}{\tau_{c2}} = \frac{1}{T_{2s}} + \sum_i \frac{1}{\tau_i}\,, \qquad (16)$$

where T_{1s}^{-1} and T_{2s}^{-1} refer to the relaxation times of the perturbing spin and the summation over τ_i^{-1} represents the contributions of the different motional components. The above equations are valid for paramagnetic relaxation due to a total electronic spin S or for dipolar relaxation of ^{13}C nuclei due to dipolar interaction with adjacent protons in proton decoupled experiments.[48,50] In the "extreme narrowing" limit, where τ_{c_2} and τ_{c_1} become equal ($T_{1s}^{-1} = T_{2s}^{-1}$) and so small that their contribution to the denominator in Equations 14 and 15 is negligible, a simplified form in terms of an effective correlation time, τ_{eff}, is appropriate:

$$\frac{1}{T_{1N}} = \frac{1}{T_{2N}} = \frac{4\,S(S+1)\gamma_I^2\gamma_S^2\hbar^2}{3\,r^6}\,\tau_{eff}. \qquad (17)$$

The general features of the above Equations 14, 15, and 17 are perhaps best illustrated in Figure 6. At small values of τ_c, characteristically less than about 10^{-10} sec for ^{13}C nuclei at 14.1 kG, Equation 17 is appropriate. At longer values of τ_c, T_1 passes through a minimum, while T_2 assymptotically approaches values characteristic of those in the solid state. Thus for diamagnetic hemoglobin, where the rotational correlation time for the molecule as a whole is on the order of 10^{-8} sec,[51] most nuclear magnetic resonance studies on nuclei undergoing dipolar relaxation will be characterized by T_1 values near the minimum of a curve as shown in Figure 6. For paramagnetic hemoglobin the relaxation time of the unpaired electron is often very short ($T_{1e} < 10^{-12}$ sec, Table 1), and hence Equation 17 may be valid for nuclei near the heme.

G. Chemical Exchange

When a given nucleus can exist in two or more different magnetic environments, pronounced effects on the observed magnetic resonance spectrum may ensue. For the sake of the present discussion, only the case of two-site exchange will be illustrated, although general treatments have appeared. Johnson has provided an excellent review of the study of rate processes by NMR with a more thorough discussion of the different approaches.[52]

A particularly straightforward treatment of exchange effects in the absence of spin-spin coupling is that of Gutowsky et al.[53] If the

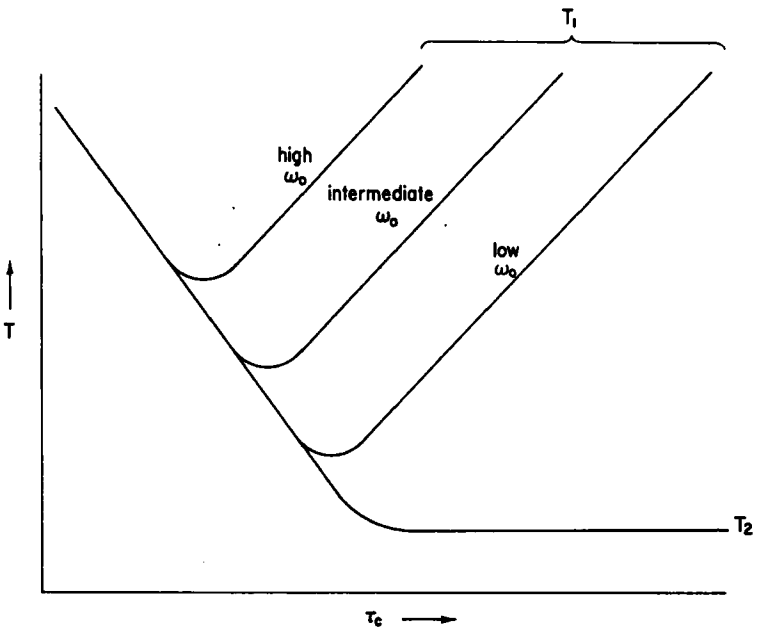

FIGURE 6. Relaxation times are plotted against correlation times for various field strengths expressed in terms of resonant frequencies. The correlation time, τ_c, can be replaced by an effective value, τ_{eff} as explained in the text.

exchange rate between two magnetic environments, characterized by respective Larmor frequencies (in radians/sec) ω_i and ω_j, is sufficiently slow such that

$$\omega_i - \omega_j >> \frac{1}{T_{2i}} + \frac{1}{\tau_i P_j} \; ; \; \tau_i P_j = \tau_j P_i, \tag{18}$$

then the two resonances will be observed. In Equation 18, τ_i or τ_j refers to the mean lifetime (in sec) of the nucleus in either state i or state j, and is related to the first order dissociation rate constant k_i (in sec^{-1}) as:

$$k_i = \tau_i^{-1} \tag{19}$$

P_i (or P_j) refers to the fractional population of site i (or j). In the limiting case each resonance (i) is Lorentzian in shape with a width (in Hz) at half-height given by:

$$(\Delta\nu_i)_{1/2} = \frac{1}{\pi T_{2i}} + \frac{1}{\pi\tau_i}. \tag{20}$$

From Equations 18 and 20 it is evident that if the two resonances are unequally populated, the weaker one will be the more broadened.

Conversely, in the case of fast exchange only a single resonance is observed. This condition obtains when exchange is so rapid that the individual resonance lines have coalesced, and

$$\omega_i - \omega_j << \frac{1}{T_{2i}} + \frac{1}{\tau_i P_j} \text{ for all i and j.} \tag{21}$$

At the highest exchange rates, the *exchange narrowed* condition, the signal is centered at an average frequency

$$\nu_\delta = P_A \nu_A + P_B \nu_B, \tag{22}$$

with a line width of:

$$(\Delta\nu)_{1/2} = \frac{1}{\pi T_2'} \; ; \; \frac{1}{T_2'} = \frac{P_i}{T_{2i}} + \frac{P_j}{T_{2j}}. \tag{23}$$

If exchange is fast enough to coalesce the signals, but slow enough to contribute to the broadening, the line width may be estimated by means of the following approximation:[35]

$$\frac{1}{T_2''} = \frac{1}{T_2'} + P_i^2 P_j^2 \, (\omega_i - \omega_j)^2 \, (\tau_i + \tau_j), \tag{24}$$

where the last term represents the excess broadening due to slow exchange.

A consideration of the above points should give the reader some appreciation for both the strengths and weaknesses of the NMR method. The method requires relatively large amounts of material, and even then its sensitivity is marginal for many nuclei, requiring many hours of signal averaging to obtain usable spectra. However, its discriminatory power is second only to X-ray crystallography. Under certain favorable circumstances, NMR may prove to be the more finely attuned to small conformational or chemical changes. Moreover, the electronic state of the iron, as well as rate processes and thermal motion at specific sites throughout the protein, may be sampled.

III. EXPERIMENTAL

A. ^{1}H NMR Studies of Hemoglobins

Up to the present, much the greater part of the NMR work on hemoglobins has been concerned with the ^{1}H nucleus. Because of the large number of hydrogen atoms incorporated in the protein, spectral overlap is severe. Pioneering studies on the utility of ^{1}H NMR for the analysis of proteins[54-57] were hindered by the low polarizing fields then available (40 to 60 MHz for ^{1}H) as well as low signal-to-noise ratios. The spectra obtained during this period were comprised largely of unresolved envelopes. With the introduction of spectrometers operating with much greater polarizing fields as well as of signal enhancement techniques, progress has been made in resolving the signals of many single protons or small groups of protons. Typically the best resolved signals have their origin in resonances shifted out from the envelopes by hyperfine interactions or ring current effects that are particularly strong in the neighborhood of a heme ring. Information is thereby provided both about the heme groups themselves and about nearby nuclei of the protein moiety. The protein structures so visualized, furthermore, bear different relations to the heme in different protein conformations. Conversely, the different ligand states responsible for differing paramagnetic behavior of the heme are themselves associated with preferred conformational states of the protein.

The proton possesses many properties that make it attractive for study. Its high magnetogyric ratio (Table 3), as well as an essentially 100% isotopic natural abundance, facilitate detection,

allowing single proton resonances to be readily observed even in hemoglobin solutions near 1 m*M* in heme. Moreover, the proton plays an essential role in determining the ligand binding behavior of hemoglobin (the Bohr effect), and hence one might hope that direct observation of this nucleus could yield information relevant to such events. Unfortunately, the chemical shift range of the proton is among the smallest, and its high abundance in the protein yields a large number of neighboring nuclei with the potential for dipolar or scalar couplings. When combined with line widths characteristically on the order of 10 to 40 Hz,[58,59] it can be appreciated that the majority of the approximately 3,500 protons in a hemoglobin molecule will not be resolved.

Thus, the oxidation state of the iron and the nature of its ligand become primary factors in modulating the utility of ^{1}H NMR for the study of hemoglobin. When the iron possesses no spin, as in oxyhemoglobin (Table 1), hyperfine shifts are absent and few individual resonances are discernible. Conversely, numerous single proton hyperfine shifted resonances are clearly observed with cyanoferrihemoglobin or deoxyhemoglobin. Hyperfine shifted resonances are also observed in ferrihemoglobin, although their line width is broader due to the slower electron spin relaxation characteristic of this species.

For these reasons, the discussion of proton studies which follows has been segregated on the basis of the heme state. Such a division is useful for descriptive purposes, but should not obscure the fact that all of the studies are measuring basically the same molecule, undergoing what usually can be described to a first approximation as a single concerted conformational change in response to appropriate perturbations of its chemical environment. The paramagnetic hemoglobin states will be examined first, followed by those hemoglobin states with zero electron spin.

1. Cyanoferrihemoglobin

A typical ^{1}H NMR spectrum of the cyanide derivative of ferric human adult hemoglobin (Fe^{3+}, S,= ½) is shown in Figure 7.[25] The spectral region from 0 to approximately −10 ppm relative to the internal standard sodium 2,2- dimethyl-2-silapentane-5-sulfonate (DSS) consists of strongly

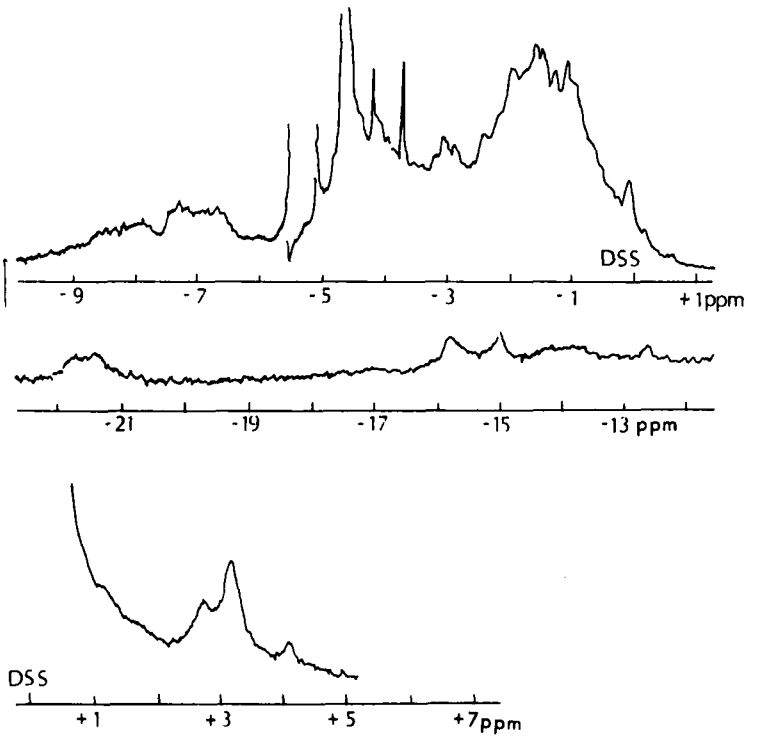

FIGURE 7. Proton NMR spectrum at 220 *M*Hz of human cyanoferrihemoglobin at 36°. (Redrawn and reprinted from Wüthrich, K., *Struct. Bonding*, 8, 53, 1970. With permission.)

overlapping resonances arising from the majority of the protons in the molecule. While some useful differences between the different states of hemoglobin are detectable in this region,[59-61] particularly for the "aromatic resonances" from -6 to -9 ppm, detailed interpretation of most of these changes is not possible. In the region below -10 ppm and in the spectral region above 0 ppm, depicted at increased gain in the middle and bottom tracings of Figure 7, a series of well-resolved lines is apparent. These resonances, removed from the "diamagnetic" envelope so prominent in the top tracing, primarily represent the hyperfine shifted protons, together with a few shifted by ring current effects.

A comparison of the upfield and downfield regions of the spectrum of cyanoferrihemoglobin A with those of the isolated cyanoferri chains is shown in Figure 8, parts a, c, and e.[62] Also shown in Figure 8b and 8d are the spectra of two valency hybrid hemoglobins discussed below. The spectra of Figure 8 have much better signal-to-noise than the one shown in Figure 7, clear peaks being resolved where there were only broad suggestions of resonances in Figure 7. The pattern of resonances present in $Hb^{III}CN$ corresponds approxi-

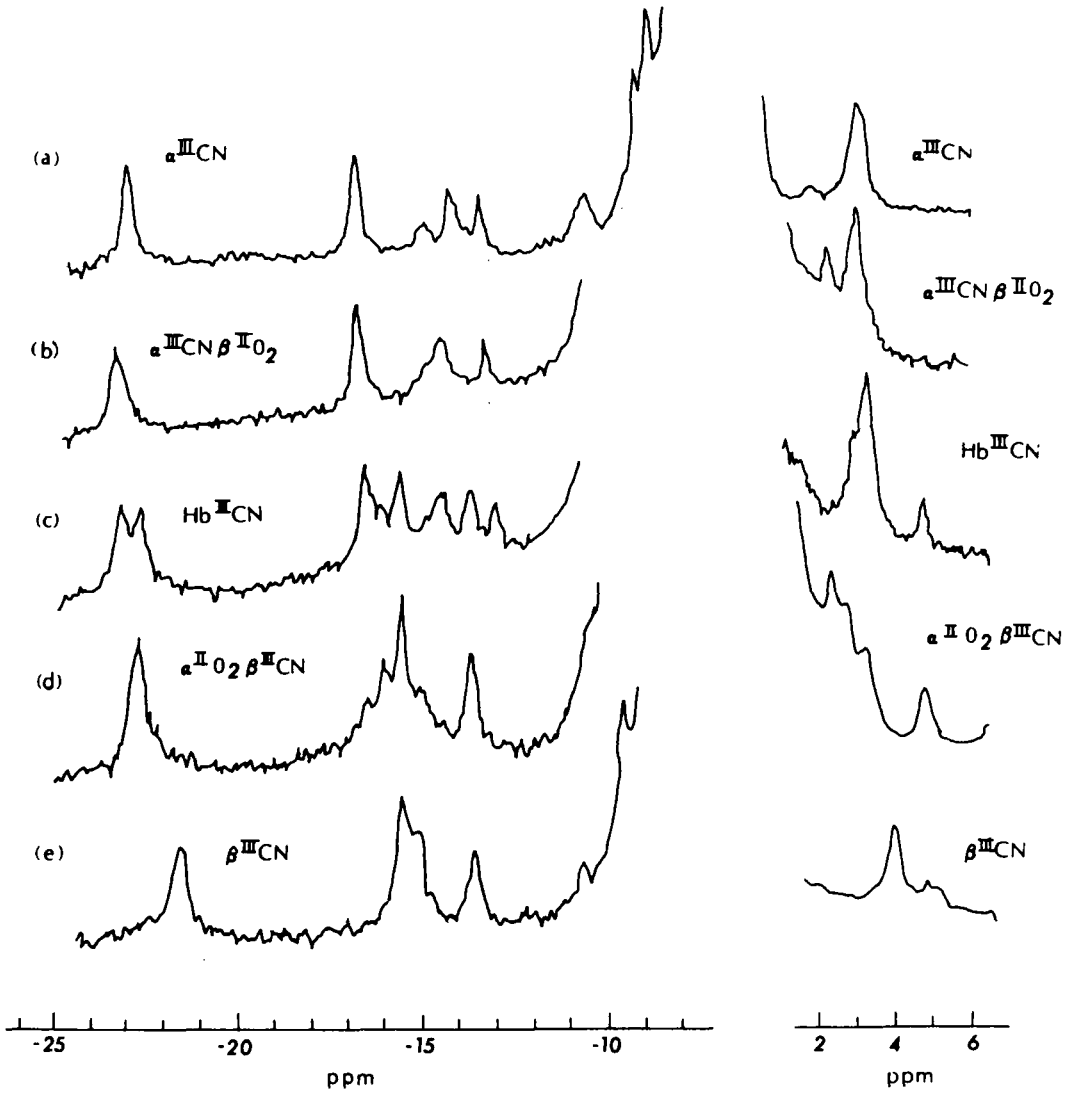

FIGURE 8. Proton NMR spectra of fully ligated hemoglobins at pH 6.6 in 0.1 *M* phosphate buffer in D_2O at 20°. The Hb^{III} CN was not rigorously stripped. Chemical shifts are shown relative to TMS. (Redrawn and reprinted from Ogawa, S., Shulman, R. G., Fujiwara, M., and Yamane, T., *J. Mol. Biol.*, 70, 301, 1972. With permission.)

mately to the superposition of the spectra of the isolated α and β cyanoferri chains, although the exact resonance positions differ slightly between the chains and the tetramer. The assignment of these resonances to specific protons within the protein has proved to be a problem of considerable magnitude.

By the criterion of their temperature dependence (Equations 8 and 9 and Figure 9),[63] all resonances clearly shown in Figure 8 may be ascribed to hyperfine interactions. Initial reports[58] suggested that pseudocontact contributions to these shifts were negligible, and hence the protons responsible for the observed resonances must be situated either on the heme itself (Figure 10) or on the proximal (F8) histidine, no other protons being so closely linked by a series of covalent bonds to the paramagnetic iron. However, theoretical calculations indicated that the pseudocontact interactions probably were not negligible.[46] Proof of this came when the measurements were repeated using H_2O rather than D_2O, first on cyanoferrimyoglobin[64] and then cyanoferrihemoglobin.[63] These measurements revealed several new hyperfine shifted resonances which were attributable to exchangeable protons and which in D_2O had been unobserved due to replacement with deuterium. With these new resonances included, more resonances were found to be shifted by hyperfine interactions than could

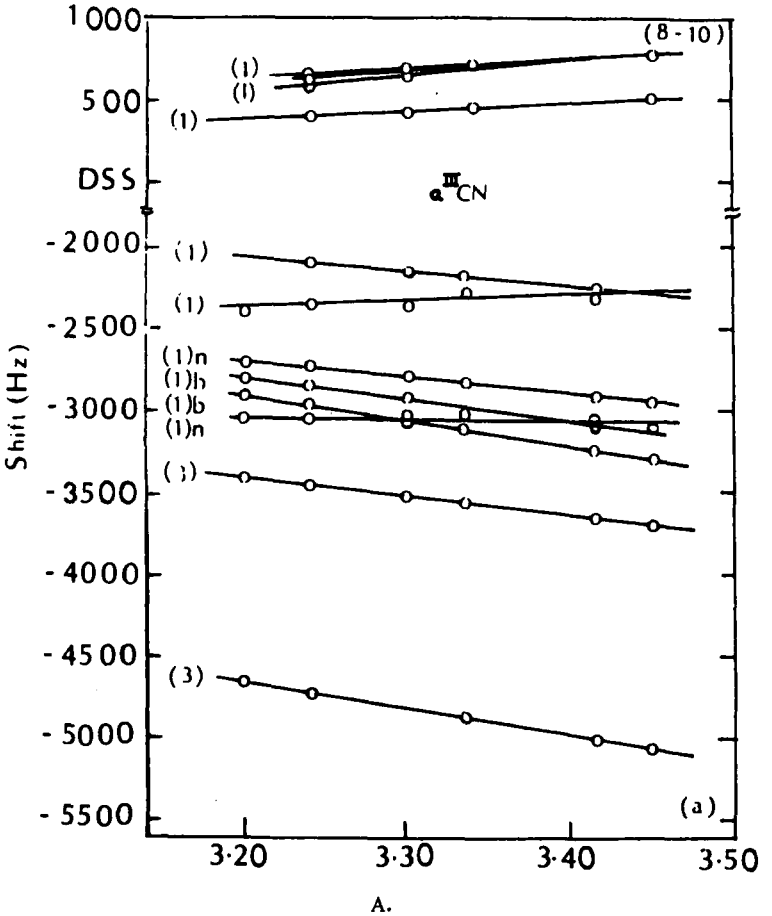

FIGURE 9. A. Temperature dependences of the shifted resonance lines of the α^{III} CN chains at pH 6.6, 0.1 *M* phosphate buffer in D_2O. The numbers in parentheses are the intensities in number of protons per heme. The letters b and n correspond to relatively broad and narrow resonance lines, as described in Ogawa et al.[63] B. Corresponding results from the same publication under comparable conditions for the β^{III} CN chains. (Redrawn and reprinted from Ogawa, S., Shulman, R. G., and Yamane, T., *J. Mol. Biol.*, 70, 291, 1972, With permission.)

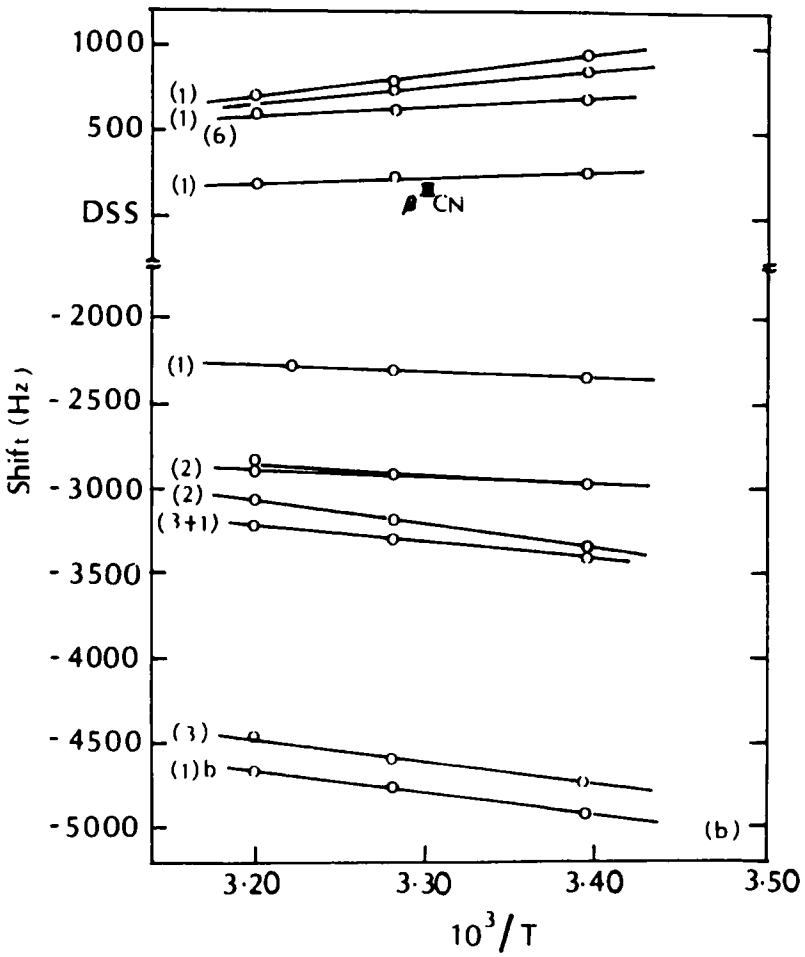

FIGURE 9B.

be accounted for by the protons on the heme alone.

A comparison of the spectra of the isolated α and β cyanoferri chains in both D_2O and H_2O is shown in Figure 11.[63] For the hemoglobin α^{III}CN chains, in the region below -12 ppm, two temperature-dependent peaks were found at -21.9 ppm and -13.5 ppm at 20° in H_2O, which were not present in D_2O, while for the β^{III}CN chain, only one such additional peak was clearly observed at -22.8 ppm in H_2O. In cyanoferric myoglobin, three additional peaks are observed in this region in H_2O and have been assigned[64] to the $N^{\delta}H$ and the peptide NH protons of the proximal histidine (F8) and the $N^{\epsilon}H$ proton of the distal histidine (E7). Thus by analogy, the peak at -13.5 ppm in the α^{III}CN and in water is assigned to the peptide NH proton of the proximal histidine (F8). The resonances at -21.9 ppm and -22.8 ppm for the α^{III}CN and β^{III}CN chains, respectively, are similarly assigned to the $N^{\delta}H$ proton of the proximal histidine. The relationship of these residues to the heme iron in the α and β chains is shown in Figure 12 which is based upon the coordinates determined by Perutz for horse oxyhemoglobin.[5,65]

Also shown in Figure 12 are several other residues which fall within 6 Å from the iron. Due to the $1/r^3$ dependence of the pseudocontact interaction (Equation 10) protons further away than 6 to 10 Å are not expected to be significantly perturbed by the heme spin state. It is clear, however, that even within 6 Å many candidates remain for assigning the nonexchangeable hyperfine shifted resonances of Figure 8. On the basis of their areas, the large resonances below -15 ppm probably represent methyl groups.[58,62,63] A recent study of cyanoferrimyoglobin utilizing

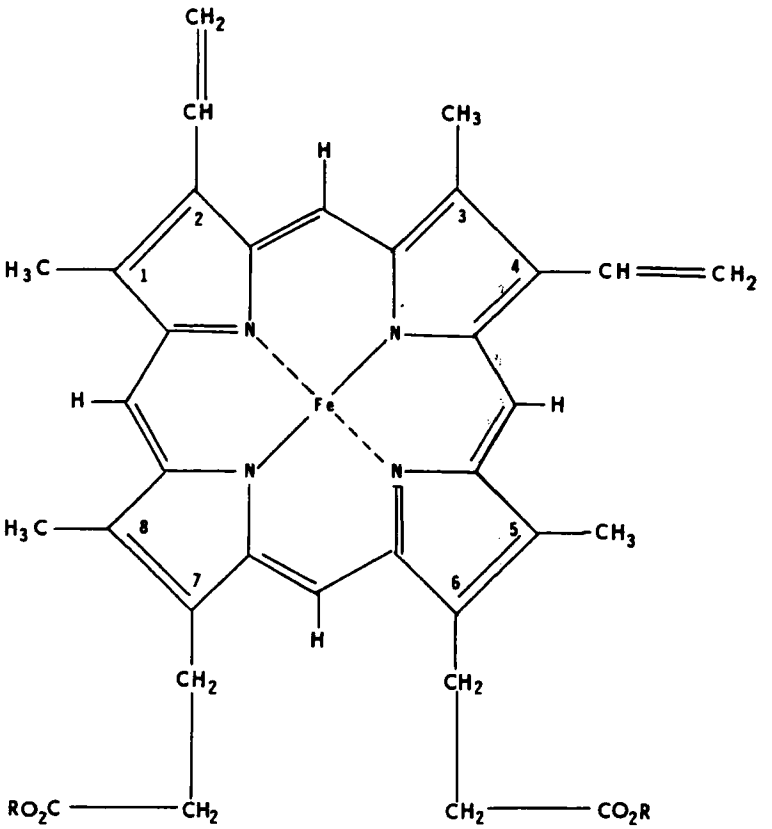

FIGURE 10. Heme group viewed from the proximal side, i.e., from the side of the histidine directly coordinated to the iron.

selectively deuterated poryphyrin groups has demonstrated the occurrence of the 1, 5, and 8 ring methyl (Figure 10) resonances at -18, -28, and -13 ppm, respectively, at 31°.[66] By analogy, the large 3-proton resonances observed in cyanoferrihemoglobin near -15 to -17 ppm and -22 to -25 ppm may be ascribed to porphyrin ring methyl groups. More specific assignments must await the completion of experiments with hemoglobin utilizing selectively deuterated prophyrins.

The resonances in the region -10 to -15 ppm, by the criterion of their area, represent primarily single proton resonances. Again Figure 12 is useful for determining potential assignments of these resonances. Based on semitheoretical considerations, the most likely candidates for these resonances would include the methylene groups of the propionates or the vinyl CH protons (Figure 10), or again, the proximal and distal histidine CHs and protons of the amino acid residues close to the heme plane, such as Phe CD 1.[63]

Similarly, the large upfield resonance near +3 ppm, a single peak in both the cyanoferri α and β chains but multiple in the tetramer, represents some methyl group. Again based on theoretical considerations and current knowledge of the anisotropy of the g-factor in cyanoferrihemoglobin, three equally likely assignments were arrived at.[62,63] These residues, all at the periphery of the heme plane, were the methyl groups of FG3 Leu, F4 Leu, and G8 Leu (Figure 12).

Regardless of the precise assignments which ultimately will be worked out, the study of changes in the pattern of hyperfine shifted resonances has proved to be a useful and sensitive marker monitoring the quaternary transitions essential to hemoglobin function.

As already mentioned and as shown in Figure 8, small changes in the observed spectrum of each chain occur upon formation of the tetramer. These changes have been interpreted[62,67] to represent small conformational adjustments in the environment of the heme groups upon tetramer formation. Although not illustrated here, the observed spectra are also quite sensitive to the presence or

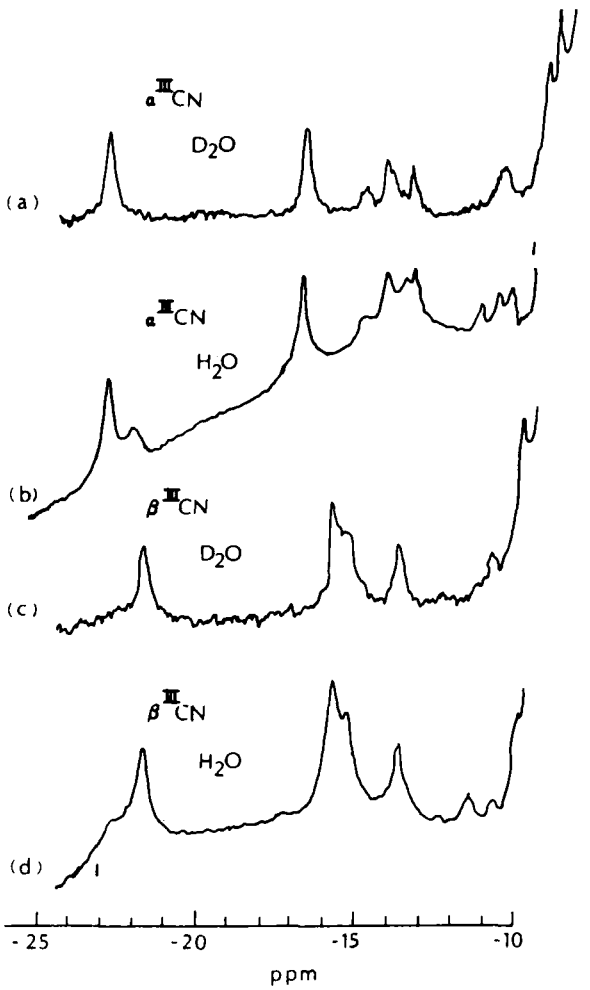

FIGURE 11. Proton NMR spectra of isolated α^{III} CN and β^{III} CN chains in D_2O (a and c) and H_2O (b and d) in 0.1 *M* phosphate buffer at pH 6.6 and 20°. (Redrawn and reprinted from Ogawa, S., Shulman, R. G., and Yamane, T., *J. Mol. Biol.*, 70, 291, 1972. With permission.)

absence of organic and inorganic phosphates and pH,[62,63] the effect of decreasing pH resembling that of increased phosphate concentrations. Since increasing either the hydrogen ion or phosphate concentration is known to stabilize the deoxy or T configuration, it is tempting to speculate that the NMR spectral changes observed in cyanoferrihemoglobin upon the addition of organic phosphates are representative of the displacement of an R → T conformational equilibrium. While such is probably the case for the valency hybrid hemoglobins discussed below, it seems less likely that fully liganded cyanoferrihemoglobin can undergo such a transition. An alternative interpretation would invoke an R → R′ conformational transition, where R′ represents a distorted R conformation. Evidence for distorted R configurations has been reported[68,69] for aquoferrihemoglobin, and Perutz et al.[70] have proposed such a conformation for cyanoferrihemoglobin.

The spectra of cyanoferrihemoglobins from different species display multiple differences.[71,72] Interpretation of such differences is complicated by a lack of resonance assignments and the unknown extent of conformational difference between the hemoglobins. Moreover, variations in experimental conditions, including organic phosphate levels or temperature and pH, may account for some of the observed differences.

2. Valency Hybrids

A model system which has proved particularly useful to the study of hemoglobin by ^{1}H NMR has been that of the valency hybrids. In these hemoglobins one set of chains in each tetramer exists in the cyanoferric state, while the remaining set remains as the ferrous chains, capable of reversible O_2 binding. Such preparations, described as either Hb $(\alpha^{II}\beta^{III\,CN})_2$ or Hb $(\alpha^{III\,CN}\beta^{II})_2$, have allowed the importance of heme-heme and subunit-subunit interactions to be assessed by monitoring the changes in the hyperfine shifted resonances of one chain induced by ligation of the neighboring chain.

Spectra typical of those obtained with the fully liganded valency hybrids are shown in Figure 8b and 8d. It is significant that the superposition of the spectra of $(\alpha^{II\,O_2}\beta^{III\,CN})_2$ and $(\alpha^{III\,CN}\beta^{II\,O_2})_2$ closely approximates the spectrum of cyanoferrihemoglobin (Figure 8c) and provides strong evidence that the conformation and electronic environment of one heme is not influenced directly by the state of neighboring heme groups.[62,67,73-75]

It was noted in the discussion of cyanoferrihemoglobin that pH and organic phosphates exerted a strong influence over the observed spectrum. This was also the case with the valency hybrids; the effect of 2,3-DPG on the spectrum of Hb $(\alpha^{III\,CN}\beta^{II})_2$ is illustrated in Figure 13.[73] The small differences between the spectrum in Figure 13b and the nearly equivalent hemoglobin preparation shown in Figure 8b are attributable primarily to temperature differences between the two spectra. It is apparent that under the conditions of Figure 13 there were no significant differences between the deoxy (Figure 13a) and oxy states

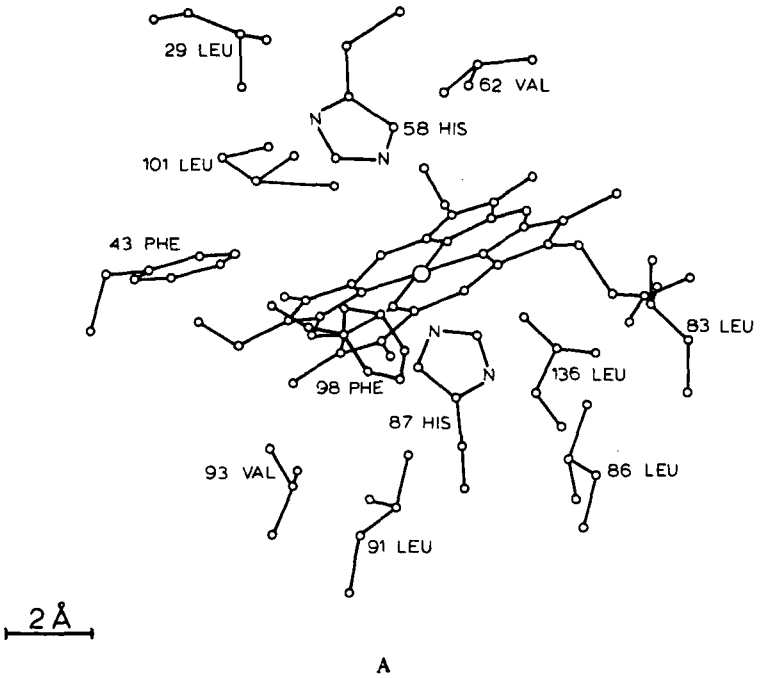

A

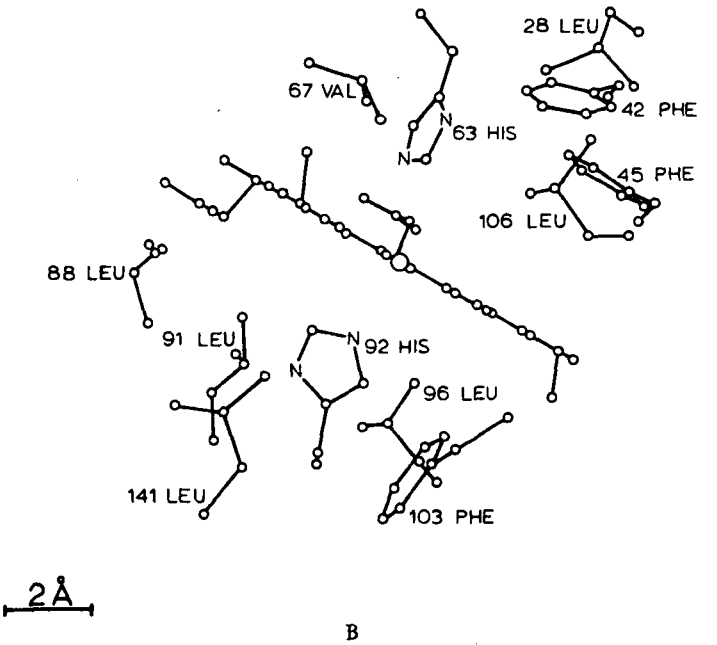

B

FIGURE 12. Views of the heme and some surrounding side chains within 6 Å of the iron in horse oxyhemoglobin based on data kindly supplied by Dr. M. F. Perutz. Views are from the +Z-axis: A.–α chain; B.–β chain. The residues are identified according to position in the sequence of the given chain. A.–For the α chain, residues shown here in numerical order have the following full identification: B10 Leu 29α, CD1 Phe 43α, E7 His 58α, Ell Val 62α, F4 Leu 83α, F7 Leu 86α, F8 His 87α, FG3 Leu 91α, FG5 Val 93α G5 Phe 98α, G8 Leu 101α, H19 Leu 136α. B.–For the β chain, the following corresponds: B10 Leu 28β, CD1 Phe 42β, CD4 Phe 45β, E7 His 63β, Ell Val 67β, F4 Leu 88β, F7 Leu 91β, F8 His 92β, FG3 Leu 96β, G5 Phe 103β, G8 Leu 106β, H19 Leu 141β.

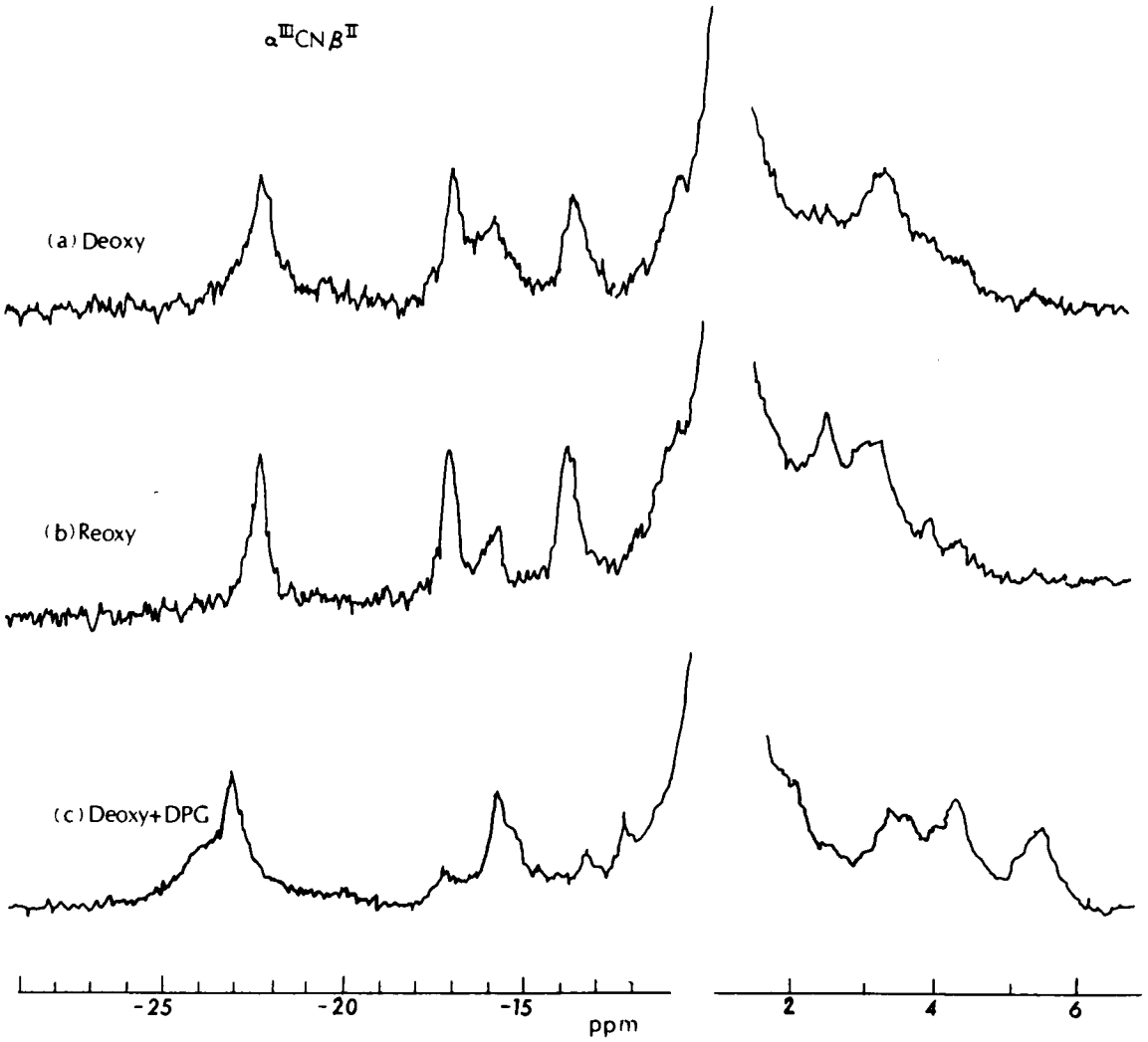

FIGURE 13. Proton NMR spectra of $(\alpha^{III}\,CN\,\beta^{II})_2$ hybrid. (a) Deoxy form in Bis Tris, pH 7.4. (b) Reoxygenated sample from a. (c) The deoxygenated form with one equivalent of 2,3-DPG per tetramer in Bis Tris buffer, ph 7.0, at 0°. The upfield and downfield regions are scaled differently. (Redrawn and reprinted from Ogawa, S. and Shulman, R. G., *J. Mol. Biol.*, 70, 315, 1972. With permission.)

(Figure 13b) unless the solutions contained 2,3-DPG (Figure 13c). Deoxygenation in 0.1 *M* phosphate at pH values near 7.1, or in the absence of phosphate at pH values below 6.74, also yielded a spectrum similar to that in Figure 13c. Conversely, for the Hb $(\alpha^{II}\,\beta^{III\,CN})_2$ hybrid, not shown in the figures, such changes in the observed NMR spectrum could be induced only by the presence of IHP, an agent possessing a very high affinity for deoxy Hb.[21,76]

It should be mentioned at this point that the broad shoulder near −24 ppm in Figure 13a, and more prominent in Figure 13c, arises not from the ferric subunit, but rather from the deoxy (high spin, S = 2) β^{II} subunit.[73,77] Similarly, the upfield resonance at +2.4 ppm in the oxygenated derivative (Figures 13b or 8b) arises from the oxygenated β^{II} subunit (S = 0), is independent of temperature, and represents a "ring-current" shifted resonance. Both of these resonances are discussed in greater detail below.

Cassoly et al.[24] studied the kinetics of CO binding in these hybrids, and found a close parallel between the observed ^{1}H NMR spectra and the relative abundance of two kinetically distinct species. The "quick" reacting species was associated with the spectrum of the oxygenated derivative (Figure 13b), while the "slow" reacting species, favored by the presence of phosphate or reduced pH, was associated with the altered spectrum as shown in Figure 13c.

These two different limiting ^{1}H NMR spectra

have been attributed to different quaternary structures, presumably similar to those of the R and T states or oxy- and deoxyhemoglobin.[73] Studies measuring the functional properties of valency hybrid hemoglobins[23,78,79] are not inconsistent with such a hypothesis. Moreover, the spectra of cyanoferrihemoglobin M Iwate (α 87 His → Tyr)[80,81] closely resemble the "altered" spectrum (Figure 13c) observed for the hybrids in the presence of phosphate. Hb M Iwate has been shown by X-ray crystallographic analysis[82] to remain in the deoxy quaternary structure, regardless of its state of ligation.

The excellent correlation of these NMR spectral changes with the conformational state, as well as with the ligand affinity, provides strong evidence that a significant change in ligand affinity at the hemes occurs with, and only with, the conformational transition between the R and T states. Such behavior is described most adequately by the two-state model of Monod et al.[11] Recently, the various models describing cooperative effects in hemoglobin have been reviewed and extended to include the effects of organic phosphates by Shulman et al.[83]

3. *Aquoferrihemoglobin*

In the absence of other ligands, the sixth coordination of the iron in ferrihemoglobin is occupied by either water or hydroxide. Few NMR studies have been reported on the aquo derivative.[10,70,84] The longer electronic relaxation time of this species, coupled with its large number of unpaired electrons (S = 5/2), would be expected to yield NMR spectra with broad hyperfine shifted resonances far removed from the diamagnetic resonance envelope. Experimentally, this has been observed. Shown in Figure 14 are the hyperfine-shifted proton resonances of aquoferrihemoglobin with and without IHP.[10] An appreciation for the line widths inherent to such species may be gained by a comparison of the abscissa scale in Figure 14 with the scales routinely used as in Figure 13. Nevertheless, the clear changes that occur in the spectrum upon the addition of IHP have been interpreted to represent a conformational change from the R to the T state, and thus have proved to be useful markers of such a conformational change.[10]

4. *Deoxyhemoglobin*

The hyperfine-shifted resonances in unmodified

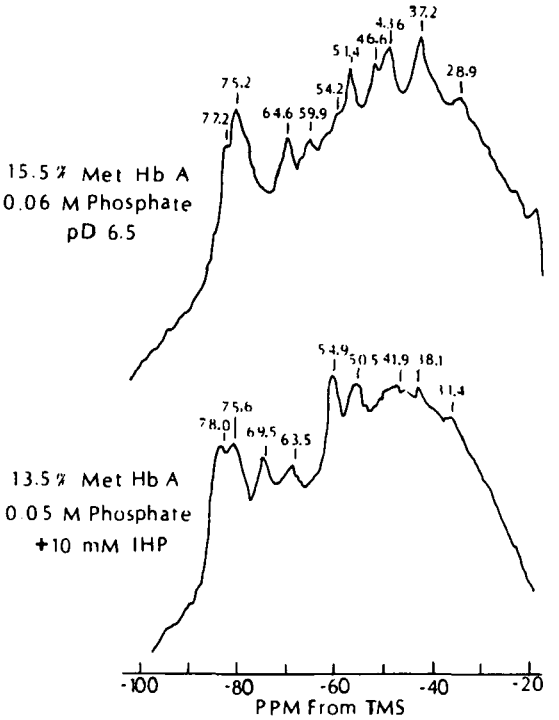

FIGURE 14. Hyperfine-shifted proton resonances of aquoferrihemoglobin in the absence and presence of IHP at 30°. The chemical shift scale, originally expressed with reference to HOD,[85] has been altered to refer to TMS. For ready reference to the original article, the chemical shifts from HOD are retained as marked on the spectra. These were obtained at 250 MHz. (Redrawn and reprinted from Perutz, M. F., Heidner, E. J., Ladner, J. E., Beetlestone, J. G., Ho, C., and Slade, E. F., *Biochemistry*, 13, 2187, 1974. With permission.)

deoxyhemoglobin (Fe^{II}, S = 4/2) have been used to assess the importance of different interchain contacts for transmitting structural information between subunits, as well as measuring the relative ligand affinities of the subunits.[67,73,77,85-92] The downfield region of the spectra of several different deoxyhemoglobins is shown in Figure 15.[77] While small variations between the different hemoglobins exist, most of them clearly demonstrate three hyperfine-shifted resonances near -23, -17 and -12 ppm at pH 7 and 25°.[77,89] On the basis of a comparison with fetal hemoglobin ($\alpha_2\gamma_2$) or hemoglobin with the β chain modified in the region of the heme,[77,80] the farthest downfield resonance near -23 ppm can be assigned to a β chain heme methyl. The assignment is consistent with the resonance appearing in this region in the deoxy valency hybrid Hb (α^{III} CN β^{II}) (Figures 13a and 13c) and with the absence of this resonance in Hb M Milwaukee,[90] a nat-

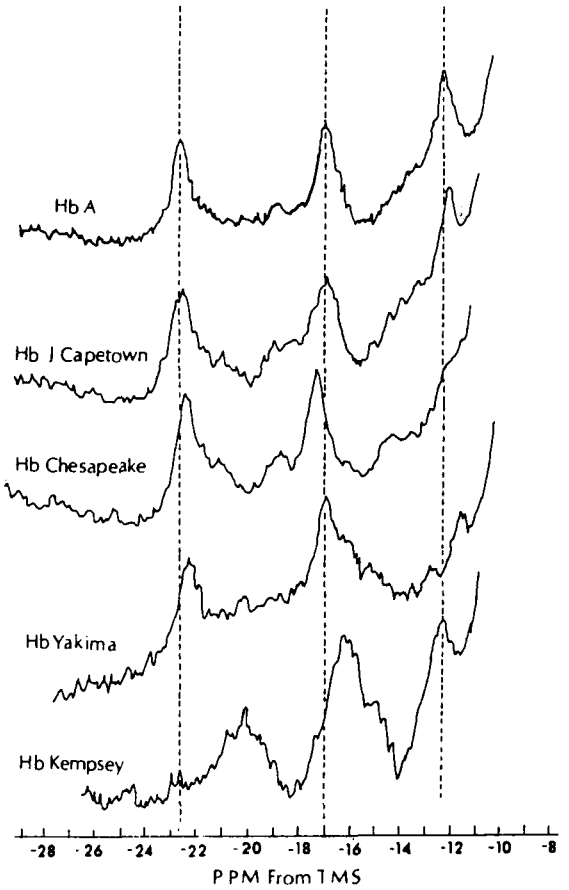

FIGURE 15. Heme proton NMR spectra at 90 MHz of deoxyhemoglobins A, J Capetown, Chesapeake, Yakima and Kempsey in 0.1 *M* phosphate buffer at pD 7 and 25°. The chemical shift scale has been altered to refer to TMS instead of HOD. (Redrawn and reprinted from Davis, D. G., Lindstrom, T. R., Mock, N. H., Baldassare, J. J., Charache, S., Jones, R. T., and Ho, C., *J. Mol. Biol.*, 60, 101, 1971. With permission.)

urally occurring valency hybrid Hb ($\alpha^{II}\beta_2{}^{III}$ Mil). By similar arguments, the resonances near -17 ppm and -12 ppm have been assigned to an α chain heme methyl.[77,89,91] A comparison of hemoglobin with mutations at the $\alpha_1\beta_2$ interface, Hb J Capetown (α 92 Arg → Gln), Hb Chesapeake (α 92 Arg → Leu), Hb Yakima (β 99 Asp → His) and Hb Kempsey (β 99 Asp → Asn) (Figure 15) shows changes in the resonance positions of each of the three hyperfine-shifted resonances, a fact consistent with the assignment to the $\alpha_1\beta_2$ interface of a critical role in the transfer of information between heme groups.[93-95] However, a separate study of Hb J Capetown[96] could demonstrate no differences between the spectra of this hemoglobin and that of Hb A for either the deoxy or cyanoferric states. Thus, while substitution of a Gln for Arg at α 92 in Hb J Capetown results in only an equivocal change in the heme environments, the changes induced by a replacement with Leu at this position, as in Hb Chesapeake,[92] are unmistakable (cf. Figure 15).

Numerous studies have sought to use these hyperfine-shifted resonances characteristic of the deoxy state as markers of the relative saturation of the subunits in a search for differences in ligand affinity between the α and β chains.[89,91,95] Such nonequivalent binding is not unexpected. Based on the stereochemical arrangement of the E11 valine residues near the face of the heme in deoxyhemoglobin, Perutz proposed that O_2 would bind preferentially to the α chains.[6] The reaction with CO, if allowance is made for its greater affinity, was thought to be equivalent.[1]

The NMR studies have tended to confirm this expected nonequivalence of the chains, although it has not always been clear whether the nonequivalence was due to equilibrium or kinetic considerations. Changes in the line width of the marker resonances due to variable exchange rates or ligand concentrations, given the poor signal-to-noise ratios inherent in many of the experiments, may easily be interpreted (erroneously) as changes in area. Thus, for Hb A and Hb Chesapeake measurements made under conditions of partial saturation in the absence of organic phosphates have revealed slight if any preferential binding of O_2 or CO to either chain.[77,89,95] However, if sufficiently high concentrations of IHP or 2,3-DPG are included in the solutions, the resonances attributable to the deoxy α-chains preferentially lose intensity.[89,91,95] This was interpreted by the authors as indicative of greater ligand affinity of the α-chains, while others[83] have interpreted it to mean a greater ligand exchange rate. For whichever reason, other ligands and other hemoglobins behave differently. In the presence of IHP, n-butylisocyanide apparently binds to the β chains in preference to the α chains.[92] In the mutant hemoglobin Yakima (β 99 Asp → His) and Kempsey (β 99 Asp → Asn), at neutral pD and in the presence of 0.1 *M* phosphate, the β chain hemes were found to possess the greater apparent affinity for CO.[87] This latter discovery finds a stereochemical explanation in the X-ray difference Fourier study of Pulsinelli,[98] in which it was shown that the (β 99 Asp → His) substitution of Hb Yakima yields a β heme with increased

exposure, while the α heme is pulled deeper within its pocket. The NMR studies have thus served to emphasize the fact that the reactions of hemoglobin are not only pH or phosphate dependent, but also ligand dependent.[89,95]

Perutz et al.[22] used ^{1}H NMR in conjunction with several other physical techniques to monitor the conformational changes induced in two chemically modified hemoglobins and in Hb Kempsey by the presence of IHP in an important study of the direct effect of the R → T transition on the ferrous hemes. The hemoglobins examined share the common property that in the absence of organic phosphates they remained in the R quaternary structure even when deoxy, but could be shifted to the T state by the addition of IHP. The NMR spectrum of deoxy Hb Kempsey in the R state was very similar to the sum of the spectra of the isolated deoxy α and β chains, and differed markedly from the spectrum of deoxy Hb A. Upon the addition of equimolar IHP to a Hb Kempsey solution, the spectrum changed to one very similar to that of deoxy Hb A.[22] These changes were interpreted as representing structural rearrangements about each heme, reflecting the R → T quaternary transition. Decreased pH showed a similar effect in another study of similarly modified hemoglobins,[99] although in this study conducted in H_2O, the observation of an exchangeable nonparamagnetically shifted resonance at -14 ppm proved to be a useful monitor of the presence of the T state.

5. *Hemoglobin Resonances Not Subject to Hyperfine Shifts*

a. Ring Current Shifted Proton Resonances

Besides the hyperfine-shifted resonances discussed above, many individual proton resonances shifted by ring current fields may be identified. The ring current fields responsible for the observed shifts arise from the porphyrin ring itself[42,60,100,101] or from imidazole[59,61] or indole[102,103] rings. Typical of the porphyrin induced ring current shifts are the upfield spectra shown in Figure 16.[101] For carboxyhemoglobin, at pD 7.0, and 0.2 *M* potassium phosphate buffer shown in Figure 16, there are resonances at 0.34, 0.58, 1.02, 1.64, and 1.74 ppm upfield of TMS, all of which are attributable to ring-current shifts. Additional resonances also occur at -0.23 and -0.02 ppm, but are not included in the figure.[100] Another peak at 0.71 ppm appears as a shoulder to the larger resonance at 0.58 ppm. On the basis of a comparison with carboxyhemoglobins containing altered β subunits, e.g., F ($\alpha_2\gamma_2$), Zürich (β 63 His → Arg) and Sydney (β 67 Val → Ala), the peaks at 1.74 and 1.02 ppm could be assigned to the γ_1 and γ_2 methyls of the β E11 valine 100 (see Figure 12). Similarly, since the sum of the spectra of the isolated carboxy chains approximated the spectrum of the tetramer,[100] the contributions of each chain to the observed spectrum could be deduced. This information, together with the integral areas of the resonances, suggested that the resonance at 1.64 ppm was a methyl of the α E11 valine.[100]

As in the case of many of the NMR studies already mentioned, both pD and phosphate concentration profoundly affected the observed NMR spectrum. In Figure 16, the effect of variations in pD at constant phosphate concentration is shown. The upfield shift of the resonances near 1.74 and 1.02 ppm, assigned to the 67 β E11 valine methyls, accompanying reduced pD or increased phosphate concentration (most strikingly noted with the organic phosphates), can be interpreted as a movement of this valine residue closer to the plane of the porphyrin ring (see Figure 4).[42,100,101] The E11 valine residues are located on the distal histidine side of the heme plane near the ligand binding site (Figure 12). Reference has already been made to the belief that they play a vital role in the stereochemical mechanism for the cooperative oxygenation of hemoglobin.[6] Significantly, the conditions favoring reduced ligand affinity[1] or increased ligand dissociation rates[104] are identical with those producing the upfield shift of the 67 β E11 valine methyl resonances. Another interesting observation to come from these studies[101] was the fact that the spectra of HbCO and HbO_2 were not identical under similar conditions. The tentative explanation of the spectral differences was that a residue, possibly the E11 valine, was positioned much closer to the iron in the oxy derivative.

b. Aromatic, Proton Resonances

While also experiencing ring-current induced shifts, the protons situated on aromatic centers characteristically are bound in a different spectral region from those resonances discussed above. Hence, they are now considered separately. The C-2 proton resonances of 5 to 9 titratable histidines have been observed in the region from

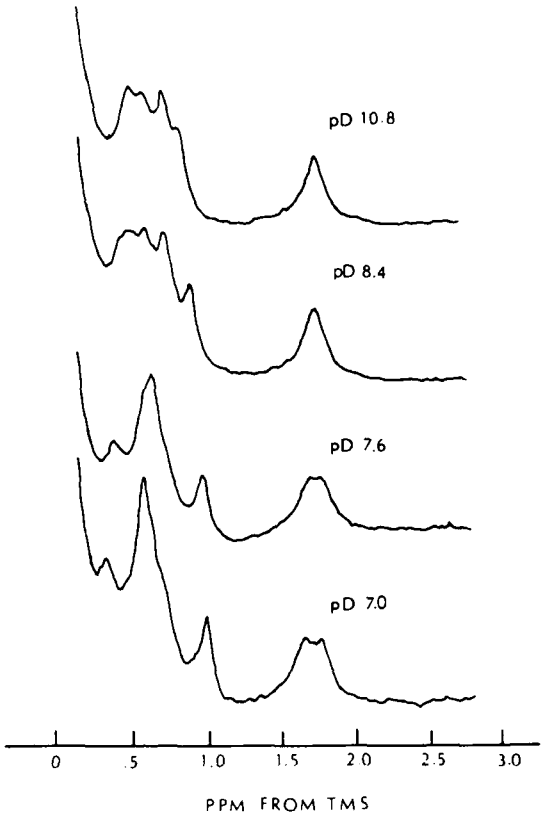

FIGURE 16. Effects of variation in pD on the ring-current shifted proton resonances of carboxyhemoglobin A in 0.2 *M* phosphate buffer, 31°. The chemical shift scale has been altered to refer to TMS instead of HOD. (Redrawn and reprinted from Lindstrom, T. R. and Ho, C., *Biochemistry*, 12, 134, 1973. With permission.)

-6.8 to -9.3 ppm for oxy, deoxy, and ferrihemoglobin.[59] These resonances exhibited similar pK values for oxy and ferrihemoglobin, but several were markedly different in deoxyhemoglobin. The results of a similar study at 250 MHz are shown in Figure 17 for hemoglobin and des-146 β His hemoglobin.[61] A resonance of the 146 β histidine residue was identified by difference; the pK determined for this resonance was 7.1 ± 0.1 in carboxyhemoglobin, and 8.0 ± 0.1 in deoxyhemoglobin. This residue was proposed by Perutz et al.[105] to account for approximately 50% of the alkaline Bohr effect. The contribution of this group to the Bohr effect was confirmed by the observation of a Bohr effect reduced by approximately 50% in des-146 β His Hb[106] or Hb Hiroshima (146 β His → Asp).[106] The direct observation of this histidine resonance by ^{1}H NMR confirmed the expected change in pK upon ligand binding. Moreover, the changes in pK of several other resonances upon deoxygenation[59] suggest that several other histidines are contributing in at least some small measure to the Bohr effect. Presumably, these multiple small contributions might account for the approximately 25% of the Bohr effect heretofore unexplained.[2]

c. Exchangeable Proton Resonances

Studies of hemoglobin in water rather than D_2O have been mentioned above. Besides the additional hyperfine shifted exchangeable resonances which appear in such solutions, several exchangeable resonances uninfluenced by the electronic spin state of the iron also make their appearance.[102,103] Notable among these are resonances near -10.6 and -10.3 ppm in oxy and carbonmonoxyhemoglobin, respectively, and near -14.2 and -11.2 ppm in deoxyhemoglobin.[102,103] While other exchangeable resonances have been observed and tentatively assigned,[99,102,103] the two pairs of resonances cited above have been shown to be useful monitors of the R and T states, respectively.[81,99,102,103]

Based on extensive studies of hemoglobin A and many different mutants or chemically modified hemoglobins, Fung and Ho[103] have arrived at assignments for some of these resonances. The resonance at -10.6 ppm in oxyhemoglobin (or -10.3 ppm in carbonmonoxyhemoglobin) can probably be assigned to the proton of the important hydrogen bond between the 94 α G1 aspartic acid and the 102 β 64 asparagine. This bond spans the $\alpha_1\beta_2$ interface in oxyhemoglobin, and is a characteristic of this structure, since it is broken upon conversion to the deoxy state.[6,7] If these assignments are correct, the 0.3 ppm difference in resonance positions between oxy and carbonmonoxyhemoglobin is intriguing, since it would imply that the $\alpha_1\beta_2$ interface senses a difference between the two hemoglobin species. The oxy and carbonmonoxy species of hemoglobin are often assumed to be identical. Exchange effects also need to be ruled out as a possible cause of the difference in chemical shift.

In deoxyhemoglobin the resonance at -14.2 ppm was assigned to the proton in the hydrogen bond between the 42 α C7 tyrosine and the 99 β G1 aspartic acid.[103] In parallel with the case of oxyhemoglobin, this hydrogen bond anchors the $\alpha_1\beta_2$ subunits in deoxyhemoglobin, but is broken upon conversion to the liganded state. Experimentally, its utility as an indication of the deoxy

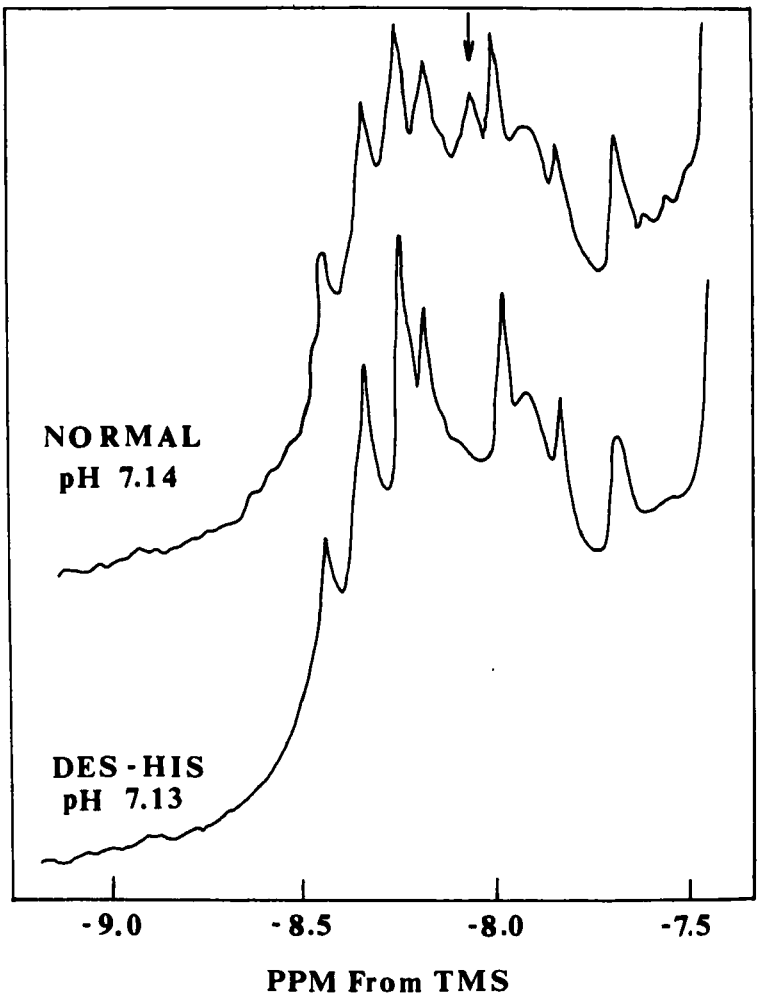

FIGURE 17. Proton NMR spectra at 250 MHz of carboxyhemoglobin at 30° in 0.2 *M* NaCl + 0.2 *M* deuterated potassium phosphate. The lower curve, DES–HIS, refers to the preparation des-(His 146β). The chemical shift scale has been altered to refer to TMS instead of HOD. (Redrawn and reprinted from Kilmartin, J. V., Breen, J. J., Roberts, G. C. K., and Ho, C., *Proc. Natl. Acad. Sci. U.S.A.*, 70, 1246, 1973. With permission.)

(T) conformation was recognized early.[81,99,102,103]

The origin of the resonance at -11.2 ppm in deoxyhemoglobin remains uncertain.[103] Possible candidates include the hydrogen bond between the HC 2 tyrosines and the FG 5 valines of both chains,[103] or else the NH proton of 37 β C3 tryptophan.[102,103]

The pattern of exchangeable resonances in ferrihemoglobin may resemble either that of deoxy or oxyhemoglobin, depending upon the conditions of measurement.[103] At pH 6.2 in the absence of phosphate, the "T" state marker at -11.2 ppm, as well as the "R" state marker at -10.7 ppm are both observed. The addition of IHP to such a solution eliminates the resonance at -10.7 ppm, to be replaced by one at -14.8 ppm. This latter resonance is believed to be analogous to the other "T" state marker found at -14.2 ppm in deoxyhemoglobin.[103] If the same experiment described above is conducted at pH 7.6, however, it is found that only the "R" state marker at -10.7 ppm is present, and that IHP is now without effect.[103] These results provide further evidence that, at least for ferrihemoglobin, intermediate states are possible, and that the equilibrium between R and T conformations may be readily tipped in either direction by small perturbations in the chemical environment.

Finally, by studying the line width of the

resonance near -14 ppm in deoxyhemoglobin, as well as the line width of some other resonances, it has been estimated that the rate of interconversion between T and R states in deoxy des -141α-Arg-hemoglobin is on the order of 10^4 sec^{-1}.[99]

B. ^{13}C NMR of Hemoglobins

The ^{13}C nucleus presents certain advantages for the study of hemoglobins. The low natural abundance, which is a disadvantage in terms of sensitivity, results in the virtual absence of homonuclear scalar coupling, so that this potential source of multiplicity can be avoided. As described previously, decoupling of protons by appropriate irradiation can be used routinely. Under these conditions the line widths for the more rapidly relaxing protonated carbon nuclei may approach 70 Hz, and those of the more slowly relaxing nonprotonated carbon nuclei will be narrower. The hyperfine interactions arising from paramagnetic centers result in shifts of the same magnitude as for ^1H NMR, which means in the context of the wider chemical shift separations characteristic of ^{13}C nuclei that the shifted resonances often will be observable within the usual observation window. Significant ring-current shifts are observed. An excellent summary of the potentialities of ^{13}C NMR for heme proteins, and its relation to ^1H NMR, has been set out by Wüthrich.[108]

1. Studies at Natural Abundance ^{13}C

As with the early ^1H NMR studies, most of the work to date studying the natural abundance ^{13}C nuclei in hemoglobin has yielded relatively meager rewards. With currently available commercial instrumentation, the observation of single carbon resonances at usable hemoglobin concentrations is not practical.[109-111] Spectra typical of hemoglobin in several different states are shown in Figure 18.[111] Such spectra have been recorded by many different workers.[51,109-111] All spectra are strikingly similar.

The relatively sharp resonances at 153 ppm and 177ppm upfield of external CS_2* represent the contributions of multiple (up to 22) ε-carbons of the lysine residues and (up to 36) β-carbons of the alanine residues, respectively. The broad resonance envelopes situated from about 115 ppm to 140 ppm and from 150 ppm to 180 ppm represent the contribution of the α-carbons and the β- and γ-carbons, respectively. Similarly, in the downfield region of the spectrum, additional resonance envelopes are found; one for each characteristic type of carbon commonly found in the protein. Thus, for example, the β and γ carboxyl resonances fall at about 9 to 14 ppm, α-carboxyls at 14 to 23 ppm, and most of the aromatic carbon resonances from 35 to 85 ppm.

Table 5 lists the expected chemical shifts of the constituent amino acids, based on studies of the free amino acids and small peptides.[49,113-121] Also shown in Table 5 are the expected ^{13}C resonance positions of the diamagnetic porphyrin ring, Zn(II) porphyrin, and the paramagnetic Fe III $(CN)_2$ protoporphyrin IX complex.[122-124] The conformational constraints imposed by the higher orders of structure characteristic of any native protein produce additional shifts of any given resonance, leading to multiple partial overlaps and the broad envelopes seen in Figure 18.

By studying the relaxation behavior of such spectra, information may be gained concerning the mobility of hemoglobin in solution. As emphasized in Section II, for molecules the size of hemoglobin, the dipole-dipole relaxation mechanism dominates the nuclear magnetic relaxation for protonated carbons. Thus, for protonated carbons which fit the model of an isotropically tumbling sphere, i.e., most of the rigidly held backbone α-carbons, the spin-lattice relaxation time T_1 may be related to the rotational correlation time, τ_R. Since T_1 is a double-valued function of τ_R (cf. Equation 15), an additional measurement is necessary to remove the ambiguity. Appropriate measurements include an estimation of the NOE or the spin-spin relaxation time (T_2), or the determination of T_1 at two different field strengths.[48]

In the case of hemoglobin, where one is dealing with overlapping resonances and limited signal-to-noise, this last approach is the most reliable. Figure 19 depicts results typical of an inversion-

*Many different markers have been used with which to reference the ^{13}C spectra. Most commonly, these have been either CS_2 or TMS. CS_2 occurs downfield of most other ^{13}C resonances while TMS appears at the upfield end of the usual spectrum. In the present discussion the reference scale used by the authors of the works considered have been retained, be it CS_2 or TMS. For purposes of comparison, external CS_2 occurs 192.8 ppm downfield of TMS.[111] The most widely useful internal reference probably is dioxane which does not appear to interact with hemoglobin and whose resonance occurs at 126.2 ppm upfield of CS_2.

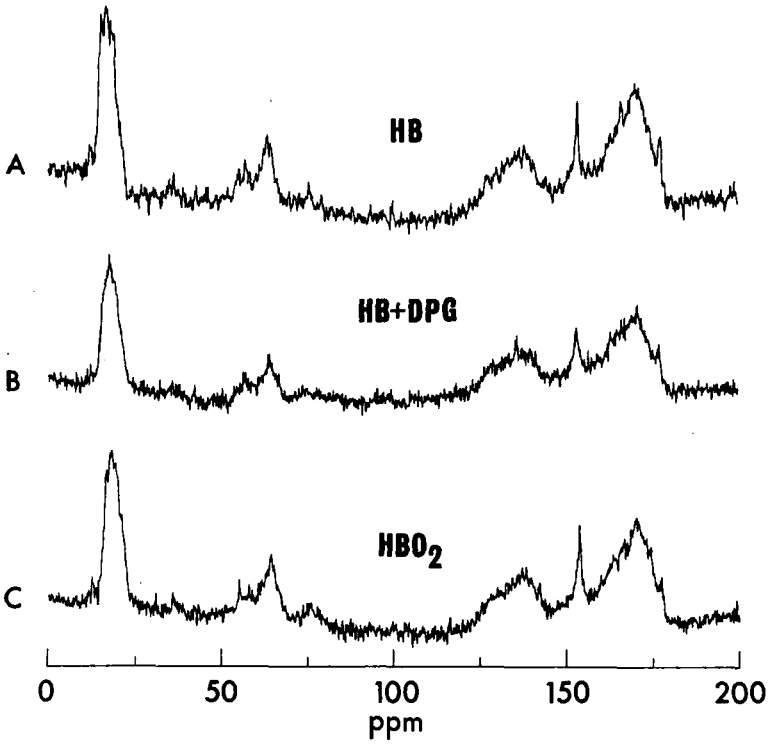

FIGURE 18. ^{13}C NMR spectra of various states of hemoglobin preparations near physiological pH. A.–Deoxyhemoglobin, pH 6.90; B.–deoxyhemoglobin containing 2,3-DPG, pH 7.32; C.–oxyhemoglobin, pH 7.10. The recycle time was 1.36 sec, and the temperature 33–34°. Hemoglobin concentrations referred to heme content varied between 12.3 and 13.6 m*M*. Spectral accumulations varied between 16,384 and 17,673; chemical shift is relative to CS_2. (From Morrow, J. S., Klein, P., Visscher, R. B., Marshall, R. C., and Gurd, F. R. N., *Proc. Natl. Acad. Sci. U.S.A.*, 70, 1414, 1973. With permission.)

recovery T_1 measurement experiment on human carboxyhemoglobin.[51] The results of conducting such an experiment at two different magnetic field strengths, and then comparing the relaxation times of different points within the α-carbon envelope, are plotted along the theoretical curves predicted at the two field strengths in Figure 20.[51] Clearly, the results correspond well with a value of τ_R of about 40 ns. This value is to be compared with the estimate of 44 ns by dielectric relaxation measurements[125] (allowing for a factor of 3 to account for differences in theoretical treatment) or a somewhat shorter value obtained by fluorescence depolarization studies.[126] When the magnetic relaxation studies are conducted on suspensions of whole erythrocytes, the derived value of τ_R is near 69 ns, suggestive of an increased viscosity within the erythrocyte.[51]

Recent instrumental improvements, most notably the introduction of large diameter (20 to 25 mm) spinning sample tubes, have attained sensitivity levels sufficient to observe single carbon resonances arising from nonprotonated aromatic and carbonyl carbons.[127] Oldfield and Allerhand have reported initial studies on carboxyhemoglobins.[127] Figure 21 shows the carbonyl and aromatic region for the adult human hemoglobin recorded at 14.2 kG. The natural abundance CO resonances are shown most downfield, with characteristic differences between the chains. The large carbonyl band falls between 170 and 185 ppm downfield of TMS. In the region between 155 and 160 ppm are seen C^{ζ} of tyrosine and arginine residues. Particularly noteworthy are tryptophan C^{γ} resonances shown as two bands on either side of the 110–ppm mark. The larger, downfield resonance has been assigned to residues 14α and 15β, and the smaller, upfield one to residue 37β. Moreover, most of the 32 nonprotonated nonequivalent aromatic carbons of the hemes were found within the range of 141 to 147 ppm downfield of TMS, although not as single carbon

TABLE 5

^{13}C NMR Positions of Amino Acids and Fe(III) Protoporphyrin $(CN)_2$ and Zn(II) Porphyrin

The positions of the amino acid are given for either the free amino acid or that amino acid in a small peptide at neutral pH (or pD). Positions may shift significantly as a function of pH; when situated in a native protein, their positions may also vary greatly. The values for the porphyrin complexes, Fe(III) PROTO $(CN)_2$ (paramagnetic) and Zn(II) POR (diamagnetic) were measured in 4:1 D_2O: d_5-pyridine solvent at 29°.

Amino Acid Chemical Shifts

	ppm Relative to external CS_2		ppm Relative to TMS		
Assignment	Peptide	Amino acid	Peptide	Amino acid	Reference
Carbonyls	16.1–25.6	15.7–25.2	(−176.7)–(−167.2)	(−178.1)–(−167.6)	A–D
Tyr C^{δ}*	38.2	N.O.*		N.O.	D
Phe C^{γ}	56.4	N.O.	−154.6	N.O.	D
His $C^{\epsilon 1}$	59.2	59.2	−136.4	−133.6	D
Tyr $C^{\delta 1}$ $C^{\delta 2}$	62.4	N.O.	−133.6	N.O.	D
Phe C^{δ}	65.6	N.O.	−130.3	N.O.	D
His $C^{\delta 2}$	75.4	75.4	−127.2	−117.4	D
Tyr $C^{\epsilon 1}$ $C^{\epsilon 2}$	77.4	N.O.	−117.4	N.O.	D
Arg C^{γ}	36.1	36.0	−115.4	−156.8	C
Thr C^{β}	125.8	126.8	−156.7	−66.0	B
Ser C^{β}	131.6	132.4	−61.2	−60.4	B
Pro C^{α}**	131.9 (*trans*)		−60.9 (*trans*)		C
	132.7 (*cis*)	131.5	−60.1 (*cis*)	−61.3	
Val C^{α}	133.0	132.1	−59.8	−60.7	A
Ile C^{α}	134.1	133.1	−58.7	−59.7	A
Thr C^{α}	133.7	132.3	−59.1	−60.5	B
Cys C^{α}	N.O.	136.8	N.O.	−56.0	E
Ser C^{α}	137.0	136.1	−55.8	−56.7	B
Tyr C^{α}	137.4	N.O.	−55.4	N.O.	D
Phe C^{α}	137.6	N.O.	−55.2	N.O.	D
Gln C^{α}	139.4	138.4	−54.3	−54.5	B
Met C^{α}	139.8	138.7	−53.0	−54.1	C
Arg C^{α}	139.1	138.4	−53.7	−54.4	C
Glu C^{α}	138.6	137.8	−54.2	−55.0	B
Lys C^{α}	139.0	138.3	−53.8	−54.5	C
Leu C^{α}	140.1	138.9	−52.7	−53.9	A
His C^{α}	140.2	139.2	−52.6	−53.6	D
Asn C^{α}	142.3	141.1	−50.5	−51.7	B
Asp C^{α}	141.2	140.4	−51.6	−52.4	B
Ala C^{α}	142.8	142.0	−50.0	−50.8	A
Gly C^{α}	150.3	151.2	−42.5	−41.6	A
Arg C^{δ}	152.0	152.2	−40.8	−40.6	C
Leu C^{β}	153.2	152.8	−39.6	−40.0	A
Lys C^{ϵ}	153.4	153.5	−39.4	−39.3	C
Phe C^{β}	156.0	N.O.	−36.8	N.O.	D
Asp C^{β}	154.2	156.2	−38.6	−36.6	B
Ile C^{β}	156.8	156.9	−36.0	−35.9	A
Tyr C^{β}	156.8	N.O.	−36.0	N.O.	D
Asn C^{β}	154.2	156.2	−38.6	−36.6	B
Glu C^{γ}	159.4	159.1	−33.4	−33.7	B
Gln C^{γ}	161.6	161.8	−31.2	−31.0	B
Met C^{β}	162.7	163.0	−30.1	−29.8	C

*N.O. – Not observed.

**_Cis_ or _trans_ refer to the configuration about the -gly-pro-bond in the study cited.

TABLE 5 continued

^{13}C NMR Positions of Amino Acids and Fe(III) Protoporphyrin $(CN)_2$ and Zn(II) Porphyrin

Amino Acid Chemical Shifts

Assignment	ppm Relative to external CS_2		ppm Relative to TMS		References
	Peptide	Amino acid	Peptide	Amino acid	
Val C^{β}	162.9	163.6	−29.9	−29.2	A
Lys C^{β}	162.7	162.9	−30.1	−29.9	C
Met C^{γ}	163.5	163.9	−29.3	−28.9	C
Pro^2 C^{β}	163.5 (*trans*)		−29.3 (*trans*)		
	160.9 (*cis*)	163.9	−31.9 (*cis*)	−28.9	C
Glu C^{β}	165.5	165.7	−27.3	−27.1	B
Arg C^{β}	164.9	165.1	−27.9	−27.7	C
Gln C^{β}	166.1	166.6	−26.7	−26.2	B
His C^{β}	166.6	166.2	−26.2	−26.6	D
Lys C^{β}	166.6	166.5	−26.2	−26.3	C
Cys C^{β}		167.8		−25.0	E
Ile $C^{\gamma 1}$	168.3	168.3	−24.5	−24.5	A
Leu C^{γ}	168.5	168.4	−24.3	−24.4	A
Pro C^{γ}	168.4 (*trans*)		−24.4 (*trans*)		
	170.8 (*cis*)	169.0	−22.0 (*cis*)	−23.8	C
Arg C^{γ}	168.4	168.9	−24.4	−23.9	C
Leu $C^{\delta 1}$	170.6	170.6	−22.2	−22.2	A
Lys C^{γ}	170.9	171.5	−21.9	−21.3	C
Leu $C^{\delta 2}$	172.1	171.6	−20.7	−21.2	A
Thr C^{γ}	174.1	173.3	−18.7	−19.5	B
Val $C^{\gamma 1}$	174.4	174.7	−18.4	−18.1	A
Val $C^{\gamma 2}$	175.2	176.0	−17.6	−16.8	A
Ala C^{β}	176.2	176.5	−16.6	−16.3	A
Ile $C^{\gamma 2}$	178.0	178.1	−14.8	−14.7	A
Met C^{ϵ}	178.7	178.7	−14.1	−14.1	C
Ile C^{ϵ}	182.4	181.7	−10.4	−11.1	A

Porphyrin Chemical Shifts[121,122]

Assignment	ppm from CS_2		ppm from TMS	
	Fe(III)Proto$(CN)_2$	Zn(II)Proto	Fe(III)Proto$(CN)_2$	Zn(II)Proto
β Carbons	88.0		−104.8	
	77.4		−115.4	
	72.5		−120.3	
	59.4	59.6	−133.4	−133.2
	57.2		−135.6	
	52.0		−140.8	
	46.4		−146.4	
	N.O.		N.O.	
Meso-carbons	158.4		−34.4	
	144.8	87.1	−48.0	−105.7
	136.8		−56.0	
	121.6		−71.2	

TABLE 5 (continued)

Porphyrin Chemical Shifts[121,122] continued

Assignment	ppm from CS_2		ppm from TMS	
	Fe(III)Proto$(CN)_2$	Zn(II)Proto	Fe(III)Proto$(CN)_2$	Zn(II)Proto
α-Carbons	163.2		−29.6	
(quaternary carbons	163.0		−29.8	
next to pyrrole	156.9		−35.9	
nitrogens)	156.2	42.0	−36.6	−150.8
	144.8		−48.0	
	144.8		−48.0	
	138.4		−54.4	
	136.8		−56.0	
Ring methyls	231.6		38.8	
	231.2	–	38.4	–
	222.0		29.2	
	218.3		25.5	
Propionates				
α-Carbon	210.9	–	18.1	–
	209.4		16.6	
β-Carbon	102.0	–	−90.8	–
	99.2		−93.6	
Carboxyl	7.3	–	−185.5	–
	7.0		−185.8	
Vinyls				
α-Carbon	126.6	–	−66.2	–
	122.5		−70.3	
β-Carbon	31.4	–	−161.4	–
	27.8		−165.0	

References: A – 117; B – 118; C – 119; D – Glushko, V., Keim, P., Lawson, P. J., and Gurd, F. R. N., unpublished observation; E – 120.

resonances. As might be expected, none of these latter resonances were detectable in the paramagnetic ferrihemoglobin. A small peak at 124.7 ppm was tentatively assigned to the C^{γ} of the proximal histidine residues of the α and β chains.

Figure 22 shows the region of the tryptophan C^{γ} resonances for a number of hemoglobins and for horse heart myoglobin. The nearly identical chemical shifts of analogous tryptophan residues of the four hemoglobins studied suggests that the conformations of these four hemoglobins in solution are nearly identical, at least in the vicinity of those residues.[127] Similarly elegant results have been reported by these workers in related studies, primarily on other proteins.[128,129]

2. Studies Employing ^{13}CO Enrichment

An alternative approach to observing single carbon resonances is the application of labels enriched in ^{13}C. Since enrichment levels of over 90% ^{13}C are routinely available from many suppliers, the potential gain in sensitivity over natural abundance ^{13}C (1.1%) is greater than 80-fold. One of the first such ^{13}C enriched labels to be applied to hemoglobin was ^{13}CO. Carbon monoxide binding to many different types of hemoglobin has been studied by ^{13}C NMR spectroscopy.[51,130-134] Representative spectra are shown in Figures 19 and 21. From such studies, it is apparent that each chain yields a distinctive ^{13}CO resonance, and that the environments about the heme are similar in a wide variety of different hemoglobins.[134]

On the basis of a comparison with the isolated pCMB α and β chains[133-135] (Figure 23), the upfield CO resonance near 206.2 ppm downfield of TMS was assigned to the β subunit, while the

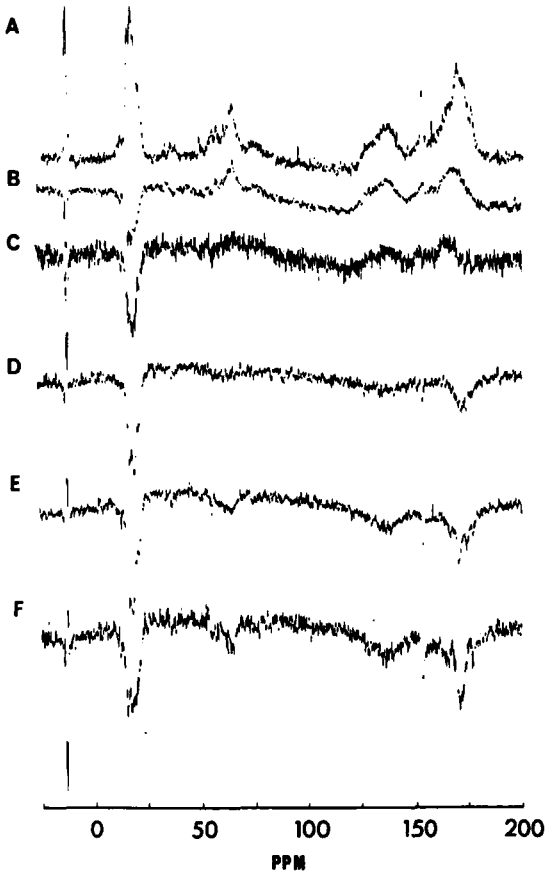

FIGURE 19. Partially relaxed Fourier transform ^{13}C NMR spectra of human carboxyhemoglobin A_0 containing ^{13}CO which appears as the narrow, most downfield resonance. Chemical shifts are referred to CS_2. A.–normal spectrum; F. to B.–spectra taken with delay times before the magnetization was sampled of 8, 16, 32, 80, and 160 msec, respectively. Other conditions corresponded to those of Figure 20, at 23.5 kG, and with instrumental operation comparable otherwise to Figure 18. (From Visscher, R. B., Investigations of the Dynamic Behavior of Hemoglobin and Myoglobin by ^{13}C Nuclear Magnetic Resonance Spectroscopy, Ph.D. thesis, Indiana University, Bloomington, 1974).

downfield resonance near 206.8 ppm (for most hemoglobins examined) was assigned to the α subunit. The close similarity of the CO environments as judged from the chemical shift data between the free chains and the intact tetramer suggests that, in the liganded state, interactions between subunits play little role in modifying the heme environment.

An interesting exception to the marked similarity of CO resonances between different hemoglobins is found in the various strains of rabbits.[25,132,134] Apparently, *three* distinct iron coordination sites can exist in hemoglobin solutions prepared from certain rabbits of the Dutch lop strain.[132] In addition to the two resonances commonly found in the hemoglobins from other animals, a third more downfield resonance is located at 208.2 ppm. The sum of the area of the two downfield resonances approximates the area of the upfield β chain resonance, implying that these rabbits have two types of α subunits. Two different α-chain alleles are in fact present[136] and yield electrophoretically indistinguishable hemoglobins. One α chain contains Val-29 (B10), Phe-48 (CD6), and Thr-49 (CD7), while its allelic partner has Leu, Leu and Ser at these positions, respectively. The markedly different CO resonance peak at 208.2 ppm in such rabbit hemoglobin solutions has been ascribed to changes in the region of the C/D helices induced by the above Val, Phe, and Thr combination.[134] The CO group would therefore seem to be primarily sensitive to effects transmitted from these helices through the porphyrin ring and heme iron, and be much less sensitive to the nature of the surrounding pocket. Such an interpretation is also consistent with the finding that there is a relatively constant separation of 0.5 ppm between the CO resonances of the α and β subunits in several different hemoglobins, perhaps reflecting the lack of a D helix in subunits of the α-type. The addition of up to a 5:1 molar excess of 2,3-DPG at pH 7.0 to 7.4, or varying the pH between pH 6 to pH 8 does not affect the chemical shift of the CO resonances.

At less than saturating levels of CO or in the presence of O_2, the α-subunit of rabbit hemoglobin displays the lower affinity for CO when compared to the β-subunit.[130] While similar measurements on other hemoglobins have not yet been reported, such an approach to monitoring the progressive saturation of hemoglobin would be complementary to the ^1H NMR studies that monitor the disappearance of hyperfine-shifted resonances with increasing saturation.

3. Interaction of $^{13}CO_2$ with Hemoglobin

Another particularly attractive ^{13}C label which may be easily introduced into hemoglobin solutions is $^{13}CO_2$.[111,131,137-139] CO_2 is an important allosteric effector of hemoglobin, increased CO_2 tensions favoring reduced O_2 affinity. The mechanism of this effect involves carbamino formation with the 4 NH_2-terminal

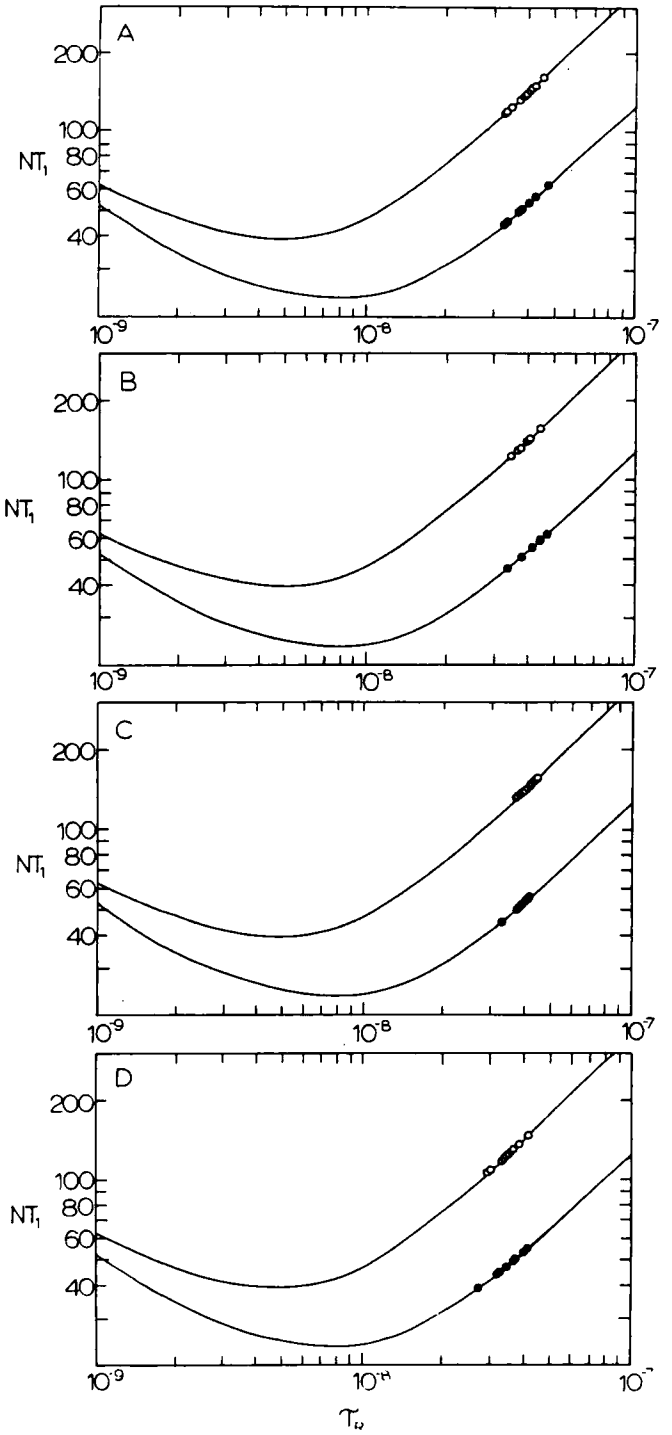

FIGURE 20. NT_1 values for hemoglobin α-carbon resonances superimposed upon computed curves for the dependence of NT_1 on τ_R for an isotropically rotating rigid sphere. Values at 23.5 kG at 28 ± 1° are shown as open circles (○), and at 14.1 kG at 32 ± 1° as closed circles (●). A.–Deoxy-; B.–carboxy-; C.–ferri-; D.–cyano-ferrihemoglobin. Both axes are in seconds. (From Visscher. R. B., Investigations of the Dynamic Behavior of Hemoglobin and Myoglobin by ^{13}C Nuclear Magnetic Resonance spectroscopy, Ph.D. thesis, Indiana University, Bloomington, 1974.)

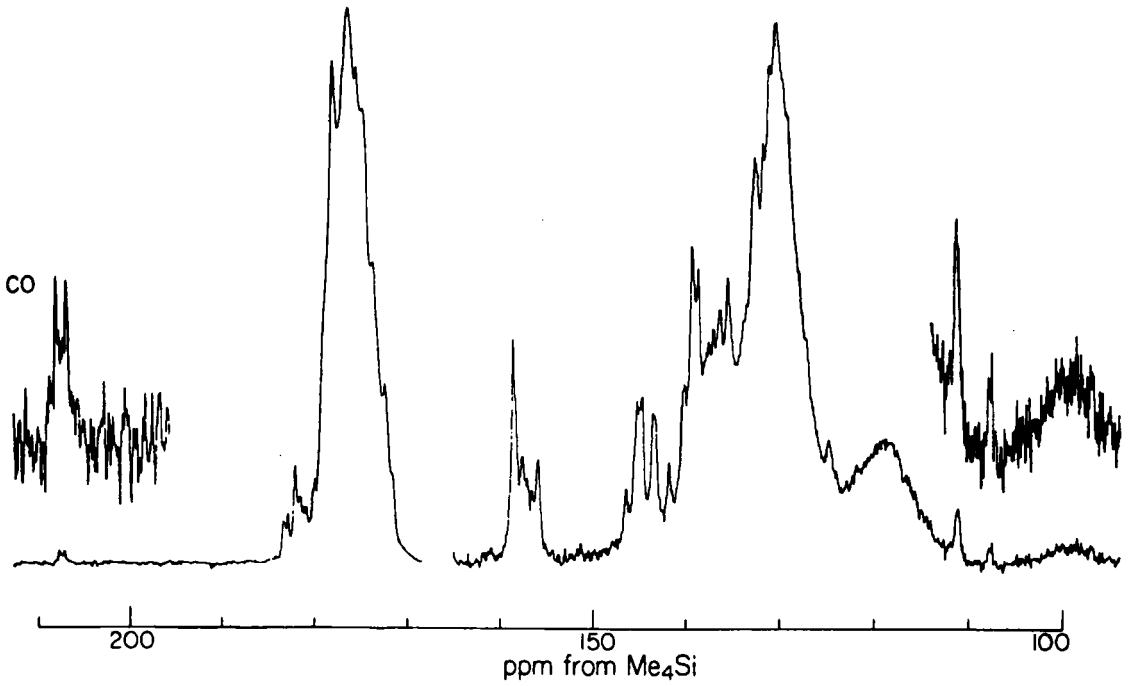

FIGURE 21. Spectrum of the carbonyl and aromatic region of human adult carbon monoxide hemoglobin 13.2 m*M* (in heme) in 0.1 *M* NaCl, 0.05 *M* phosphate buffer, pH 7.0, 34°. The spectrum was recorded under conditions of noise-modulated off-resonance proton-decoupling using 131,072 accumulations. The spectrum was recorded at 15.18 *M*Hz with 1.105 s recycle time. The vertical gain of the main carbonyl printout is 0.4 times that of the aromatic region. The insert at about 210 ppm has a fourfold vertical expansion (relative to the aromatic region) and a twofold horizontal expansion. The insert at 100 to 105 ppm has a fourfold vertical expansion. (Redrawn and reprinted from Oldfield, E. and Allerhand, A., *J. Biol. Chem.*, 250, 6403, 1975. With permission.)

groups of the α and β chains.[140-142] The carbamino reaction is just one of the potential fates of CO_2 in aqueous solutions of amines, however, in competition with the formation of bicarbonate and carbonate.[2,143,144] These different pathways of reaction are set forth in Figure 24.

The binding to CO_2 at other sites besides the NH_2-terminus within the protein is considered negligible under physiological conditions,[2,140-142] although noncarbamate binding has been reported.[20,145-152] Until the advent of ^{13}C NMR spectroscopy, no other spectroscopic method had been able to detect directly the presence of the carbamates in hemoglobin. Figure 25 shows spectra obtained after equilibration of different hemoglobin solutions with $^{13}CO_2$.[139] In Figure 25A, 13.07 m*M* deoxy human adult hemoglobin was equilibrated with 68 m*M* total carbonates at pH 8.47. Four large narrow resonances are discernible, in addition to the broad protein carbonyl envelope. The largest and most upfield resonance near 32.5 ppm represents dissolved bicarbonate and carbonate, which yield a single resonance due to fast exchange (see Section II). Immediately downfield of this resonance are 3 additional resonances at 29.8, 29.2, and 28.4 ppm, which represent carbamino formation with the β chain NH_2-terminal valine, the α chain NH_2-terminal valine, and one or more ϵ-amino groups of lysine residues, respectively.[139,143] Dissolved CO_2, expected at 68.3 ppm, is not apparent in these spectra due to the high pH (cf. Figure 24).

In Figure 25B, 16.80 m*M* adult carboxyhemoglobin at pH 8.47 was equilibrated with 46 m*M* total carbonates. Strikingly, carboxyhemoglobin displays only two carbamino resonances, in addition to the bicarbonate-carbonate resonance. The small peaks on either side of the bicarbonate-carbonate resonance are artifacts (spinning side bands). The largest carbamino resonance at 29.8 ppm now represents contributions from carbamino formation at the NH_2-terminals of both chains, and the small resonance at 28.4 ppm again represents the ϵ-amino adducts. Clearly, in adult human hemoglobin, the conformation change

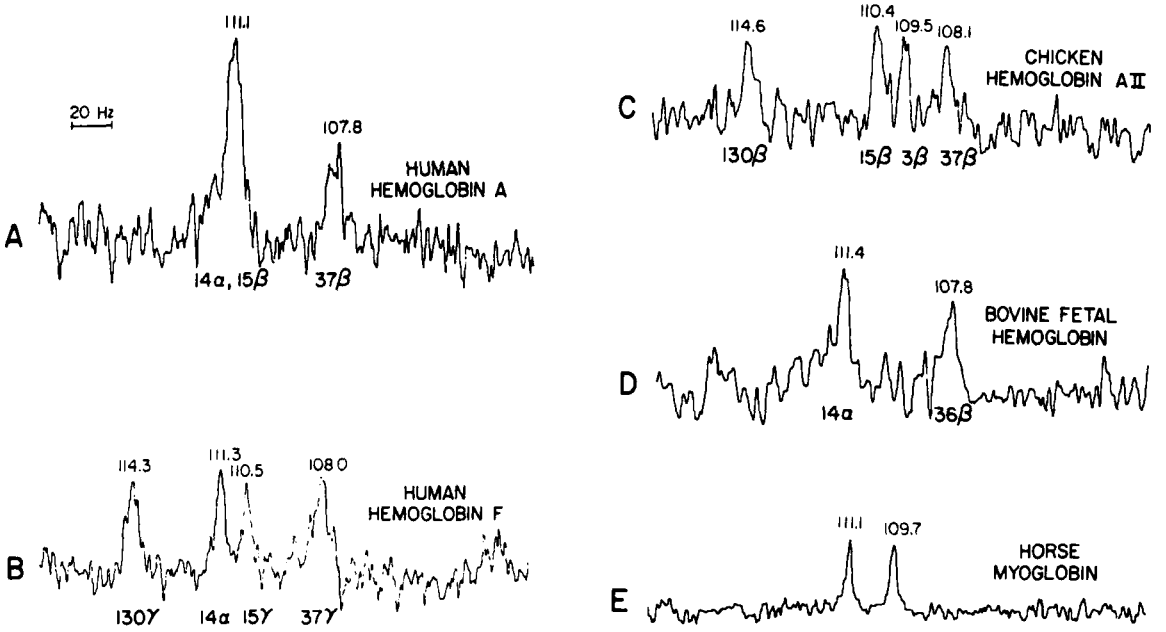

FIGURE 22. Region of C^{γ} resonances of tryptophan residues in natural-abundance ^{13}C Fourier transform NMR spectra of some carbon monoxide hemoglobins and horse carbon monoxide myoglobin in 0.1 *M* NaCl, 0.05 *M* phosphate buffer. Contributions from broad methine carbon bands were removed digitally from the hemoglobin spectra. Chemical shifts are given in parts per million downfield from Me_4Si. A.–Human adult hemoglobin (see Figure 21) fully proton-decoupled. Digital broadening 0.93 Hz. B.–Human fetal (Fo) hemoglobin, 2.3 m*M* in tetramer, at 36°, fully proton-decoupled, after 251,167 accumulations with a recycle time of 1.105 s. Digital broadening, 0.93 Hz. C.–Chicken (A_{II}) hemoglobin 2.6 m*M* in tetramer, pH 7.0, 36°, fully proton-decoupled, 131,072 accumulations with a recycle time of 1.105 s. Digital broadening 1.55 Hz. D.–Bovine fetal hemoglobin, 3.3 m*M* in tetramer, pH 7.0, 36°, fully proton-decoupled, after 98,304 accumulations with a recycle time of 1.105 s. Digital broadening 1.55 Hz. E.–Horse carbon monoxide myoglobin, 9.7 m*M*, pH 6.7, 36°, 32,768 accumulations, 1.105 s recycle time. Digital broadening 0.62 Hz. (Redrawn and reprinted from Oldfield, E. and Allerhand, A., *J. Biol. Chem.*, in press, 1975. With permission.)

accompanying deoxygenation (R → T) removes the degeneracy of the NH_2-terminal adducts characteristic of the R state.

In Figure 25C, ferrihemoglobin at pH 8.23 was equilibrated with 49 m*M* total carbonates. This latter spectrum was recorded at 15.1 MHz, while the other two were recorded at 25.2 MHz. The pattern of resonances is nearly identical to that of the carboxy derivative. Such a result is not unexpected, since the solutions studied here were free of any phosphates, and hence under such conditions ferrihemoglobin would be expected to exist primarily in the R state.[70]

By monitoring carbamino formation at the various sites at different pH values (Figure 26), it was found that the major fraction of CO_2 bound by adult deoxyhemoglobin is carried by the β chain NH_2-terminus.[139] In carboxyhemoglobin, both chains contributed approximately equally to the CO_2 binding, although relative differences in chain affinity of up to 20% could not be excluded. By fitting the measured binding curves to the appropriate mathematical models,[143] estimates of pK_z, the acid dissociation constant for the amine group in question, and pK_c, the carbamate formation constant (Figure 24), were arrived at, as shown in Table 6.

These values may be compared with the best available estimate of pK_c in the literature of 4.62 at 37° calculated for deoxyhemoglobin by Rossi-Bernardi and Roughton.[153] Current theories regarding the origin of the Bohr effect attribute a substantial role (~25%) to a change in the pK_z of the α chain NH_2-terminus.[140,141,154] Estimates of the pK by other methods have been made. Differential titration studies suggest that pK^{α}_{oxy} = 7.3, and pK^{α}_{deoxy} = 7.8.[2] Hill and Davis estimated pK^{β}_{CO} = 6.7 by a kinetic method.[155] Recently Garner et al.[156] determined the individual pK values directly using the rate of

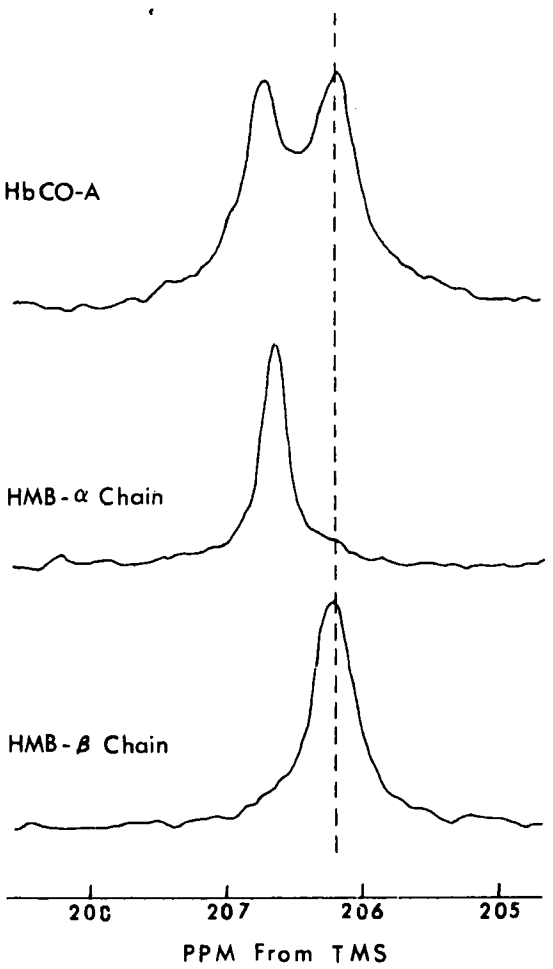

FIGURE 23. Spectra of the ^{13}CO resonances of a sample of intact human adult hemoglobin and the isolated HMB (p-hydroxymercuribenzoate) derivatives of its α and β subunits. (Redrawn and reprinted from Moon, R. B. and Richards, J. H., *Biochemistry*, 13, 3437, 1974. With permission.)

reaction with HNCO as a probe. The values so obtained were $pK^{\alpha}_{CO} = 6.95 \pm 0.13$; $pK^{\alpha}_{deoxy} = 7.79 \pm 0.10$; $pK^{\beta}_{CO} = 7.05 \pm 0.05$; $pK^{\beta}_{deoxy} = 6.84 \pm 0.12$. The values estimated from the $^{13}CO_2$ binding experiments cited above agree satisfactorily with these values.

Since the interaction of CO_2 with the amine groups in hemoglobin is readily reversible, under appropriate conditions exchange rates may be estimated for the various sites directly from the observed NMR spectrum (see Section II). The theoretical ^{13}C NMR spectra produced by two carbamino resonances experiencing exchange with dissolved CO_2 but not with each other nor directly with bicarbonate or carbonate is shown in Figure 27. Estimates of the carbamate dissociation rate in deoxyhemoglobin by potentiometric methods[151] have approximated its value as 500 sec^{-1} at pH values slightly above neutrality. A comparison of the spectra in Figure 27 with experiment (Figure 26) clearly indicates that the dissociation rate in the solutions studied by NMR is much slower, certainly no greater than 10 to 50 sec^{-1}.

The addition of 2,3-DPG or IHP to deoxyhemoglobin solutions equilibrated with $^{13}CO_2$ suppresses the β chain carbamate resonance as expected, but does not shift the resonance position of either the α or the β chain carbamino resonance.[139] Interestingly, the addition of 2,3-DPG markedly retards the formation of the ε-amino adduct in deoxyhemoglobin at pH values less than approximately 9. One may speculate that the appearance of this resonance in deoxyhemoglobin at relatively low pH values may be attributed to a single lysine residue, probably near the DPG binding site, with an abnormally low pK_z value. Lysine 82β may be such a residue (Figure 28).[9]

The results with several hemoglobins other than human adult have displayed a large variability in their response to CO_2 (Figure 29),[139] suggestive that as in their interactions with 2,3-DPG,[157] different hemoglobins may exhibit physiological nonequivalence.

4. Other ^{13}C Labels

Another readily introduced label which may prove useful to the study of hemoglobin is $^{13}CS_2$. As with CO_2, CS_2 reacts reversibly with uncharged amino groups to yield the dithiocarbamate.[158] In Figure 30 is shown the result of adding a saturating amount of 61% ^{13}C enriched in CS_2 to a 10.34 m*M* solution of adult carboxyhemoglobin at pH 6.8. The lower spectrum, A, was recorded immediately after the addition of the $^{13}CS_2$; two resonances are apparent downfield of the large free CS_2 peak at 0.0 ppm. Presumably, these resonances represent the dithiocarbamate adducts on the NH_2-terminals, and possibly some ε-amino adduct. When the spectrum of the same sample was again recorded 24 hr later, numerous additional resonances were apparent, as seen in the upper spectrum, B, of Figure 30. Because of the extreme sensitivity of dithiocarbamates to oxidation, some of these additional resonances undoubtedly represent oxidation products. The possibility that additional sites within the protein are being labeled, however, cannot be excluded.

$$CO_2 + H_2O \rightleftharpoons H_2CO_3 \rightleftharpoons HCO_3^- + H^+; \quad K_1' = \frac{[HCO_3^-][H^+]}{[CO_2]}$$

$$R\text{-}NH_3^+ \rightleftharpoons R\text{-}NH_2 + H^+; \quad Kz = \frac{[R\text{-}NH_2][H^+]}{[R\text{-}NH_3^+]}$$

$$R\text{-}NH_2 + CO_2 \rightleftharpoons R\text{-}NHCOOH \rightleftharpoons R\text{-}NHCO_2^- + H^+;$$

$$Kc = \frac{[R\text{-}NHCO_2^-][H^+]}{[R\text{-}NH_2][CO_2]}$$

FIGURE 24. Scheme of reactions involving CO_2 and amines with definitions of equilibrium constants.

TABLE 6

Values of pK_z and pK_c for Deoxy- and Carboxyhemoglobin

Measurements were made in 0.05 *M* NaCl with ionic strength ranging between 85 to 133 m*M*. Temperature range was 29–32°.

	Deoxy		Carboxy*	
	pK_c	pK_z	pK_c	pK_z
α	4.69 ± 0.12	7.96 ± 0.20	5.57 ± 0.10	6.57 ± 0.22
β	4.64 ± 0.08	6.91 ± 0.32		
ϵ**	4.83 ± 0.16	8.91 ± 0.20	~4.20	~9.87

*Individual resonances not resolved for α and β chains. See text.
**May represent multiple lysine adducts, especially for carboxyhemoglobin.

Adapted from Morrow, J. S., Ph.D. thesis, Indiana University, Bloomington, 1974.

A nonreversible label which is of considerable interest in its own right is cyanate (RHN - $C\lesssim^{NH_2}_{O}$). The reaction of potassium cyanate in vitro with red blood cells of patients with sickle cell disease has been shown to be of value.[159-162] Hemoglobin S so treated demonstrates an increased oxygen affinity and a diminished propensity to gel when deoxygenated. Erythrocytes containing hemoglobin S exhibit an increased mean survival time when so treated.

The pattern of resonances apparent when carboxyhemoglobin S has been reacted with $KN^{13}CO$ (and ^{13}CO) under various conditions is shown in Figure 31.[163] The two closely spaced, large downfield resonances represent ^{13}CO, as previously described. The two $N^{13}CO$ resonances at 161.82 and 160.99 ppm represent the ϵ-amino and α-amino cyanate adducts, and are highly reminiscent of the pattern observed with the similar compound $^{13}CO_2$. Free cyanate, with a resonance expected near 129.17 ppm, was not present in these solutions. From these NMR measurements, it was possible to substantiate directly the enhanced reactivity of the α-amino groups under conditions of approximately neutral pH. Unfortunately, no chemical shift difference was observed between the cyanate adducts of the α and β chain NH_2-termini in carboxyhemoglobin, precluding direct

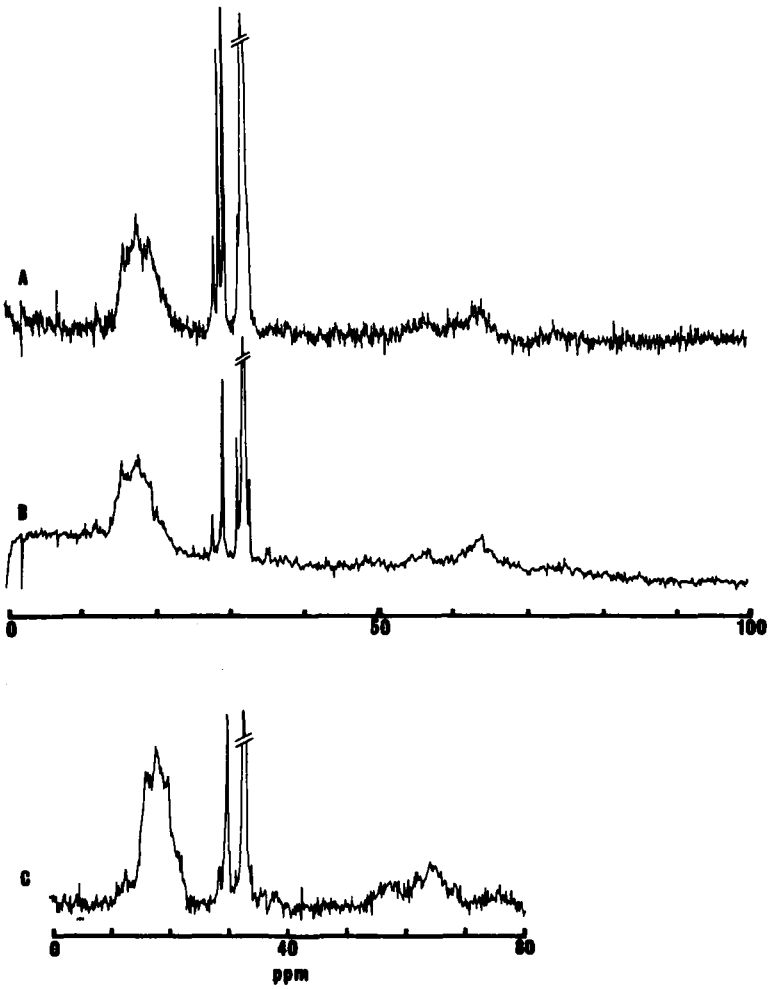

FIGURE 25. ^{13}C NMR spectra of purified hemoglobin A_0 equilibrated with $^{13}CO_2$ in various ligand states. A.–Deoxyhemoglobin, pH 8.47, 68 m*M* total carbonates; B.–carboxyhemoglobin, Ph 8.47, 46 m*M* total carbonates; C.–ferrihemoglobin, pH 8.23, 49 m*M* total carbonates. Spectra A and B were recorded at 23.5 kG, 30°, and spectrum C at 14.1 kG, 33 to 34°. Chemical shifts are relative to CS_2. (From Morrow, J. S., The Interaction of Carbon Dioxide with Amino Acids, Peptides, and Hemoglobin: A study by ^{13}C Nuclear Magnetic Resonance, Ph.D. thesis, Indiana University, Bloomington, 1974.)

monitoring of the extent of reaction at each of these sites individually. Similar experiments on deoxyhemoglobin have not yet been reported. In analogy with the CO_2 results, one might hope that at least for adult deoxyhemoglobin, the α and β chain carbamates would be magnetically nonequivalent.

C. ^{19}F NMR Studies

Several other nuclei have also proved useful to the study of hemoglobin by magnetic resonance. The most fruitful of these has been ^{19}F. The ^{19}F nucleus is an attractive label from the standpoint of both its spin (1/2) and high sensitivity (Table 3). The lack of ^{19}F in native hemoglobin may be conveniently remedied by the reaction of 3-bromo-1,1,1-trifluoropropanone with the accessible βF9 cysteine sulfhydryl, yielding the trifluoroacetonyl group.[164,165] The βF9 cysteine lies at the $\alpha_1\beta_2$ interface, near to 92 βF8 His (the proximal heme ligand) and 94 βFG1 Asp a residue salt-linked to the imidazole of 146 βH24 His in deoxyhemoglobin.[6] The changes which are believed to occur about this site upon ligand binding are shown schematically in Figure 32. Since the α chain is about 10 Å away from this

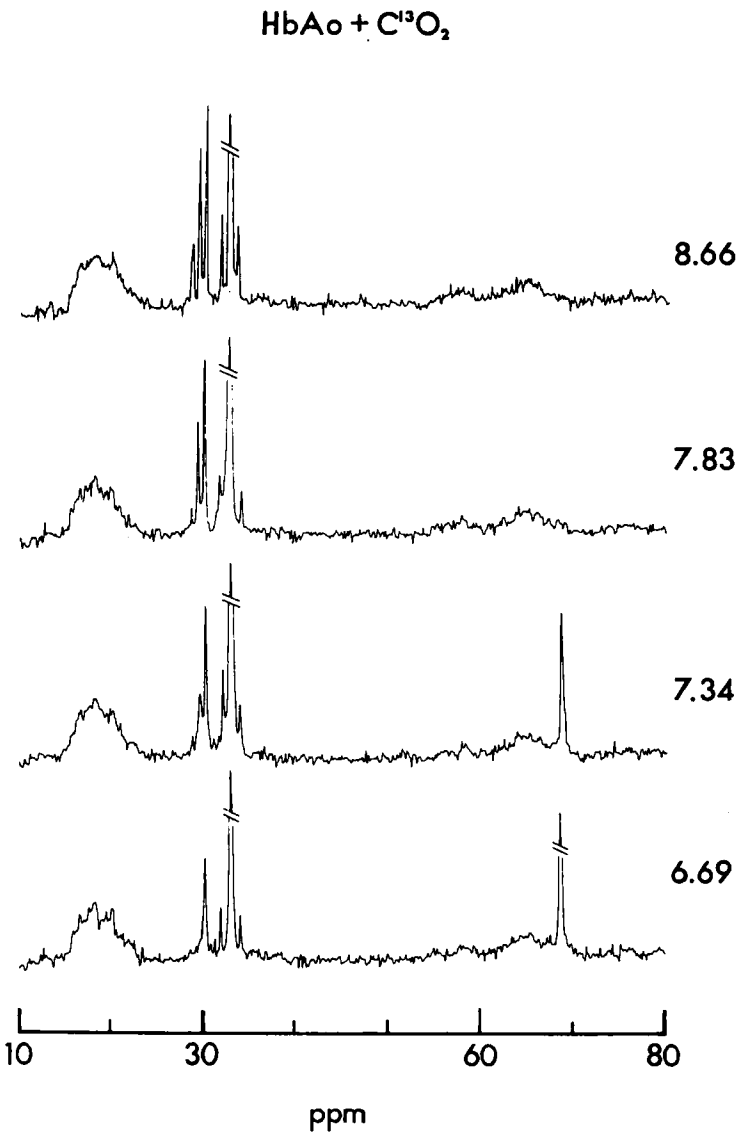

FIGURE 26. ^{13}C NMR spectra of purified hemoglobin A_0 equilibrated with $^{13}CO_2$ at various pH values.

site, it would be expected that a ^{19}F label so placed would primarily be sensitive to tertiary and perhaps quaternary structural changes involving the β chain alone.

In Figure 33 are shown the ^{19}F spectra obtained with a Hb^{TFA} preparation under various degrees of saturation with CO.[165] The addition of 2,3-DPG to such solutions shifts the observed resonance to higher fields in deoxyhemoglobin and in the valency hybrid ($\alpha_2{}^{III\,CN}\beta_2$).[164,165] One fact apparent from the spectra is the slow interchange that the different molecular species responsible for each resonance must undergo, since the resonance position of each peak is independent of the CO pressure. Less obvious is the presence of the small resonances identified as I_2 and I_3 in Figure 33, which were resolved by the aid of a computer fitting procedure.[165] These resonances have formed the basis for the contention that intermediate states such as $\alpha_2{}^{CO}\beta_2$ and $\alpha_2{}^{CO}\beta^{CO}\beta^*$ exist, where β^* is an unliganded β chain with a conformation unlike that found in either fully deoxy or oxyhemoglobin.[165] The invariance in either position or line width of these resonances upon replacement of CO with the more rapidly exchanging O_2 has allowed Shulman et al.

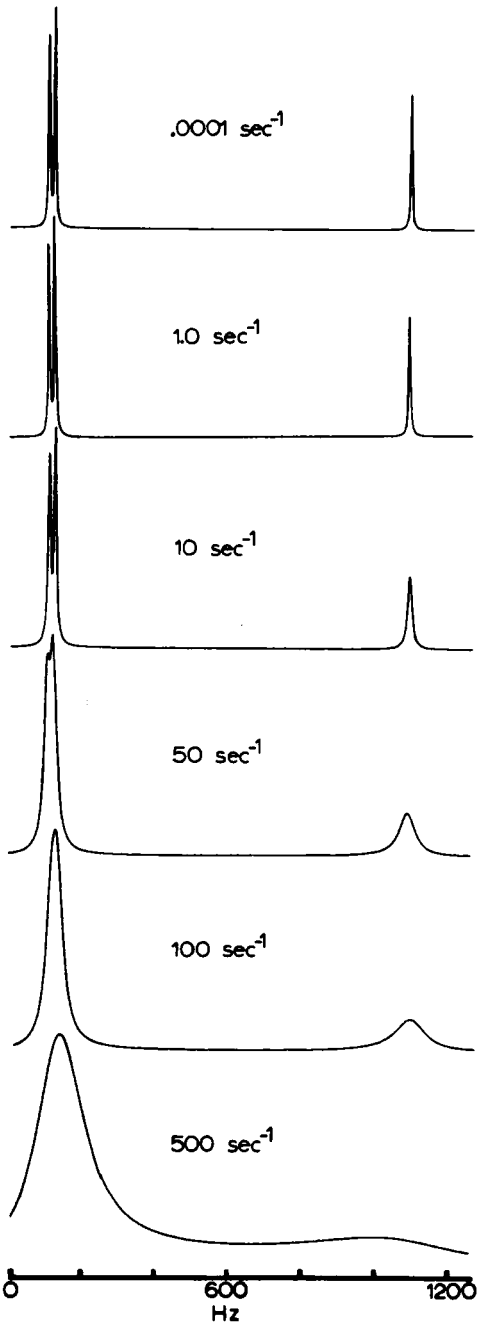

FIGURE 27. Computer simulated spectra illustrating the effects of site exchange between 2 carbamino resonances at 735 and 755 Hz, and dissolved CO_2 at 1720 Hz. The exchange rate between the 2 carbamino resonances was set at 0 in all cases, and the relative populations were held constant at 0.35, 0.40, and 0.25, respectively. The carbamino dissociation rate used for each calculation is listed in the center. (From Morrow, J. S., The Interaction of Carbon Dioxide with Amino Acids, Peptides, and Hemoglobin: A Study by ^{13}C Nuclear Resonance, Ph.D. thesis, Indiana, University, Bloomington, 1974.)

to establish that the species represented by I_2 and I_3 also possess ligand binding properties intermediate to the T and R states.[83] However, further experiments are necessary to verify these resonances and to rule out contributions from dimers.

The TFA label has also been used to monitor the ionization of nearby charged groups within the $\alpha_1\beta_2$ interface, believed to reflect predominantly the imidazole ionization of 146 βH24 His.[69] Measuring the chemical shift changes as a function of pH, an apparent pK_a of 7.4 was determined for this ionization in deoxy Hb^{TFA}.[69] However, the steepness of the titration suggested that other processes were also important, the most probable being cooperative ionization involving nearby charged groups[69] or possibly conformational transitions induced by the pH change.[13]

This value of pK_a equal to 7.4 found by ^{19}F NMR studies of deoxy Hb^{TFA} is difficult to reconcile with the value of 8.0 found for the ionization of the same residue in deoxyhemoglobin by ^1H NMR methods[61] in D_2O. Isotope effects appear unimportant.[61] Moreover, the ^1H NMR studies showed no evidence of cooperative ionizations. It is likely that the effect of 146 βH24 His on the chemical shift of the TFA group is linked not only to its ionization state, but also to its particular geometrical relationship to the label. That the environment of the TFA group changes with pH is strongly implied by the finding that the rate of reaction of pCMB with the 93 β F9 cysteine-SH group shows a fivefold greater pH dependence in deoxyhemoglobin than in the liganded species.[166]

A similar conflict of results between methods also has arisen over the preferential binding of n-butylisocyanide (BIC) to the different subunits of hemoglobin. The ^1H NMR studies,[92] as well as kinetic measurements,[167,168] indicated that the β subunits bind BIC preferentially, while the ^{19}F measurements[169] with Hb^{TFA} were interpreted as providing evidence for preferential binding by the α chains. Structural and functional perturbations caused by the addition of the TFA label cannot be excluded. However, the small differences observed between native and the TFA hemoglobins, when they are systematically compared,[170] diminish the likelihood that such a change is sufficient to account for the discrepancies. What is more likely is that the chemical shift of the ^{19}F label is primarily sensitive to

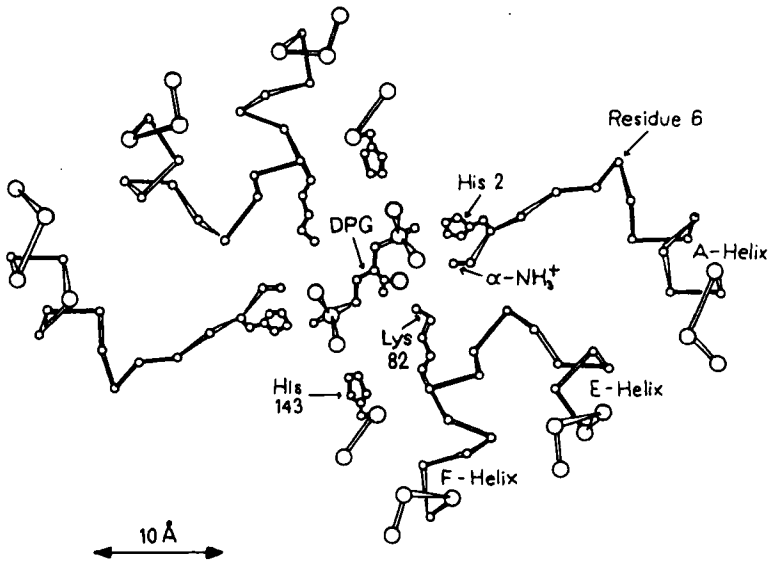

FIGURE 28. Sketch showing the amino- and carboxyl-terminal regions of the β chains of human deoxyhemoglobin. Also depicted is the binding position of 2,3-DPG at this site. (Redrawn and reprinted from Arnone, A., *Nature*, 237, 146, 1972. With permission.)

quaternary conformational changes of the protein rather than simply to local tertiary changes linked only to the ligation state of the β chain.

Edelstein has more explicitly confronted the problem of conformational change by extending the two state model of Monod et al. to the case of hemoglobin with nonequivalent α and β chains.[13] By this model, two functions are defined which describe the transition from the T to the R state. The first is the *saturation function*, $\bar{Y}'$, which defines the fractional ligand saturation of the molecule and which may be resolved into the individual contributions from each chain. Distinct from the saturation function is the *state function*, $\bar{R}'$, which is a measure of the fraction of the tetramers which have shifted from the T to the R configuration. Under this scheme, it was proposed[13] that the ^{19}F resonance of the TFA group, although bound to the β chain, was a more reliable monitor of the state function ($\bar{R}'$) than of the β chain saturation function ($\bar{Y}'$).

A point particularly relevant to all NMR studies of hemoglobin and perhaps illustrated by the foregoing case was also made.[13] Whenever one is dealing with probes which may actually monitor the T → R transition rather than the ligand saturation, extreme caution must be exercised with interpretations postulating preferential binding to either chain.

D. Other Nuclei

^{31}P magnetic resonance has been used in the study of the interaction of 2,3-DPG with hemoglobin,[171] and has also been found to provide a useful indicator of intraerythrocyte pH.[172] As with ^{19}F, ^{31}P is a particularly attractive label from the standpoint of its high magnetogyric ratio and its 100% natural abundance. One drawback of the ^{31}P nucleus, however, is a significant contribution to its relaxation modes by chemical shift anisotropy. While not discussed earlier, this relaxation process is described by a second order term in the magnetic field strength (H_0). Therefore, as higher frequency spectrometers become available, the relative merits of the ^{31}P nucleus may fade due to vastly increased line widths.

The ^{31}P spectrum of 2,3-DPG yields 2 resonances, representative of the 3-phosphate and 2-phosphate moieties for the low field and high field resonances at neutral pH, respectively.[172] In the presence of deoxyhemoglobin, both of these resonances are shifted to lower field, the 2-phosphate being shifted the greater amount, approximately 0.75 ppm.[171] With increasing CO saturation, the phosphate resonances shifted gradually upfield. Moreover, the fraction of DPG released lagged behind the fractional CO saturation, a fact consistent with the interpretation that the intial stages of ligand binding do not perturb

the required deoxy conformation of the β chains.

By a comparison with their ^{19}F results on TFA treated Hb,[164] the authors concluded that the DPG release exactly correlated with the degree of ligation of the β chains, and hence conflicted with the "two state model" in that the species $\alpha_2{}^{CO}\beta^{CO}\beta^{deO_2}$ would bind 2,3-DPG with intermediate affinity. However, as discussed above, if the ^{19}F label monitors the state function rather than the saturation function, then the evidence of the lagging DPG binding is not inconsistent with a two state model.[13,83]

A few studies employing other nuclei have appeared. By comparing the line widths of $^{35}Cl^-$ free and in solutions of oxy, carboxy, and deoxyhemoglobin, and myoglobin, it was determined that in hemoglobin there are at least two classes of chloride binding sites, one of which (the high affinity site) is oxygen linked.[173] Moreover, by studying the competition with ATP, it was determined that the high affinity site for Cl^- binding corresponds to the site of organic phosphate binding.

Attempts have also been made to observe the ^{17}O resonance of oxyhemoglobin[174,175] without success. The low sensitivity of this nucleus and its quadrupole moment, when taken with the fact that it is undergoing rapid exchange between molecules[1] suggests that this resonance in hemoglobin will not soon be observed.

IV. DISCUSSION

A few generalizations may be distilled from the mass of NMR studies discussed in the preceding sections. NMR has done much to establish for the protein in solution the interpretation that direct

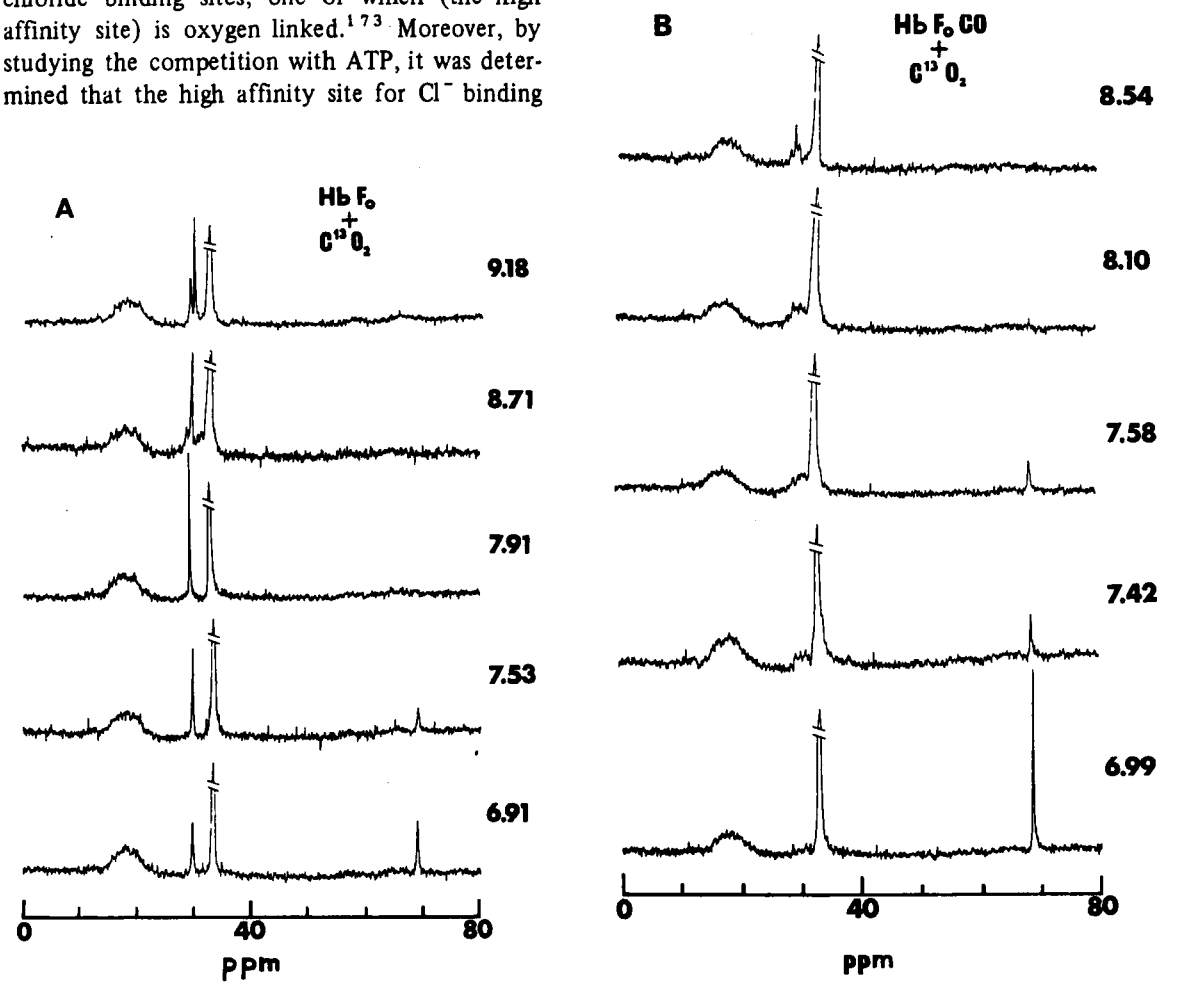

FIGURE 29. ^{13}C NMR spectra of human fetal hemoglobin F_0 equilibrated with 63 m*M* total carbonates in the deoxy state (A) and with 64 mM total carbonates in the carboxy state (B). Protein concentration was 11.3 m*M*; all spectra were proton decoupled. (From Morrow, J. S., The Interaction of Carbon Dioxide with Amino Acids, Peptides, and Hemoglobin: A Study by ^{13}C Nuclear Magnetic Resonance, Ph.D. thesis, Indiana University, Bloomington, 1974.)

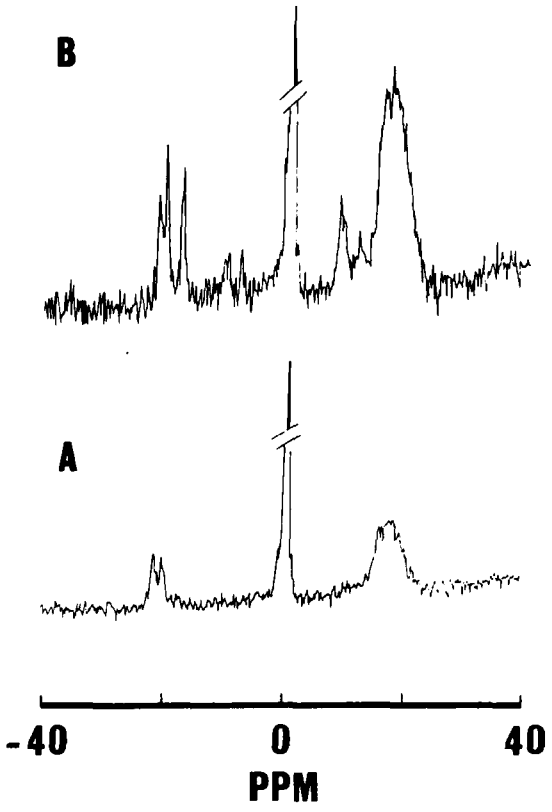

FIGURE 30. Interaction of CS_2 with adult carboxyhemoglobin. The 10.34 m*M* protein solution (referred to heme) at pH 6.8 was treated with a saturating amount of CS_2 enriched to 61% in the ^{13}C isotope. A.—spectrum recorded immediately after the addition of the $^{13}CS_2$. B.—spectrum of the same solution recorded 24 hr later. The free CS_2 is represented by the prominent peak at 0 ppm.

heme-heme interactions are not involved in the thermodynamics of the cooperative transition and that changes are propagated by alterations in interfacial contacts between subunits. The sensitivity of the NMR method to structural parameters has contributed to the recognition of the course of conformational changes within the protein as a function of ligand binding; limits of rate processes have been defined in a few instances. Largely because of the NMR studies, in conjunction with kinetic determinations, it has become clear that to a first approximation, the cooperativity of hemoglobin may be more adequately described phenomenologically by a modified "two-state" model than by a model postulating progressive increases in ligand affinity as each subsequent ligand is bound. This latter model has been termed the induced fit hypothesis.[176] Mathematical models have also been proposed which fit these data well.[177] However, the NMR studies have also demonstrated clearly that intermediate conformational states may exist, as well as more than one form of the "T" or "R" state. Such results serve as a caveat to those who are tempted to believe that the detailed molecular mechanism for the oxygenation of hemoglobin is fully understood.

Rather than reiterate here the various models of ligand binding in hemoglobin that have been developed, this essay will close with a discussion of some of the questions concerning hemoglobin function which NMR might reasonably be expected to address in the near future. The reader interested in the models describing the cooperative transition is referred to the numerous recent and excellent papers on this subject.[11-13,83,178-180]

No other protein has been so intensively studied as has hemoglobin. Indeed, hemoglobin or its closely similar brother myoglobin, have long provided the models *par excellence* against which theories of protein conformation,[181] ionization,[182,183] cooperativity,[11] allostery,[184] and stability[185] have been tested. It is unlikely that this role will soon change. For a protein such as hemoglobin, which can and should be studied in concentrated solutions, the NMR method promises to be a major tool for unraveling further subtleties of function and stability. However, if the method is to accomplish this, single sites in the protein must be observed with sufficient sensitivity that assignments become feasible. As has been discussed in the preceding sections, single site resonances have been observed and assigned in a few instances. As further instrumental improvements are made, it is probable that many further such assignments will become practical at natural abundance of a given isotope, particularly for groups situated near the heme or near other aromatic centers. Obviously, the ability to make such measurements at natural abundance will have many advantages.

A. Enrichment Procedures

The broadest prospect, however, for monitoring single sites within the protein by NMR methods is given by the specific enrichment with respect to an appropriate nucleus. While the easiest such enrichments are gained by the attachment of an extrinsic "labeled" molecule such as the TFA group,

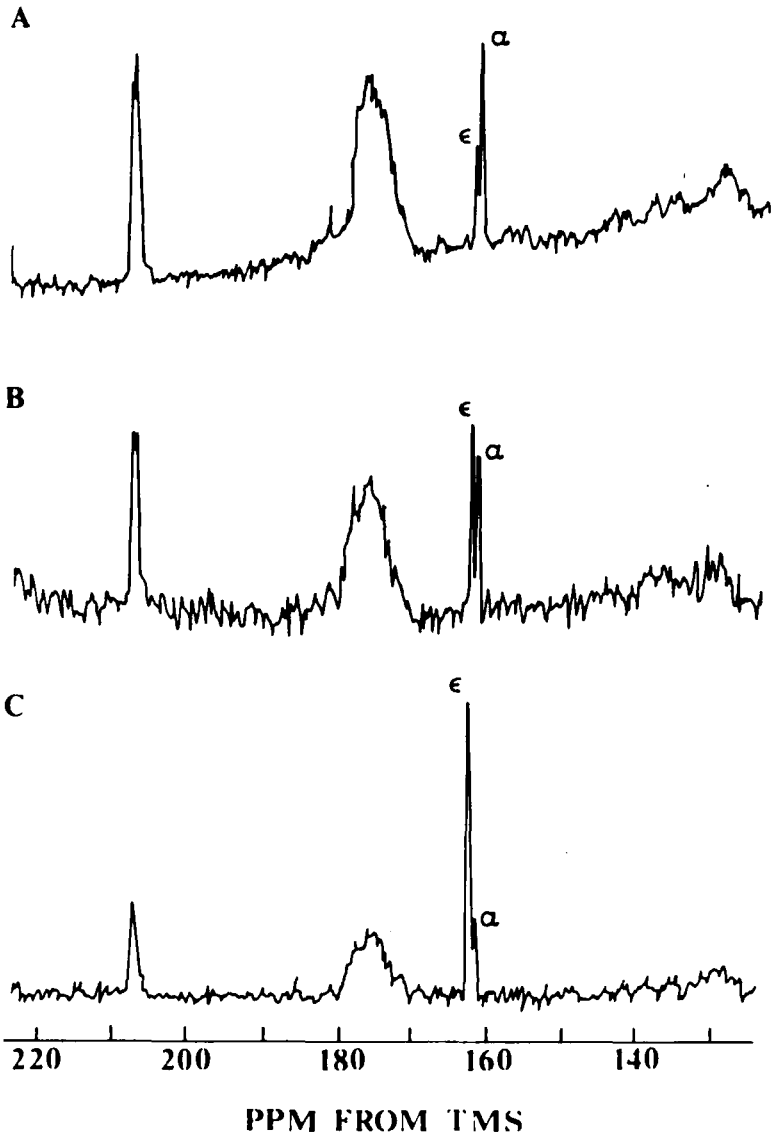

FIGURE 31. Typical spectra of carbamylated (KNCO-treated) carboxyhemoglobin S showing the ^{13}CO resonances near 206 ppm, the broad carbonyl region at 175 to 180 ppm, and the ε- and α-amino carbamyl adduct resonances near 161 ppm downfield of TMS. The reactions were performed on red cell suspensions followed by isolation of the hemoglobin preparations. (Redrawn and reprinted from Moon, R. B., Nelson, M. J., Richards, J. H., and Powars, D. F., *Physiol. Chem. Phys.*, 6, 31, 1974. With permission.)

$N^{13}CO$, or $^{13}CS_2$, the most useful and subtle of enrichments will utilize the substitution of amino acids enriched at specific sites with either ^2H or ^{13}C into the primary sequence. The incorporation of ^2H may be useful in two ways. Extensive replacement of ^1H with ^2H in a protein acts to simplify the resulting ^1H spectrum, significantly facilitating assignments and resolution.[186,187] Such an approach has been successfully employed with staphlococcal nuclease.[188] Alternatively, the ^2H nucleus possesses a nuclear spin of its own, and its resonance may be readily observed under favorable conditions.

In theory, ^2H is a relatively unfavorable nucleus for observation, due to its low magnetogyric ratio (low sensitivity), small chemical shift range, and nonvanishing quadrupole moment (which yields short relaxation times and large line widths). In

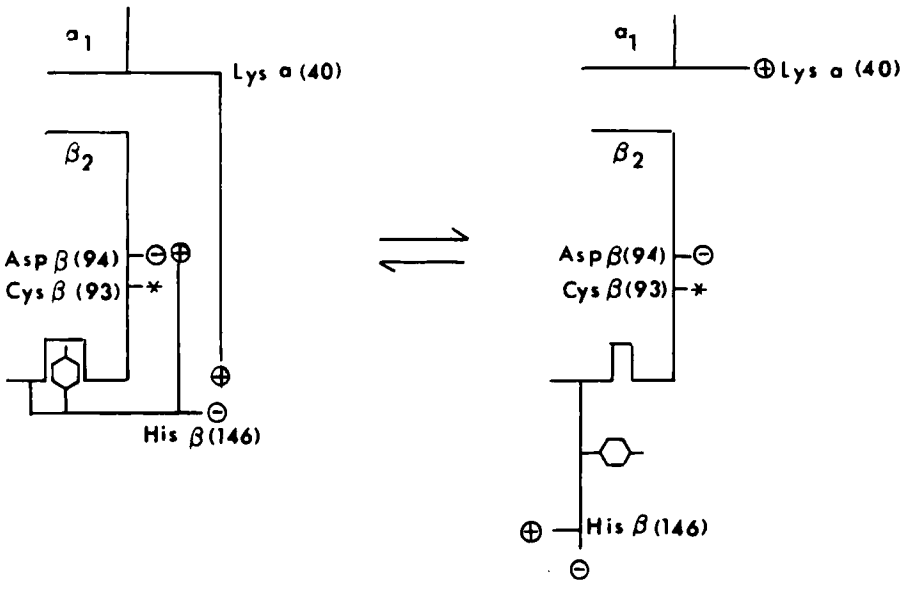

FIGURE 32. Schematic representation, adapted from Huestis and Raftery[162] after Perutz[6] of the conformational equilibrium of the carboxyl terminus of the β chain, showing effects of pH and ligand binding in the $\alpha_1\beta_2$ contact region. The position of the ^{19}F probe is indicated by the asterisk. On the left is pictured the predominant deoxy form; on the right, the predominant oxy form. (Redrawn and reprinted from Huestis, W. H. and Raftery, M. A., *Biochemistry*, 11, 1648, 1972. With permission.)

practice, however, the economics of ^2H substitutions, its ease of incorporation, and the fact that selectively enriched sites are observed in the complete absence of any other resonances often should make ^2H an isotope useful for protein NMR studies. Furthermore, line broadening by paramagnetic centers such as the heme in deoxyhemoglobin or ferrihemoglobin should be minor.[189, 190] These points are illustrated in Figure 34. In this figure the ^2H spectrum is shown[191] of cyanoferrimyoglobin of sperm whale in which the heme has been replaced by one selectively deuterated at the positions shown in Figure 35.[192] The manageable line width seen in Figure 34 depends on the rapid internal rotational motion of the $-CD_3$ groups.[191]

The categories of enrichment strategy to be considered are broadly either biological or chemical. The biological strategies include growth of strains of microorganisms yielding the desired protein, and the use of cell free protein synthesizing systems. The latter type of procedure has proved applicable to mammalian hemoglobins on a small scale.[193] In general, such strategies do not allow pinpointing a given residue position in the protein synthesized since at the least all residues of a given amino acid will be enriched. The potentialities should not be underestimated, however.[186,187,194]

The chemical strategies for enrichment deal either with changes involving side chains or with changes involving the polypeptide sequence itself. In the first category are substitutions with ^2H in some cases,[195] as well as the enrichment of methionine methyl groups with ^{13}C, a method suited to ^2H enrichment as well. An example of such enrichment of the methionine methyl with ^{13}C, again applied to myoglobin, is shown in Figure 36.[196] The twin resonances at 176.77 and 178.15 ppm upfield of external CS_2 represent partial enrichment of the methyl groups of the two methionine residues, 55 and 131, in sperm whale myoglobin. The preparative procedure involves selective methylation with $^{13}CH_3I$ of these residues in the intact apomyoglobin chain, followed by random demethylation with a sulfhydryl compound as methyl group acceptor.[196] In unpublished experiments, T. M. Rothgeb has applied this procedure successfully to the enrichment of the methyl group of the amino-terminal methionine residue in the α chain of chicken hemoglobin A_I.[197]

The second category deals with the general procedure which is to control the polypeptide

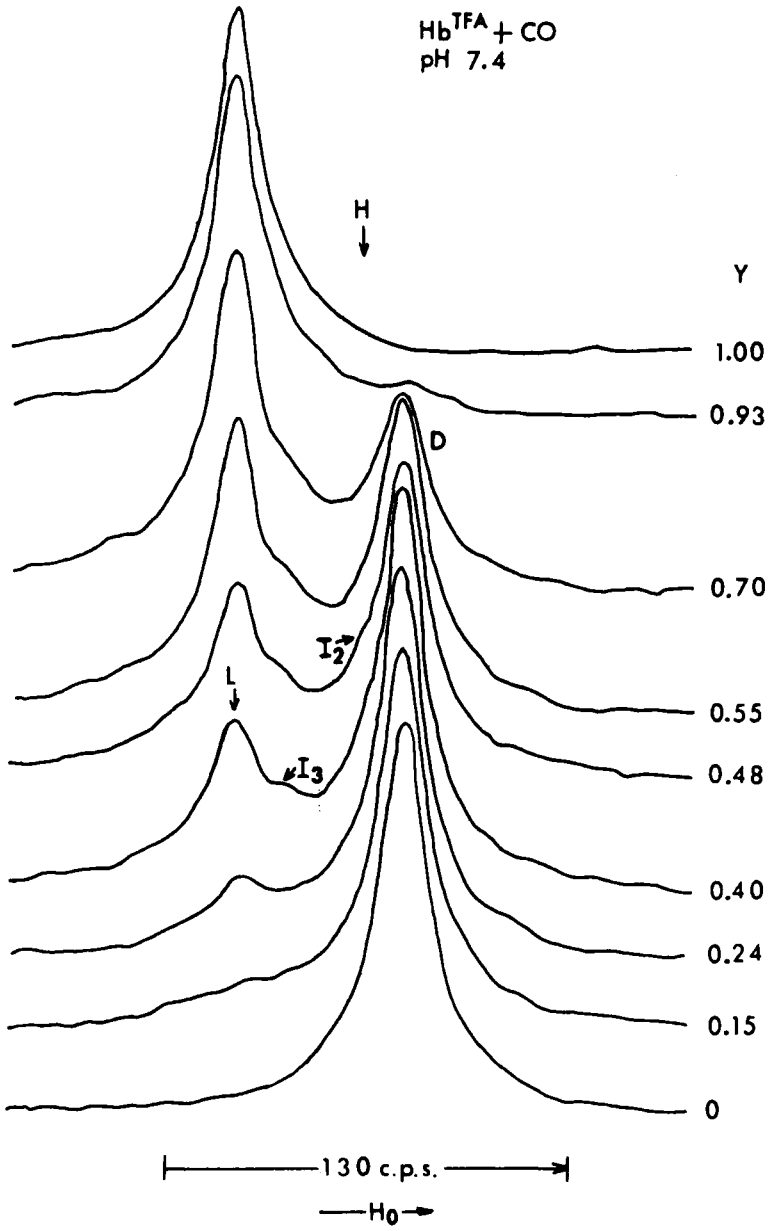

FIGURE 33. ^{19}F NMR spectrum of Hb^{TFA} as a function of increasing fraction bound to carbon monoxide (Y). Peak D is the absorbance due to Hb^{TFA}-deO_2; L is due to Hb^{TFA}-$(CO)_4$; I_2 and I_3 are due to partially liganded intermediate species. The arrow H marks the chemical shift position of the high-affinity (β^*) unliganded form. (Redrawn and reprinted from Huestis, W. H. and Raftery, M. A., *Biochemistry*, 12, 2531, 1973. With permission.)

sequence either by complete chemical synthesis or by semisynthesis. In either case, the complete sequence is obtained by joining fragments that are themselves of known purity. In semisynthesis only part of the polypeptide is reconstructed, and much of it is obtained from fragments prepared from the natural protein. In *ab initio* synthesis to obtain the complete sequence, protective groups and activating functions are built in from the first; the successes have been remarkable with more to be anticipated.[198] Semisynthesis is in principle less heroic and should prove flexible enough to be applied systematically for purposes of isotopic enrichment. Technically it draws a great deal from

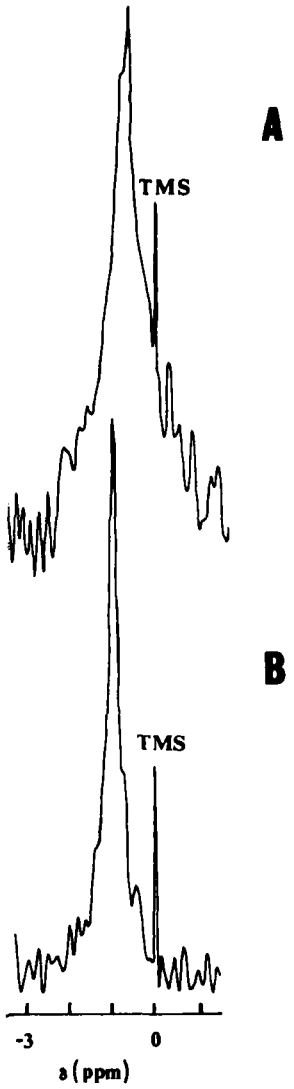

FIGURE 34. Spectra obtained by pulsed Fourier transform ^2H NMR, referred to the resonance position of external D_{12}-TMS (shown overlaid). A. – D_6- diacetyldeutero-hemin-cyanoferrimyoglobin in 0.1 *M* ionic strength phosphate buffer at pH 6.7. B. – D_6-diacetyldeuterohemin-OMe in a mixture of pyridine and water, 0.75 ml and 0.25 ml, respectively, containing 4 mg KCN. (From Oster, O., Neireiter, G. W., and Gurd, F. R. N., *Biochem. Biophys. Res. Commun.*, 64, 1, 1975. With permission.)

such key procedures of total synthesis as the solid phase method of Merrifield.[199]

In certain favorable cases an active protein may be reassembled from fragments that are not rejoined covalently.[200-204] Such systems have been studied with considerable success by NMR following isotopic enrichment.[205-207] Valuable as it is, this approach is not general, and has failed so far with hemoglobin and myoglobin. Furthermore, the discontinuity in the covalent polypeptide chain clearly may be a disadvantage for testing the freedom of conformational adaptability and stability.

The pattern of semisynthesis can be visualized as follows:[208-211] The natural protein is cleaved chemically or enzymatically. Polypeptide fragments are isolated and purified. The protein is reassembled with introduction of residues as desired in one or more fragments. The altered fragments are obtained either by complete synthesis or by substituting certain residues in a natural peptide. The general application of the technique requires protective group strategies that are to some degree specific to semisynthesis. Since the starting materials are mainly intact peptides, it is important to devise methods compatible with aqueous solvents or based on coupling to resins. Both amino groups and carboxyl groups must be protected by suitable reagents at certain points in any general synthesis. Reversible protection of amino groups is conveniently obtained by treatment with methylacetimidate,[211] a reagent that can modify ϵ-amino groups completely while leaving the greater part of the terminal α-amino group unmodified if desired.[211-213] Differential specificity for the α-carboxyl group can be based on the esteratic activity of a peptidase, opening the way for an active ester coupling reaction.[208,214] Much depends on the feasibility of making repeated small adjustments in reaction conditions, testing for completeness of reaction, separation of products, and detailed characterization of the final reconstituted product. The NMR labels themselves are helpful markers for the progress of the chemistry.[211] The inherent tendency of the polypeptide chain segments to associate in appropriate media may help promote the covalent recombination in favorable cases, recently illustrated by Corradin and Harbury with cytochrome c.[215] The strongest examples of such entropic advantage are shown in the proteinase inhibitor systems.[216,217]

In Figure 37 are illustrated the spectra at several pH values of a carbonyl-enriched [^{13}C]-glycine attached to the amino-terminus of sperm whale myoglobin. Because of the sensitivity of the chemical shift of carbons in such a terminal

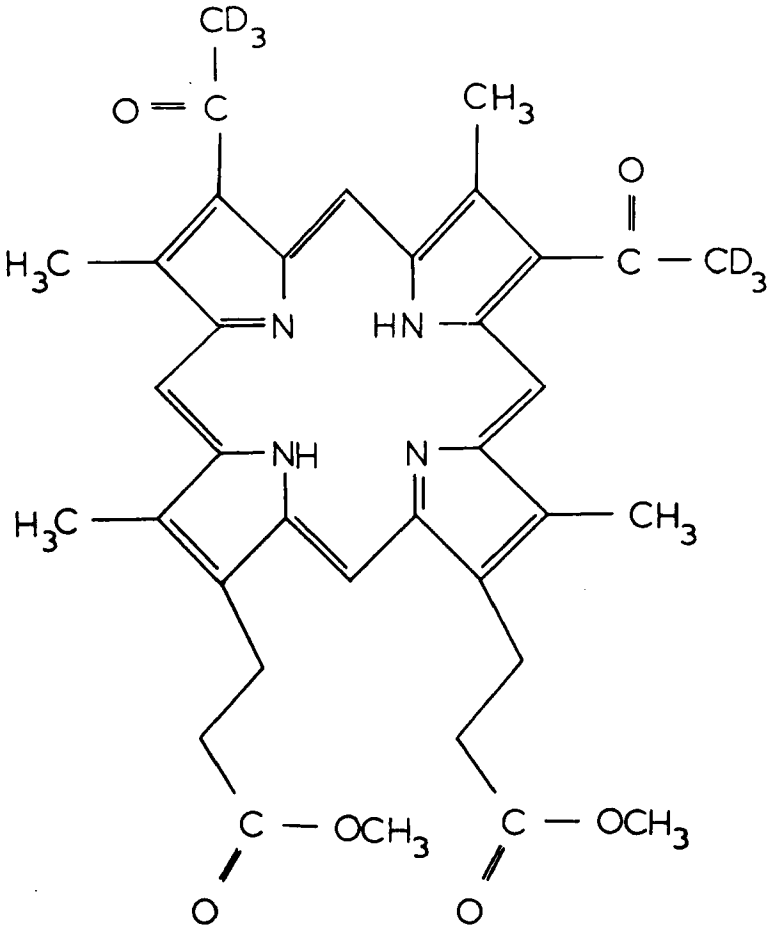

FIGURE 35. Structure of D_6-diacetyldeuteroporphyrin-OMe, the basis for the heme form studied in Figure 34. (From Oster, O., Neireiter, G. W., and Gurd, F. R. N., *Z. Naturforsch.*, 30b, 37, 1975. With permission.)

residue,[117,119] the enriched locus titrates with the state of protonation of the amino group, as illustrated further in Figure 38. Separate measurements of T_1 for the corresponding adduct enriched in the α-carbon of the glycine residue confirm that the adduct undergoes internal rotation in addition to the overall tumbling motion of the protein.[218] The same point has emerged from unpublished experiments by W. H. Garner in which the terminal valine of the sperm whale myoglobin was removed and replaced by enriched glycine. These results correspond with the crystallographic evidence of mobility of the two terminal residues in sperm whale myoglobin.[219]

Other semisynthetic procedures are being developed for myoglobin, and the beginning of hemoglobin β chain applications is in hand. The procedures are appliable not only to the replacement of a residue with the corresponding isotopically enriched form, but to the introduction of residues not native to the given protein species.

The prospect of altering the sequence at will and of being able to introduce enriched residues as desired in the α and β chains opens the full power of the NMR methods to the analysis of hemoglobin structure and function. For many purposes the ^{13}C isotope will be the nucleus of choice. However, ^{2}H will be of interest for sites such as methyl groups in which considerable internal rotational motion may occur. The ^{15}N nucleus should be borne in mind as another spin ½ case that could be explored advantageously by NMR following specific enrichment.

B. Correlation of Chemical Shifts with Structure

Ideally one would like to test the observed

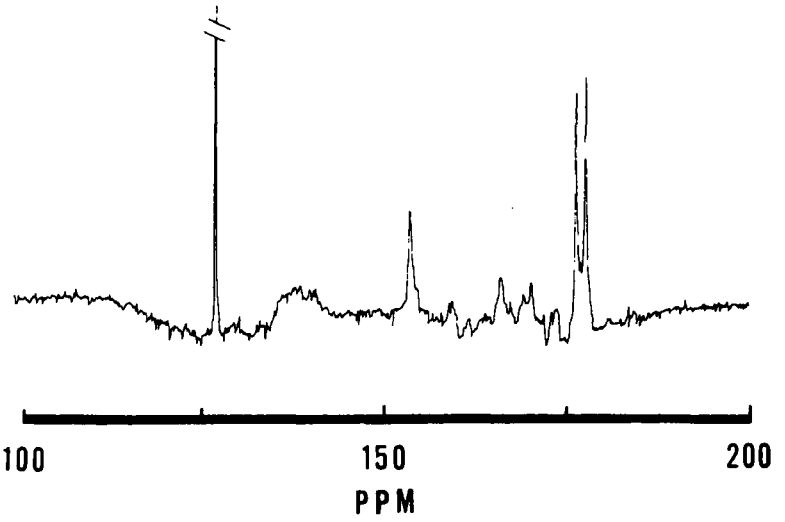

FIGURE 36. Proton-decoupled Fourier transform ^{13}C NMR of carboxymyoglobin prepared with enrichment of the methyl groups of the two methionine residues. Chemical shifts are referenced to external CS_2, with internal dioxane at 126.30 shown as the most prominent resonance. Data were accumulated from 32 K transients with 16 K data points, at 23.5 kG at 30°. The methionine resonances are prominent at 176.77 ppm and 178.15 ppm upfield of CS_2. (From Jones, W. C., Rothgeb, T. M., and Gurd, F. R. N., *J. Am. Chem. Soc.*, 97, 3875, 1975. With permission.)

chemical shifts with ^{13}C enrichment, for example, against shifts predicted from the appropriate crystalline structure. For most cases at present, such predictions will be too approximate to be very valuable. However, satisfactory interpretations may be made when different forms of the hemoglobin are compared, whether they be different molecular species or different conformations of a given molecule.

In practice it appears likely that the most effective correlations will be based on internal evidence developed by the technique itself in which a given nucleus in a given amino acid residue type can be observed in various different positions in the molecule. Comparisons between molecular species can be anchored in the evidence of identity of chemical shift for certain resonances in the different species. Several excellent examples of such identity between species have already been cited in the foregoing sections, including many of the contact shifted ^{1}H resonances as well as the tryptophan ^{13}C resonances. Although the exact quantitative shift values will remain empirically based, the cumulative evidence from numerous concurrently observed specifically enriched sites should serve to correlate the main structural features of the protein in solution with those of the crystal.

C. Interactions with Effectors

The analysis of hemoglobin structure and function through NMR observations of specifically enriched preparations can be discussed under two headings, one dealing directly with effectors and their (external) sites of interaction and the other dealing with the internal sites whose chemical shifts may be sensitive to the state of ligation and effector binding. Appropriate enrichment, usually with ^{13}C, should be particularly valuable in studying the interaction of hemoglobin with the effectors H^+, CO_2 DPG, and IHP, as well as various anions such as phosphate, bicarbonate, and chloride. These interactions are of the greatest importance to hemoglobin function and could be studied readily with and without the presence of various heme ligands. An effective combination would be to have the small molecule or ion be enriched itself, as well as sufficient sites in the protein to monitor the principal and secondary loci of effector interaction and to report on the conformational state of the protein. In the case of H^+, the components of the protein itself provide all the NMR information. In the case of the other effectors, much information can be obtained about binding exchange rates and the extent of binding at equilibrium directly from the NMR observations on the effector molecule itself.

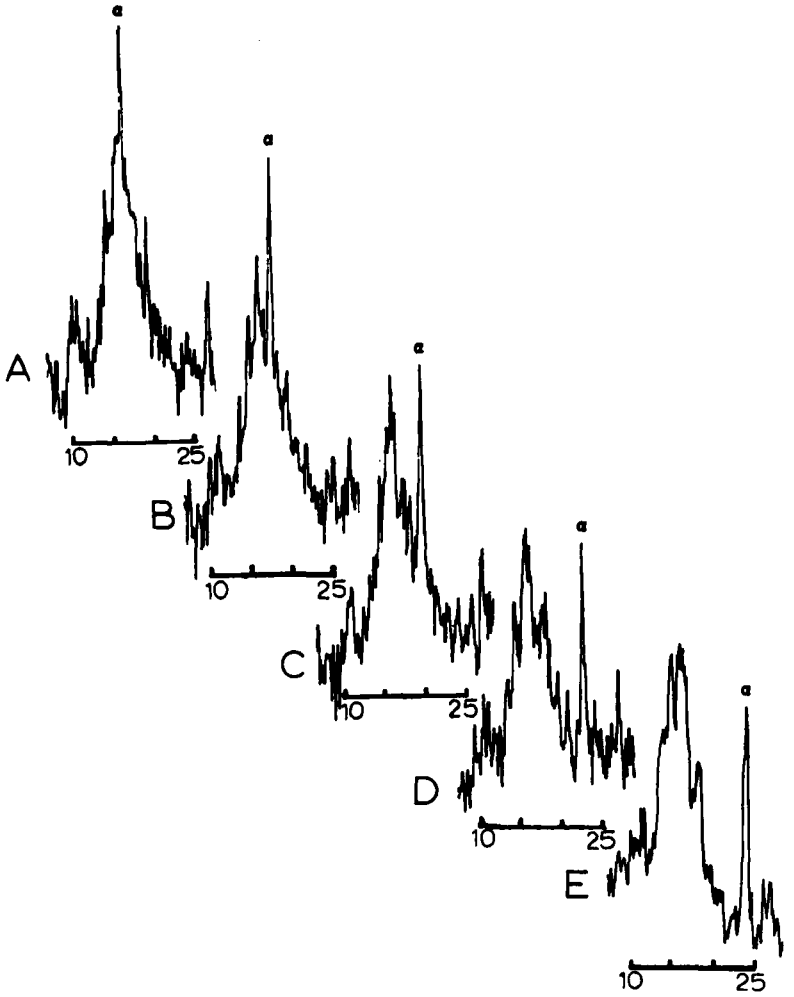

FIGURE 37. ^{13}C Fourier-transform nuclear magnetic resonance spectra of N^{α}-[1-^{13}C] glycylmyoglobin at various pH values; A.–pH 9.27; B.–pH 8.82; C,–pH 7.99; D.–pH 7.11; E.–pH 6.48. The single adduct peak is marked α. Proton-decoupled spectra were accumulated 16,384 times at 32 ± 1°. Recycle time was 1.6 s. Protein concentration was 3.2 m*M*. Chemical shifts are expressed upfield of external CS_2, with internal dioxane standards in every case taken as 126.2 ppm. (From Garner, W. H. and Gurd, F. R. N., *Biophys. Biochem. Res. Commun.*, 63, 262, 1975. With permission.)

The enrichment of sites such as terminal regions of the chains has obvious value for monitoring the binding sites of the effectors listed. For example, with appropriate labeling of the amino-terminal residues of both α and β chains (cf. Figure 37) it should be possible to follow the individual CO_2 adducts[143] even in the liganded form of the protein where the carbamino resonances are not themselves distinguishable (cf. Figure 25).

In addition to making possible the determination of the stoichiometry of reactions of effectors at individual sites under given conditions, the method would have other immediate applications. First, it would be possible to monitor subtle responses to conformational changes or to binding of heme ligands, and to correlate the sequence and timing of these changes with the gross R-T conformational transition. Second, it would be possible to monitor changes in reactivity with substitutions in the protein sequence in the region of the site of interest (see Table 2 and Figures 12, 28, and 32). Third, it would be possible to monitor effects of ionic strength and ion competition that are difficult to follow by less direct methods.

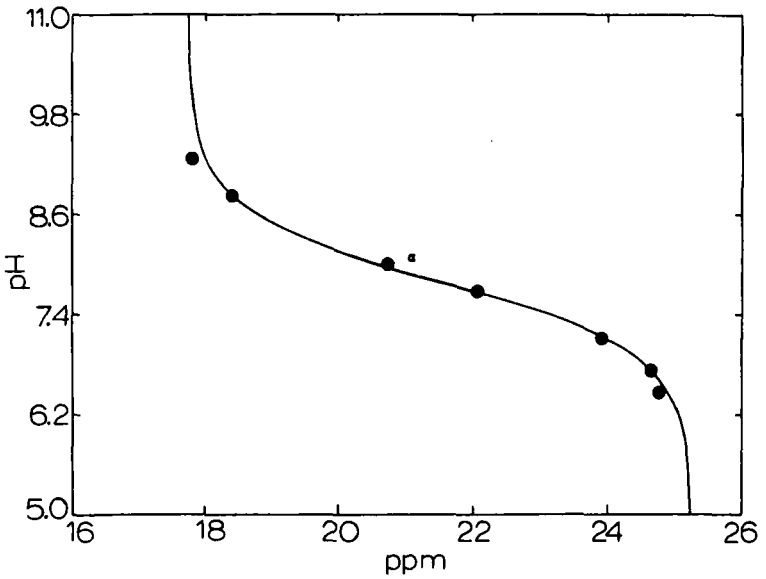

FIGURE 38. Dependence on pH of the chemical shift of the adduct resonance shown in Figure 37. Chemical shift values were taken from computer channel positions. The curve is theoretical according to the Henderson-Hasselbalch equation. (From Garner, W. H. and Gurd, F. R. N., *Biophys. Biochem. Res. Commun.*, 63, 262, 1975. With permission.)

D. Internal Residues

Residues that are neither part of effector binding sites nor near the heme are well worth monitoring for the information that may be obtained about the propagation of changes brought on by ligand or effector binding. In the absence of specific enrichment, however, such residues are usually unresolved and hence inaccessible to NMR examination. The residues that are in contact with solvent in a given conformational state will be accessible to dissolved reagents including the effectors discussed above. Some degree of distinction between external and internal sites in the dissolved protein can be obtained through preferential changes in the resonances of the former in the presence of free radicals that do not bind to the protein. An unanchored organic "spin label" will usually be more reliable for this purpose than a paramagnetic metal ion.[220] The pattern of response of internal residues to structural changes in hemoglobin should help greatly to follow the progression of the R-T transition. It may also prove valuable for detecting intermediate forms not conforming strictly to the Monod-Wyman-Changeux hypothesis.

E. Motions within the Molecule

The rates of transitions within the hemoglobin molecule, although not specified by the crystallographic information, are clearly of the greatest importance for function. As has already been demonstrated, under appropriate conditions NMR measurements can provide direct information about rates of exchange or interconversion between forms. It is useful to discuss here the general problem of motions within a molecule such as hemoglobin and the role of NMR in recognizing their existence.

Relaxation measurements for ^{13}C fit a model for both myoglobin and hemoglobin in which the α-carbons are viewed as being relatively rigid within the protein framework and undergoing rotational reorientation controlled by the tumbling of the protein according to Equation 15. The correlation time for overall reorientation, τ_R, is approximately 40 nsec for hemoglobin at 30°.[51] This conclusion does not rule out some internal freedom of certain individual α-carbons.

Deviation of both myoglobin and hemoglobin from rigid invariant structures has long been recognized. In the first place, access to the heme iron atom by O_2 or other ligands is restricted or shows other evidence of having a complex reaction pattern.[1,27,51,219,221-226] Second, various compounds such as xenon, cyclopropane, and mercury triiodide penetrate the protein molecule readily

even in the crystalline array and lodge themselves in an interior pocket. This process is accompanied by displacement of side chains by bond rotation to produce a locally different protein conformation.[227,228] Third, changes in reactivity patterns between the crystalline and dissolved states of myoglobin have been observed[226,229] and other evidence of structural transition has been adduced.[230] Fourth, exchange of ^{2}H or ^{3}H with hydrogen atoms in the interior of the molecule occurs at limited rates.[231,232] All of these processes require motions at some depth within the molecule, as well as the expected motion of side chains that actually project into the surrounding solvent. The motional requirements for penetration need not be identical with those that contribute most directly to the relaxation effects sampled by ^{13}C NMR measurements.

A body of NMR evidence for myoglobin as well as some for hemoglobin indicates that methyl groups have considerable freedom to spin in the intact molecule, that bulky aromatic side chains are much more limited in rotational freedom, and that some other side chain components constitute a class of intermediate rotational freedom.[51,196,221]

Two aspects of the hemoglobin or myoglobin structure may facilitate the motion of carbons not protruding into the solvent. The first is the presence of cavities within the structure.[222] An obvious process to facilitate internal rotational motions is cavitation, and the statically identified cavities may well allow more or less continuous small movements or may themselves undergo intermittent extension to a size into which even a group of some bulk may twist. The second aspect of the structure is the ease with which surface side chains may rotate to protrude into the surrounding solvent.[221] Since the components of nonpolar side chains are not subject to direct polar constraints, they should be favored candidates for such behavior. The classification of Lee and Richards, moreover, lists about 60% of the valine, leucine, and isoleucine residues in myoglobin, taken together, as touching the surface.[222] For them to gain considerable rotational freedom would require relatively small departures from the crystallographic structure in many cases. It is tempting to look upon such motion as a reasonable prelude to the more cooperative effects required for the penetration processes alluded to several times above or for the structure adjustments involved in conformational transitions and ligand interactions.

Motions within a molecule that can be detected by NMR involve rotational reorientation generally appreciably more rapid than that of the overall tumbling of the protein. For hemoglobin this means contributing correlation times of the order of 1 nsec or less. Detecting and pinpointing the motion can be very useful even when the details of rotations about the different bonds in a side chain are not interpretable conclusively.[49] The freedom to rotate will express itself in two particularly important ways.[51] First, it will go with the fluidity that allows the local or longer range, interlinked movements within the subunits and the sliding motions between the subunits. In dealing with the fluidity of the mobile, imperfectly packed,[233] internal structures, Lumry has used the apt expression "mobile defect."[234] In comparison with small model systems one may also anticipate that the proteins will contain some regions or foci of particularly limited freedom.[235] Second, the nature of the rotational motion of side chains making up the outermost boundary of any protein will have a general bearing on the behavior of active sites with respect to (a) the adaptation to the arrival of a substrate or interacting molecule, and (b) the ability to provide directed kinetic motion during a chemical reaction.

F. Thermodynamic Considerations

The prospect of being able to monitor directly some features of these motions within the intact protein is quite exciting. To appreciate this, one need only consider the factors which determine the stability of any given conformation of the protein in solution. An excellent review of protein stability is given by Tanford.[236,237]

Briefly, a protein may be considered as existing in any given state, as opposed to an alternate or denatured state, as the result of a balance of interactions involving both entropic and enthalpic components. For hemoglobin, the two states of primary interest are "T" and "R". If the allosteric equilibrium constant for the interconversion of the two forms in the absence of ligands is defined by $L = [T]/[R]$, for $R \rightleftharpoons T$, then the free energy of the conformational change above, irrespective of ligand binding, is determined by the relation

$$\Delta G = -RT \ln L. \quad (25)$$

The free energy change may also be expressed more generally as:

$$\Delta G = \Delta G_{conf} + \sum_i \Delta g_{i\ int} + \sum_i \Delta g_{is} + \Delta W_{el} \quad (26)$$

The terms $\Sigma\Delta g_{i\ int}$ and $\Sigma\Delta g_{is}$ represent summations over the free energy differences between states for i groups within the protein, due to short-range internal interactions and short range solvent interactions respectively. The latter term probably contributes little to the R ⇌ T transition, although it does become significant for native ⇌ random coil transitions.

Of greater interest is the ΔG_{conf} term, or the "order-disorder term." This term represents the contributions to the free energy arising from the degrees of randomness available to the atoms of the molecule. This randomness, of course, has its origins in the rotation that occurs about single bonds of the polypeptide backbone and side-chain groups.[238,239] Besides these entropic contributions to ΔG_{conf}, however, there are also enthalpic components arising from the fact that different rotation angles have unequal energy. Thus, one rotational angle may be greatly favored over the others, diminishing the entropy but introducing enthalpic considerations. Since the free energy minima themselves are often not sharp, mobility in a given rotational state will increase both the enthalpy and entropy over that expected for the crystal structure. The general expression for ΔG_{conf} is thus[237]

$$\Delta G_{conf} = \Delta H_{conf} - T\Delta S_{conf} \quad (27)$$

Satisfactory estimates of ΔG_{conf} have not been possible. In the limiting case of the transition from a rigid native protein to a random coil, ΔG_{conf} has been estimated to be prohibitively large and negative.[236] Little is known of the contribution of ΔG_{conf} to the R ⇌ T transition in hemoglobin. X-ray studies have suggested that the factors determining the relative stability of the R or T states are concentrated in the interactions occurring at the $\alpha_1\beta_2$ and $\alpha_2\beta_1$ interfaces.[6,7,240] Salt bridges are believed to play a significant role in stabilizing the T state, several of which bridges must be broken when going to the R state. The contributions to ΔG arising from salt bridges would be included in the remaining term in Equation 26, ΔW_{el}.

ΔW_{el} represents the contributions to the free energy due to the long-range electrostatic interactions. These are primarily the Coulombic interactions between charged groups, groups which may exert measurable effects over a considerable distance.[183,237] The magnitude of this term will be pH dependent. Electrostatic interactions may be an important factor in determining the sharpness of the free energy minima limiting the mobility of charged side chains.

Since the motions that can be detected by NMR are often the same as those involved in the "order-disorder term," the motion at several different loci may be monitored, and then by comparing the changes in this motion between ligand states, a determination of some of the groups which are contributing to ΔG_{conf} in the R ⇌ T transition should be possible. In favorable cases, it may even be possible to estimate the entropic contributions based on a comparison with limiting models. For example, it has been estimated that ΔG_{conf} for a lysine side chain, when passing from a completely immobilized state with no degree of freedom to a completely random state is -3.9 cal/mol.[238,239] It goes without saying, however, that the model of completely immobilized conformation of any structural element in any state of hemoglobin will often be inappropriate. Indeed, the stability of a native protein will depend in part on the thermodynamic consequences of its normal internal motions.

Of particular interest would be the influence of ligands per se, in the absence of the R ⇌ T transition, on the mobility of groups near the heme. Suitable systems for studying such changes would include the valency hybrids, as well as those mutant hemoglobins which can retain the deoxy structure regardless of ligation state (such as hemoglobin M Iwate). Significant changes in mobility, and hence ΔG_{conf}, subsequent to ligand binding may be important in destabilizing the T state and initiating the sequence of events leading to the flip between conformations.

G. Conclusion

Finally, the NMR techniques are peculiarly well adapted to measurements under conditions of physiological interest. As pointed out already, the high concentration within the red blood cell is compatible with these techniques. Furthermore,

the methods are compatible with measurements of effector binding at physiologically important levels and in realistic electrolyte media.[1,2,137-154,241,242] A certain amount of kinetic information may come out of such measurements. The introduction of stopped flow techniques in NMR is intriguing in this connection.[243] Particularly important is the prospect of observing the consequences of CO_2 binding, both within the range of normal metabolic variation in the transit cycle of the red cell and under conditions corresponding to respiratory or metabolic abnormality.[244] The adaptive and regulatory consequences[245] of the finite dissociation rate of carbamino adducts can be explored in detail with the help of ^{13}C NMR techniques, as outlined above.[144] Lastly, the NMR techniques can be applied with some success to red cell suspensions,[51,111,131,172] and in the long run it should be feasible to reincorporate modified or enriched hemoglobin preparations into suitably treated red cell ghosts.[246]

ACKNOWLEDGMENTS

We wish to acknowledge helpful discussions with G. Ackers, J. T. Edsall, G. I. H. Hanania, B. S. Hartley, A. B. Hastings, F. Haurowitz, B. E. Offord, M. F. Perutz, R. Lumry, and A. Szabo, as well as the patience of A. Allerhand, R. G. Shulman, T. Vänngård, and K. Wüthrich in guiding us into magnetic resonance techniques. The advice and cooperation of many colleagues in the laboratory, notably R. A. Bogardt, M. H. Garner, W. H. Garner, P. Keim, J. B. Matthew, T. M. Rothgeb, R. Ruth, R. B. Visscher, and R. J. Wittebort is gratefully acknowledged. A. Allerhand kindly made available results in advance of publication. The assistance of A. O. Clouse, T. Roseberry, and R. Addleman is much appreciated.

GLOSSARY

T – The unliganded state of hemoglobin.

R – The liganded state of hemoglobin.

A to H – Helix designations in α and β chains of hemoglobin. Taken with a number, e.g., E11, the symbol represents the 11th residue in the E-helix. Interhelical segments are indicated by the two bounding helix letters. A numeral immediately following α or β indicates the overall sequence number in the particular subunit chain.

α^{III}, β^{II} – Symbols to indicate oxidation level of iron in valency hybrid hemoglobins identified according to the subunit incorporating the particular heme form. Symbol for a ligand may follow immediately.

2,3-DPG – 2,3-Diphosphoglycerate.

IHP – Inositol hexaphosphate.

ΔE – An energy separation between states.

E_i – A particular energy level.

P_i – A population of spins in an energy level. The fractional population of spins in a given magnetic environment.

γe – Electron magnetogyric ratio.

NOE – Nuclear Overhauser enhancement factor.

TMS – Tetramethylsilane.

DSS – 2,2-dimethyl-2-silapentane-5-sulfonate.

H_0 – Applied external magnetic field.

H_1 – Various radio frequency fields as designated in the text.

h – Planck's constant = 6.62554×10^{-27} erg·sec.

$\hbar$ – Planck's constant divided by 2π.

I, S – Spin quantum numbers usually of nucleus and electron, respectively.

k – Boltzmann's constant = 6.62377×10^{-16} erg·deg^{-1}.
k_i – First order dissociation rate constant.
$\bar{M}$ – Net macroscopic magnetization; subscripts (without the bar) refer to components along the coordinate axes.
T – Absolute temperature.
T_{1_i} – Spin–lattice relaxation time (sec); subscript "i" refers to specific relaxation mechanisms.
$T^*_{2_i}$ – Spin–spin relaxation time; subscript refers to specific relaxation mechanism and superscript * (if present) refers to inclusion of field inhomogeneity and spectrometer instability.
W_{ij} – Transition probability per unit time for exchange between spin states i and j.
γ_N – Magnetogyric ratio of nucleus N.
μ_N – Magnetic moment of nucleus N.
ν – Frequency in sec^{-1}; subscript "o" refers to the resonance or Larmor frequency and all other subscripts are defined in the text.
τ_i – Mean residence time of an exchangeable nucleus in site i.
τ_c – Generalized correlation time.
τ_e – Correlation time for electron-nuclear scalar interactions.
τ_{eff} – Effective correlation time; "effective" includes anisotropic or internal motion or other motional factors not explicitly separable by analysis.
τ_R – Rotational correlation time for overall molecular motion.
ω_i – Frequency in radians sec^{-1}; subscript "o" refers to the resonance or Larmor frequency and all other subscripts are defined in the text.
Q – Electric quadrupole moment.
pCMB – p-Chloromercuribenzoate.
TFA – Trifluoroacetonyl.
X_0 – Static nuclear magnetic susceptibility.
β – Bohr magneton.

REFERENCES

1. **Antonini, E. and Brunori, M.,** *Hemoglobin and Myoglobin in Their Reactions with Ligands,* North-Holland Publishing, London, 1971.
2. **Kilmartin, J. V. and Rossi-Bernardi, L.,** Interaction and hemoglobin of hydrogen ions, carbon dioxide, and organic phosphates, *Physiol. Rev.,* 53, 836, 1973.
3. **Lehmann, H. and Huntsmann, E. G.,** *Man's haemoglobins,* Lippincott, Philadelphia, 1966.
4. **Perutz, M. F. and Lehmann, H.,** Molecular pathology of human haemoglobin, *Nature,* 219, 902, 1968.
5. **Perutz, M. F., Muirhead, H., Cox, M., and Goaman, C. G.,** Three-dimensional Fourier synthesis of horse oxyhaemoglobin at 2.8 A resolution: the atomic model, *Nature,* 219, 131, 1968.
6. **Perutz, M. F.,** Stereochemistry of cooperative effects in haemoglobin, *Nature,* 228, 726, 1970.
7. **Perutz, M. F. and Ten Eyck, L. F.,** Stereochemistry of cooperative effects in hemoglobin, *Cold Spring Harbor Symp. Quant. Biol.,* 36, 295, 1971.
8. **Perutz, M. F.,** Nature of haem-haem interaction, *Nature,* 237, 495, 1972.
9. **Arnone, A.,** X-ray diffraction study of binding of 2,3-disphosphoglycerate to human deoxyhaemoglobin, *Nature,* 237, 146, 1972.
10. **Perutz, M. F., Heidner, E. J., Ladner, J. E., Beetlestone, J. G., Ho, C., and Slade, E. F.,** Influence of globin structure on the state of the heme. III. Changes in heme spectra accompanying allosteric transitions in methemoglobin and their implications for heme-heme interaction, *Biochemistry,* 13, 2187, 1974.

77. Davis, D. G., Lindstrom, T. R., Mock, N. H., Baldassare, J. J., Charache, S., Jones, R. T., and Ho, C., Nuclear magnetic resonance studies of hemoglobins. VI. Heme proton spectra of human deoxyhemoglobins and their relevance to the nature of co-operative oxygenation of hemoglobin, *J. Mol. Biol.*, 60, 101, 1971.
78. Haber, J. E. and Koshland, D. E., Jr., Evidence for β-β interactions during the binding of oxygen to hemoglobin, *Biochim. Biophys. Acta*, 194, 339, 1969.
79. Brunori, M., Amiconi, G., Antonini, E., Wyman, J., and Winterhalter, K. H., Artificial intermediates in the reaction of haemoglobin. Functional and conformational properties of the cyanmet intermediates, *J. Mol. Biol.*, 49, 461, 1970.
80. Shulman, R. G., Ogawa, S., Mayer, A., and Castillo, C. L., High-resolution proton NMR studies of low affinity hemoglobins, *Ann. N.Y. Acad. Sci.*, 222, 9, 1973.
81. Mayer, A., Ogawa, S., Shulman, R. G., and Gersonde, K., High resolution nuclear magnetic resonance studies of the quaternary state of hemoglobin M Iwate, *J. Mol. Biol.*, 81, 187, 1973.
82. Greer, J., Three-dimensional structure of abnormal human haemoglobins M Hyde Park and M Iwate, *J. Mol. Biol.*, 59, 107, 1971.
83. Shulman, R. G., Hopfield, J. J., and Ogawa, S., Allosteric interpretation of hemoglobin properties, *Quart. Rev. Biophys.*, in press, 1975.
84. Kurland, R. J., Davis, D. G., and Ho, C., Paramagnetic proton nuclear magnetic resonance shifts of metmyoglobin, methemoglobin, and hemin derivatives, *J. Am. Chem. Soc.*, 90, 2700, 1968.
85. Lindstrom, T. R., Baldassare, J. J., Bunn, H. F., and Ho, C., Nuclear magnetic resonance and spin-label studies of hemoglobin Kempsey, *Biochemistry*, 12, 4212, 1973.
86. Davis, D. G., Mock, N. H., Lindstrom, T. R., Charache, S., and Ho, C., Nuclear magnetic resonance studies of hemoglobins. V. The heme proton spectra of human deoxyhemoglobins A, F, Zürich, and Chesapeake, *Biochem. Biophys. Res. Commun.*, 40, 343, 1970.
87. Ho, C., Lindstrom, T. R., Baldasssare, J. J., and Breen, J. J., Magnetic resonance studies of human hemoglobins and their implications to the structure-function relationships in human normal and abnormal hemoglobins, *Ann. N.Y. Acad. Sci.*, 222, 21, 1973.
88. Breen, J. J., Bertoli, D. A., Dadok, J., and Ho, C., Proton magnetic resonance studies of human adult hemoglobin in water, *Biophys. Chem.*, 2, 49, 1974.
89. Johnson, M. E. and Ho, C., Effects of ligands and organic phosphates on functional properties of human adult hemoglobin, *Biochemistry*, 13, 3653, 1974.
90. Lindstrom, T. R., Ho, C., and Pisciotta, A. V., Nuclear magnetic resonance studies of haemoglobin M Milwaukee, *Nat. New Biol.*, 237, 263, 1972.
91. Lindstrom, T. R. and Ho, C., Functional nonequivalence of α and β hemes in human adult hemoglobin, *Proc. Natl. Acad. Sci. U.S.A.*, 69, 1707, 1972.
92. Lindstrom, T. R., Olson, J. S., Mock, N. H., Gibson, Q. H., and Ho, C., Nuclear magnetic resonance studies of hemoglobins. VIII. Evidence for preferential ligand binding to β chains within deoxyhemoglobins, *Biochem. Biophys. Res. Commun.*, 45, 22, 1971.
93. Baldassare, J. J., Charache, S., Jones, R. T., and Ho, C., Electron paramagnetic resonance studies of spin-labeled hemoglobins. II. Roles of subunit interactions and of intermediate structures in the cooperative oxygenation of hemoglobin and the results on hemoglobin J Capetown, and carboxypeptidases A and B treated hemoglobin A, *Biochemistry*, 9, 4707, 1970.
94. Perutz, M. F., The haemoglobin molecule, *Proc. Roy. Soc. London, Ser. B*, B173, 113, 1969.
95. Wiechelman, K. J., Charache, S., and Ho, C., Nuclear magnetic resonance studies of hemoglobin Chesapeake: An $\alpha_1\beta_2$ mutant, *Biochemistry*, 13, 4772, 1974.
96. Ogawa, S., Shulman, R. G., Kynoch, P. A. M., and Lehmann, H., High resolution nuclear magnetic resonance studies of haemoglobin J Capetown, *Nature*, 225, 1042, 1970.
97. Nagel, R. L., Gibson, Q. H., and Charache, S., Relation between structure and function in hemoglobin Chesapeake, *Biochemistry*, 6, 2395, 1967.
98. Pulsinelli, P. D., Structure of deoxyhemoglobin Yakima: a high-affinity mutant form exhibiting oxy-like $\alpha_1\beta_2$ subunit interactions, *J. Mol. Biol.*, 74, 57, 1973.
99. Ogawa, S., Patel, D. J., and Simon, S. R., Proton magnetic resonance study of the switch between the two quaternary structures in high-affinity hemoglobins in the deoxy state, *Biochemistry*, 13, 2001, 1974.
100. Lindstrom, T. R., Noren, J. B. E., Charache, S., Lehmann, H., and Ho, C., Nuclear magnetic resonance studies of hemoglobins. VII. Tertiary structure around ligand binding site in carbonmonoxy hemoglobin, *Biochemistry*, 11, 1677, 1972.
101. Lindstrom, T. R. and Ho, C., Effects of anions and ligands on the tertiary structure around ligand binding site in human adult hemoglobin, *Biochemistry*, 12, 134, 1973.
102. Patel, D. J., Kampa, L., Shulman, R. G., Yamane, T., and Fujiwara, M., Proton NMR studies of hemoglobin in H_2O, *Biochem. Biophys. Res. Commun.*, 40, 1224, 1970.
103. Fung, L. W. M. and Ho, C., A proton nuclear magnetic resonance study of the quaternary structure of human hemoglobins in water, *Biochemistry*, 14, 2526, 1975.
104. McDonald, M. J. and Noble, R. W., The effect of pH on the rates of ligand replacement reactions of human adult and fetal hemoglobins and their subunits, *J. Biol. Chem.*, 247, 4282, 1972.

105. Perutz, M. F., Muirhead, H., Mazzarella, L., Crowther, R. A., Greer, J., and Kilmartin, J. V., Identification of residues responsible for the alkaline Bohr effect in haemoglobin, *Nature*, 222, 1240, 1969.
106. Kilmartin, J. V. and Wootton, J. F., Inhibition of Bohr effect after removal of C-terminal histidines from haemoglobin β-chains, *Nature*, 228, 766, 1970.
107. Perutz, M. F., Pulsinelli, P. D., Ten Eyck, L., Kilmartin, J. V., Shibata, S., Iuchi, I., Miyaji, T., and Hamilton, H. B., Haemoglobin Hiroshima and the mechanisms of the alkaline Bohr effect, *Nat. New Biol.*, 232, 147, 1971.
108. Wüthrich, K., Studies of the molecular conformation in proteins by ^{1}H and ^{13}C N.M.R. spectroscopy, *Pure Appl. Chem.*, 37, 235, 1974.
109. Moon, R. B. and Richards, J. H., Conformational studies of various hemoglobins by natural abundance ^{13}C NMR spectroscopy, *Proc. Natl. Acad. Sci. U.S.A.*, 69, 2193, 1972.
110. Matwiyoff, N. A. and Burnham, B. F., Carbon-13 NMR spectroscopy of tetrapyrroles, *Ann. N.Y. Acad. Sci.*, 206, 265, 1973.
111. Morrow, J. S., Keim, P., Visscher, R. B., Marshall, R. C., and Gurd, F. R. N., The interaction of [^{13}C] carbon dioxide and bicarbonate with human hemoglobin preparations, *Proc. Natl. Acad. Sci. U.S.A.*, 70, 1414, 1973.
112. Levy, G. C. and Cargioli, J. D., Carbon-13 chemical shifts on the TMS scale, *J. Magn. Reson.*, 6, 143, 1972.
113. Glushko, V., Lawson, P. J., and Gurd, F. R. N., Conformational states of bovine pancreatic ribonuclease A observed by normal and partially relaxed carbon 13 nuclear magnetic resonance, *J. Biol. Chem.*, 247, 3176, 1972.
114. Horsley, W. J., Sternlicht, H., and Cohen, J. S., Carbon-13 magnetic resonance studies of amino acids and peptides. II, *J. Am. Chem. Soc.*, 92, 680, 1970.
115. Christl, M. and Roberts, J. D., Nuclear magnetic resonance spectroscopy. Carbon-13 chemical shifts of small peptides as a function of pH, *J. Am. Chem. Soc.*, 94, 4565, 1972.
116. Deslauriers, R. and Smith, I. C. P., Conformation and structure of peptides, in *Topics in Carbon-13 NMR Spectroscopy*, Vol. 2, Levy, G. C., Ed., Interscience, New York, 1975, chap. 1.
117. Keim, P., Vigna, R. A., Marshall, R. C., and Gurd, F. R. N., Carbon 13 nuclear magnetic resonance of pentapeptides of glycine containing central residues of aliphatic amino acids, *J. Biol. Chem.*, 248, 1604, 1973.
118. Keim, P., Vigna, R. A., Morrow, J. S., Marshall, R. C., and Gurd, F. R. N., Carbon 13 nuclear magnetic resonance of pentapeptides of glycine containing central residues of serine, threonine, aspartic and glutamic acids, asparagine and glutamine, *J. Biol. Chem.*, 248, 7811, 1973.
119. Keim, P., Vigna, R. A., Nigen, A. M., Morrow, J. S., and Gurd, F. R. N., Carbon 13 nuclear magnetic resonance of pentapeptides of glycine containing central residues of methionine, proline, arginine, and lysine, *J. Biol. Chem.*, 249, 4149, 1974.
120. Flohé, L., Breitmaier, E., Gunzler, W. A., Voelter, W., and Jung, G., Zum Dissoziationsuerhalten von Cystein und verwandten SH-Verbindungen, *Hoppe-Seyler's Z. Physiol. Chem.*, 353, 1159, 1972.
121. Bradbury, J. H. and Norton, R. S., Carbon-13 NMR spectra of tryptophan, tryptophan peptides and of native and denatured proteins, *Biochim. Biophys. Acta*, 328, 10, 1973.
122. Wüthrich, K. and Baumann, R., Hyperfine shifts of the ^{13}C-NMR in low spin iron (III) complexes, *Helv. Chim. Acta*, 56, 585, 1973.
123. Wüthrich, K. and Baumann, R., Recent developments in the investigation of the paramagnetic centers in low-spin ferric hemoproteins: carbon-13 hyperfine shifts in iron porphyrin complexes, *Ann. N. Y. Acad. Sci.*, 222, 709, 1973.
124. Wüthrich, K. and Baumann, R., Hyperfine shifts of the ^{13}C-NMR in protoporphyrin IX iron (III) dicyanide and deuteroporphyrin IX iron III diyamide, *Helv. Chim. Acta*, 57, 336, 1974.
125. Schlecht, P., Vogel, H., and Mayer, A., Effect of oxygen binding on the dielectric properties of hemoglobin, *Biopolymers*, 6, 1717, 1968.
126. Anderson, S. R., Brunori, M., and Weber, G., Fluorescence studies of Aplysia and sperm whale apomyoglobins, *Biochemistry*, 9, 4723, 1970.
127. Oldfield, E. and Allerhand, A., Studies of individual carbon sites of hemoglobins in solutions by natural abundance carbon 13 nuclear magnetic resonance spectroscopy, *J. Biol. Chem.*, 250, 6403, 1975.
128. Oldfield, E., Norton, R. S., and Allerhand, A., Studies of individual carbon sites of proteins in solution by natural abundance carbon 13 nuclear magnetic resonance spectroscopy. Relaxation behavior, *J. Biol. Chem.*, 250, 6368, 1975.
129. Oldfield, E., Norton, R. S., and Allerhand, A., Studies of individual carbon sites of proteins in solution by natural abundance carbon 13 nuclear magnetic resonance spectroscopy. Strategies for assignments, *J. Biol. Chem.*, 250, 6381, 1975.
130. Moon, R. B. and Richards, J. H., Nuclear magnetic resonance studies of ^{13}CO binding to various heme globins, *J. Am. Chem. Soc.*, 94, 5093, 1972.
131. Matwiyoff, N. A. and Needham, T. E., Carbon-13 NMR spectroscopy of red blood cell suspensions, *Biochem. Biophys. Res. Commun.*, 49, 1158, 1972.
132. Matwiyoff, N. A., Vergamini, P. J., Needham, T. E., Gregg, C. T., Volpe, J. A., and Caughey, W. S., Carbon-13 nuclear magnetic resonance and infrared spectroscopic studies of ^{13}CO binding to rabbit hemoglobin, *J. Am. Chem. Soc.*, 95, 4429, 1973.
133. Antonini, E., Brunori, M., Conti, F., and Geraci, G., NMR studies of ^{13}CO-hemoglobin. α and β chain identification, *Fed. Eur. Biochem. Soc. Lett.*, 34, 69, 1973.

134. Moon, R. B. and Richards, J. H., ^{13}C magnetic resonance studies of the binding of carbon monoxide to various hemoglobins, *Biochemistry*, 13, 3437, 1974.
135. Vergamini, P. J., Matwiyoff, N. A., Wohl, R. C., and Bradley, T., Carbon-13 NMR studies of ^{13}CO binding to human hemoglobin, *Biochem. Biophys. Res. Commun.*, 55, 453, 1973.
136. Hunter, T. and Munro, A., Allelic variants in the amino-acid sequence of the α chain of rabbit haemoglobin, *Nature*, 223, 1270, 1969.
137. Gurd, F. R. N., Morrow, J. S., Keim, P., Visscher, R. B., and Marshall, R. C., ^{13}C NMR studies of the interaction of hemoglobin and carbonic anhydrase with $^{13}CO_2$, in *Protein-Metal Interactions*, Friedman, M., Ed., Plenum Publishing, New York, 1974, 109.
138. Morrow, J. S., Wittebort, R. J., and Gurd, F. R. N., Ligand-dependent aggregation of chicken hemoglobin A_I, *Biochem. Biophys. Res. Commun.*, 60, 1058, 1974.
139. Morrow, J. S., The Interaction of Carbon Dioxide with Amino Acids, Peptides, and Hemoglobins: A Study by ^{13}C Nuclear Magnetic Resonance, Ph.D. thesis, Indiana University, Bloomington, 1974.
140. Kilmartin, J. V. and Rossi-Bernardi, L., Inhibition of CO_2 combination and reduction of the Bohr effect in haemoglobin chemically modified at its α-amino groups, *Nature*, 222, 1243, 1969.
141. Kilmartin, J. V. and Rossi-Bernardi, L., The binding of carbon dioxide by horse haemoglobin, *Biochem. J.*, 124, 31, 1971.
142. Kilmartin, J. V., Fogg, J., Luzzana, M., and Rossi-Bernardi, L., Role of the α and β chains of human hemoglobin in oxygen-linked binding of carbon dioxide, *J. Biol. Chem.*, 248, 7039, 1973.
143. Morrow, J. S., Keim, P., and Gurd, F. R. N., CO_2 adducts of certain amino acids, peptides, and sperm whale myoglobin studied by carbon 13 and proton nuclear magnetic resonance, *J. Biol. Chem.*, 249, 7484, 1974.
144. Morrow, J. S., Gurd, R. S., and Gurd, F. R. N., The chemical basis and possible role of carbamino homeostatic mechanisms, in *Peptides, Polypeptides and Proteins*, Blout, E. R., Bovey, F. A., Goodman, M., and Lotan, N., Eds., John Wiley & Sons, New York, 1974, 594.
145. Roughton, F. J. W., Some recent work on the interactions of oxygen, carbon dioxide and haemoglobin, *Biochem. J.*, 117, 801, 1970.
146. Milla, E., Giustina, G., and Margaria, R., L'esistenza di due tipi di composti dell'Hb col CO_2, *G. Biochim.*, 2, 153, 1953.
147. Guistina, G., Milla, E., and Margaria, R., La capacita dell' emoglobina e di alcune altre proteine a formare cabamino composti, *G. Biochem.*, 2, 357, 1953.
148. Kernohan, J. C., Kreuzer, F., Rossi-Bernardi, L., and Roughton, F. J. W., The effects of bicarbonate and carbon dioxide on the affinity of haemoglobin for oxygen, *Biochem. J.*, 100, 49P, 1966.
149. Kreuzer, F., Diskussionsbemerkung (on the specific effect of CO_2 on the affinity of Hb for O_2 at constant pH), in *Gesellschaft für Biologische Chemie; Biochemie des Sauerstoffs*, Hess, B. and Staudinger, Hj., Eds., Springer-Verlag, Berlin, 1968, 93.
150. Kreuzer, F., Transport of O_2 and CO_2 at altitude, in *Exercise at Altitude*, Margaria, R., Ed., Exerpta Medica, Amsterdam, 1967, 148.
151. Kreuzer, F., Roughton, F. J. W., Rossi-Bernardi, L., and Kernohan, J. C., Specific effect of CO_2 and bicarbonate on the affinity of hemoglobin for oxygen, in *Oxygen Affinity of Hemoglobin and Red Cell Acid Base Status*, Rørth, M. and Astrup, P., Eds., Academic Press, New York, 1972, 208.
152. Sidwell, A. E., Jr., Munch, R. H., Guzman Barron, E. S., and Hogness, T. R., The salt effect on the hemoglobin-oxygen equilibrium, *J. Biol. Chem.*, 123, 335, 1938.
153. Rossi-Bernardi, L. and Roughton, F. J. W., The specific influence of carbon dioxide and carbamate compounds on the buffer power and Bohr effect in human haemoglobin solutions, *J. Physiol.*, 189, 1, 1967.
154. Forster, R. E., Constantine, H. P., Craw, M. R., Rotman, H. H., and Klocke, R. A., Reaction of CO_2 with human hemoglobin solution, *J. Biol. Chem.*, 243, 3317, 1968.
155. Hill, R. J. and Davis, R. W., The pK of specific groups of proteins. I. The α-amino group of the α chain of human co-hemoglobin, *J. Biol. Chem.*, 242, 2005, 1967.
156. Garner, M. H., Bogardt, R. A., Jr., and Gurd, F. R. N., Determination of the pK values for the α-amino groups of human hemoglobin, *J. Biol. Chem.*, 250, 4398, 1975.
157. Tomita, S. and Riggs, A., Studies of the interaction of 2,3-diphosphoglycerate and carbon dioxide with hemoglobins from mouse, man, and elephant, *J. Biol. Chem.*, 246, 547, 1971.
158. Levy, A. L., The removal of terminal groups from peptides, *J. Chem. Soc.*, Part I., p. 404, 1950.
159. Cerami, A. and Manning, J. M., Potassium cyanate as an inhibitor of the sickling of erythrocytes *in vitro*, *Proc. Natl. Acad. Sci. U.S.A.*, 68, 1180, 1971.
160. Cerami, A., Cyanate as an inhibitor of red-cell sickling, *N. Engl. J. Med.*, 287, 807, 1972.
161. Gillette, P. N., Manning, J. M., and Cermai, A., Increased survival of sickle-cell erythrocytes after treatment *in vitro* with sodium cyanate, *Proc. Natl. Acad. Sci. U.S.A.*, 68, 2791, 1971.
162. Nigen, A. M., Njikam, N., Lee, C. K., and Manning, J. M., Studies on the mechanism of action of cyanate in sickle cell disease, *J. Biol. Chem.*, 249, 6611, 1974.
163. Moon, R. B., Nelson, M. J., Richards, J. H., and Powars, D. F., ^{13}C Magnetic resonance studies of hemoglobin carbamylation, *Physiol. Chem. Phys.*, 6, 31, 1974.

164. **Heustis, W. H. and Raftery, M. A.,** A study of cooperative interactions in hemoglobin using fluorine nuclear magnetic resonance, *Biochemistry,* 11, 1648, 1972.
165. **Heustis, W. H. and Raftery, M. A.,** Characterization of intermediate states in the ligation of hemoglobin, *Biochemistry,* 12, 2531, 1973.
166. **Gibson, Q. H.,** p-Mercuribenzoate as an indicator of conformation change in hemoglobin, *J. Biol. Chem.,* 248, 1281, 1973.
167. **Olson, J. S. and Gibson, Q. H.,** The reaction of *n*-butyl isocyanide with human hemoglobin. I. Determination of the kinetic parameters involved in the last step in ligand binding, *J. Biol. Chem.,* 246, 5241, 1971.
168. **Olson, J. S. and Gibson, Q. H.,** The reaction of n-butyl isocyanide with human hemoglobin. II. The ligand-binding properties of the α and β chains within deoxyhemoglobin, *J. Biol. Chem.,* 247, 1713, 1972.
169. **Huestis, W. H. and Raftery, M. A.,** The binding of *n*-butyl isocyanide to human hemoglobin, *Biochem. Biophys. Res. Commun.,* 48, 678, 1972.
170. **Lee, T., Huestis, W. H., and Raftery, M. A.,** A comparison of the functional properties of human hemoglobin A and its (β-93) – trifluoroacetonylated derivative, *Biochemistry,* 13, 2535, 1973.
171. **Huestis, W. H. and Raftery, M. A.,** ^{31}P-NMR studies of the release of diphosphoglyceric acid on carbon monoxide binding to hemoglobin, *Biochem. Biophys. Res. Commun.,* 49, 428, 1972.
172. **Moon, R. B. and Richards, J. H.,** Determination of intracellular pH by ^{31}P magnetic resonance, *J. Biol. Chem.,* 248, 7276, 1973.
173. **Chiancone, E., Norne, J. E., Forsén, S., Antonini, E., and Wyman, J.,** Nuclear magnetic resonance quadrupole relaxation studies of chloride binding to human oxy- and deoxyhaemoglobin, *J. Mol. Biol.,* 70, 675, 1972.
174. **Pifat, G., Maricić, S., Petrinović, M., Kramer, V., Marsel, J., and Bonhard, K.,** Oxygen bonding to haemoglobin. ^{17}O NMR spectrum – a second look, *Croat. Chem. Acta,* 41, 195, 1969.
175. **Velenik, A. and Lynden-Bell, R. M.,** ^{17}O nuclear magnetic resonance chemical shift in oxyhaemoglobin, *Croat. Chem. Acta,* 41, 205, 1969.
176. **Koshland, D. E., Jr., Nemethy, G., and Filmer, D.,** Comparison of experimental binding data and theoretical models in proteins containing subunits, *Biochemistry,* 5, 365, 1966.
177. **Szabo, A. and Karplus, M.,** A mathematical model for structure-function relations in hemoglobin, *J. Mol. Biol.,* 72, 163, 1972.
178. **Ogata, R. T. and McConnell, H. M.,** The binding of a spin-labeled triphosphate to hemoglobin, *Cold Spring Harbor Symp. Quant. Biol.,* 36, 325, 1971.
179. **Ogata, R. T. and McConnell, H. M.,** Mechanism of cooperative oxygen binding to hemoglobin, *Proc. Natl. Acad. Sci. U.S.A.,* 69, 335, 1972.
180. **Baldwin, J. M.,** Structure and Function of Haemoglobin Prog. Biophys. Molec. Biol., 29, 225, 1975.
181. **Perutz, M. F., Rossmann, M. G., Cullis, A. F., Muirhead, H., Will, G., and North, A. C. T.,** Structure of haemoglobin. A three-dimensional Fourier synthesis at 5.5 Å resolution, obtained by x-ray analysis, *Nature,* 185, 416, 1960.
182. **Wyman, J.,** Linked functions and reciprocal effects in hemoglobin: a second look, *Adv. Protein Chem.,* 19, 223, 1964.
183. **Shire, S. J., Hanania, G. I. H., and Gurd, F. R. N.,** Electrostatic effects in myoglobin. Hydrogen ion equilibria in sperm whale ferrimyoglobin, *Biochemistry,* 13, 2967, 1974.
184. **Monod, J., Changeux, J. P., and Jacob, F.,** Allosteric proteins and cellular control systems, *J. Mol. Biol.,* 6, 306, 1963.
185. **Polet, M. and Steinhardt, J.,** Sequential stages in the acid denaturation of horse and human ferrihemoglobins, *Biochemistry,* 8, 857, 1969.
186. **Crespi, H. L. and Katz, J. J.,** Preparation of deuterated proteins and enzymes, *Methods Enzymol.,* 26, 627, 1972.
187. **Markley, J. L.,** High-resolution proton magnetic resonance spectroscopy of selectively deuterated enzymes, *Methods Enzymol.,* 26, 605, 1972.
188. **Markley, J. L., Putter, I., and Jardetzky, O.,** High-resolution nuclear magnetic resonance spectra of selectively deuterated staphlococcal nuclease, *Science,* 161, 1249, 1968.
189. **Diehl, P. and Leipert, T.,** Deuteronen-kernresonanzspektroskopie, *Helv. Chim. Acta,* 47, 545, 1964.
190. **Diehl, P.,** A survey of recent advances in ^{2}D and ^{3}T NMR, in *Nuclear Magnetic Resonance Spectroscopy of Nuclei Other Than Protons,* Axenrod, T. and Webb, G. A., Eds., John Wiley & Sons, New York, 1974, 275.
191. **Oster, O., Neireiter, G. W., and Gurd, F. R. N.,** Observation of deuterium-labeled diacetyldeuteroporphyrin incorporated in cyanoferrimyoglobin by deuterium nuclear magnetic resonance, *Biochem. Biophys. Res. Commun.,* 64, 1, 1975.
192. **Oster, O., Neireiter, G. W., and Gurd, F. R. N.,** Specific acid catalyzed deuteration of the acetyl groups of 2,4-diacetyldeuterohemin-OMe, *Z. Naturforsch.,* 30b, 37, 1975.
193. **Morrison, M. R., Brinkley, S. A., Gorski, J., and Lingrel, J. B.,** The separation and identification of α- and β-globin messenger ribonucleic acids, *J. Biol. Chem.,* 249, 5290, 1974.
194. **Hunkapiller, M. W., Smallcombe, S. H., Whitaker, D. R., and Richards, J. H.,** Carbon nuclear magnetic resonance studies of the histidine residue in α-lytic protease. Implications for the catalytic mechanism of serine proteases, *Biochemistry,* 12, 4732, 1973.

195. **Markley, J. L.,** High-resolution proton magnetic resonance studies of two trypsin inhibitors: soybean trypsin inhibitor (Kunitz) and ovomucoid (hen egg white), *Ann. N.Y. Acad. Sci.*, 222, 347, 1973.
196. **Jones, W. C., Rothgeb, T. M., and Gurd, F. R. N.,** Specific enrichment with ^{13}C of the methionine methyl groups of sperm whale myoglobin, *J. Am. Chem. Soc.*, 97, 3875, 1975.
197. **Morrow, J. S., Wittebort, R. J., and Gurd, F. R. N.,** Ligand-dependent aggregation of chicken hemoglobin A_I, *Biochem. Biophys. Res. Commun.*, 60, 1058, 1974.
198. **Gutte, B.,** A synthetic 70-amino acid residue analog of ribonuclease S-protein with enzymic activity, *J. Biol. Chem.*, 250, 889, 1975.
199. **Stewart, J. M. and Young, J. D.,** *Solid Phase Peptide Synthesis*, W. H. Freeman, San Francisco, 1969.
200. **Richards, F. M.,** On the enzymic activity of subtilisin-modified ribonuclease, *Proc. Natl. Acad. Sci. U.S.A.*, 44, 162, 1958.
201. **Hodges, R. S. and Merrifield, R. B.,** The role of serine-123 in the activity and specificity of ribonuclease, *J. Biol. Chem.*, 250, 1231, 1975.
202. **Corradin, G. and Harbury, H. A.,** Reconstitution of horse heart cytochrome c: interaction of the components obtained upon cleavage of the peptide bond following methionine residue 65, *Proc. Natl. Acad. Sci. U.S.A.*, 68, 3036, 1971.
203. **Fisher, W. R., Taniuchi, H., and Anfinsen, C. B.,** On the role of heme in the formation of the structure of cytochrome c, *J. Biol. Chem.*, 248, 3188, 1973.
204. **Chaiken, I. M.,** Purification and properties of semisynthetic staphlococcal nuclease-T', *J. Biol. Chem.*, 246, 2948, 1971.
205. **Chaiken, I. M., Cohen, J. S., and Sokoloski, E.,** Microenvironment of histidine 12 in ribonuclease-S as detected by ^{13}C nuclear magnetic resonance, *J. Am. Chem. Soc.*, 96, 4703, 1974.
206. **Chaiken, I. M.,** Carbon 13 as a probe of helix formation in semisynthetic ribonuclease-S', *J. Biol. Chem.*, 249, 1247, 1974.
207. **Freedman, M. H., Cohen, J. S., and Chaiken, I. M.,** Carbon-13 fourier transform nuclear magnetic resonance studies of peptides, *Biochem. Biophys. Res. Commun.*, 42, 1148, 1971.
208. **Offord, R. E.,** Protection of peptides of biological origin for use as intermediates in the chemical synthesis of proteins, *Nature*, 221, 37, 1969.
209. **Saunders, D. J. and Offord, R. E.,** The use of semisynthetically-introduced ^{13}C probes for nuclear magnetic resonance studies on insulin, *Fed. Eur. Biochem. Soc. Lett.*, 26, 286, 1972.
210. **Lode, E. T., Murray, C. L., Sweeney, W. V., and Rabinowitz, J. C.,** Synthesis and properties of clostridium acidi-urici [Leu^2]-ferredoxin: a function of the peptide chain and evidence against the direct role of the aromatic residues in electron transfer, *Proc. Natl. Acad. Sci. U.S.A.*, 71, 1361, 1974.
211. **Garner, W. H. and Gurd, F. R. N.,** Semisynthesis of a specific NH_2-terminal [$1-^{13}C$] glycine adduct to sperm whale myoglobin: intermediate protection of ϵ-amino groups with methyl acetimidate, *Biochem. Biophys. Res. Commun.*, 63, 262, 1975.
212. **Hunter, M. J. and Ludwig, M. L.,** The reaction of imidoesters with proteins and related small molecules, *J. Am. Chem. Soc.*, 84, 3491, 1962.
213. **Ludwig, M. L. and Byrne, R.,** Reversible blocking of protein amino groups by the acetimidyl group, *J. Am. Chem. Soc.*, 84, 4160, 1962.
214. **Coleman, J. E. and Vallee, B. L.,** Metallocarboxypeptidases, *J. Biol. Chem.*, 235, 390, 1960.
215. **Corradin, G. and Harbury, H. A.,** Reconstitution of horse heart cytochrome c: reformation of the peptide bond linking residues 65 and 66, *Biochem. Biophys. Res. Commun.*, 61, 1400, 1974.
216. **Kowalski, O. and Laskowski, M., Jr.,** Inactivation of enzymatically modified trypsin inhibitors upon chemical modification of the α-amino group in the reactive site, *Biochemistry*, 11, 3451, 1972.
217. **Dyckes, D. F., Creighton, T., and Sheppard, R. C.,** Spontaneous re-formation of a broken peptide chain, *Nature*, 247, 202, 1974.
218. **Garner, W. H.,** The Specific Incorporation of [^{13}C] Glycine into Sperm Whale Myoglobin: An Investigation by ^{13}C Nuclear Magnetic Resonance, Ph.D. thesis, Indiana University, Bloomington, 1974.
219. **Watson, H. C.,** The stereochemistry of the protein myoglobin, *Progr. Stereochem.*, 4, 299, 1969.
220. **Espersen, W. G., Hutton, W. C., Chow, S. T., and Martin, R. B.,** Cautions concerning uses of copper (II) selective broadening in nuclear magnetic resonance spectroscopy for determination of ligand binding sites, *J. Am. Chem. Soc.*, 96, 8111, 1974.
221. **Visscher, R. B. and Gurd, F. R. N.,** Rotational motions in myoglobin assessed by carbon-13 relaxation measurements at two magnetic field strengths, *J. Biol. Chem.*, 250, 2238, 1975.
222. **Lee, B. and Richards, F. M.,** The interpretation of protein structures: estimation of static accessibility, *J. Mol. Biol.*, 55, 379, 1971.
223. **Nobbs, C. L., Watson, H. C., and Kendrew, J. C.,** Structure of deoxymyoglobin: a crystallographic study, *Nature*, 209, 339, 1966.
224. **Stryer, L., Kendrew, J. C., and Watson, H. C.,** The mode of attachment of the azide ion to sperm whale metmyoglobin, *J. Mol. Biol.*, 8, 96, 1964.
225. **Ver Ploeg, D. A., Cordes, E. H., and Gurd, F. R. N.,** Comparison of myoglobins from harbor seal, porpoise, and sperm whale. VII. Mechanism and catalysis for addition of cyanide to myoglobins, *J. Biol. Chem.*, 246, 2725, 1971.

226. Chance, B., On the measurement of reactivity of hemoproteins in the crystalline state, in *Hemes and Hemoproteins*, Chance, B., Estabrook, R. W., and Yonetani, T., Eds., Academic Press, New York, 1966, 213.
227. Schoenborn, B. P., Watson, H. C., and Kendrew, J. C., Binding of xenon to sperm whale myoglobin, *Nature*, 207, 28, 1965.
228. Schoenborn, B. P., Binding of cyclopropane to sperm whale myoglobin, *Nature*, 214, 1120, 1967.
229. Hugli, T. E. and Gurd, F. R. N., Carboxymethylation of sperm whale myoglobin in the crystalline state, *J. Biol. Chem.*, 245, 1930, 1970.
230. Atanasov, B. P., Models of conformers on the native state of myoglobin, *Mol. Biol.* (Russia), 4, 348, 1970.
231. Benson, E. S., Fanelli, M. R. R., Giacometti, G. M., Rosenberg, A., and Antonini, E., Effects of ligand binding on the rates of hydrogen exchange in myoglobin and hemoglobin, *Biochemistry*, 12, 2699, 1973.
232. Englander, S. W. and Staley, R., Measurement of the free and the H-bonded amides of myoglobin, *J. Mol. Biol.*, 45, 277, 1969.
233. Richards, F. M., The interpretation of protein structures: total volume, group volume distributions and packing density, *J. Mol. Biol.*, 82, 1, 1974.
234. Lumry, R. and Rosenberg, A., The mobile-defect hypothesis of protein function, Proceedings of the Alfsen Conference on Water, Roscoff, France, June 2–6, 1975, in press.
235. Morishima, I. and Iizuka, T., Nuclear magnetic resonances of hemoproteins. Restricted rotation of a heme side chain methyl group in some ferric myoglobin complexes and its implication in van der Waals contact in the heme side chain environments, *J. Am. Chem. Soc.*, 96, 7365, 1974.
236. Tanford, C., Protein denaturation, parts A and B, *Adv. Protein Chem.*, 23, 121, 1968.
237. Tanford, C., Protein denaturation, part C., *Adv. Protein Chem.*, 24, 1, 1970.
238. Ramachandran, G. N. and Sasisekharan, V., Conformation of polypeptides and proteins, *Adv. Protein Chem.*, 23, 283, 1968.
239. Nemethy, G., Leach, S. J., and Scheraga, H. A., The influence of amino acid side chains on the free energy of helix-coil transition, *J. Phys. Chem.*, 70, 998, 1966.
240. Perutz, M. F., The Bohr effect and combination with organic phosphates, *Nature*, 228, 734, 1970.
241. Benesch, R. E. and Benesch, R., The mechanism of interaction of red cell organic phosphates with hemoglobin, *Adv. Protein Chem.*, 28, 211, 1974.
242. Bansil, R., Herzfeld, J., and Stanley, H. E., Hemoglobin kinetics and the effect of organic phosphates, *Science*, 186, 929, 1974.
243. Grimaldi, J. J. and Sykes, B. D., Concanavalin A: a stopped flow nuclear magnetic resonance study of conformational changes induced by Mn^{++}, Ca^{++}, and α-methyl-D-mannoside, *J. Biol. Chem.*, 250, 1618, 1975.
244. Davenport, H. W., *The ABC of Acid-Base Chemistry*, The University of Chicago Press, Chicago, 1950.
245. Hastings, A. B., A biochemist's anabasis, *Annu. Rev. Biochem.*, 39, 1, 1970.
246. Wood, P. G., The preparation of hemoglobin free resealable red blood cell ghosts by a gel filtration technique, *Fed. Proc.*, 34, 248, 1975.